UNIVERSITY OF OKLAHOMA

GRADUATE COLLEGE

AN ENHANCER-TRAP AND SPLICE-TRAP SCREEN FOR REGULATORS OF ENDOCRINE FUNCTIONS IN THE CENTRAL NERVOUS SYSTEM AND THE EPITRACHEAL GLAND OF *DROSOPHILA MELANOGASTER*

A DISSERTATION

SUBMITTED TO THE GRADUATE FACULTY

in partial fulfillment of the requirements for the

Degree of

DOCTOR OF PHILOSOPHY

By

CHUNJING QU
Norman, Oklahoma
2010

AN ENHANCER-TRAP AND SPLICE-TRAP SCREEN FOR REGULATORS OF ENDOCRINE FUNCTIONS IN THE CENTRAL NERVOUS SYSTEM AND THE EPITRACHEAL GLAND OF *DROSOPHILA MELANOGASTER*

A DISSERTATION APPROVED FOR THE
DEPARTMENT OF ZOOLOGY

BY

_____
Dr. Randall Hewes, Chair

_____
Dr. Tyrell Conway

_____
Dr. David Durica

_____
Dr. Rosemary Knapp

_____
Dr. Donald Wilson

Acknowledgements

First of all, I wish to thank my advisor Dr. Randall Hewes, for his patience in providing guidance to me during my stay in his lab. He set a good example for me as to how to be a scientist and an educator. I wish to thank my advisory committee members, Dr. Tyrell Conway, Dr. David Durica, Dr. Rosemary Knapp and Dr. Donald Wilson for their assistance, expertise and guidance. I am thankful to professors and staffs in the department of Zoology, it has been such a great experience to be in the midst of so many talented and friendly people.

I wish to thank my parents, Zhiren Qu and Chuanhua Wang, my sister and brother, Chunmei and Kaishan Qu for their sustained support through so many years. Their encouragement and help are indispensible factors for each step of my achievement.

At last, but not the least, I wish to thank my husband Donghui Li and my daughters Lisa and Leah Li for their strong support in my research work and the happiness they are bringing to me.

This work was supported by the Department of Zoology (Adams scholarship, 2005-2007, 2009), the University of Oklahoma Graduate College (Robberson and travel awards, 2009) and the University of Oklahoma Graduate Student Senate (research/travel grant in 2006, 2007, 2009), the National Science Foundation (NSF grant numbers IOS-0744447 (PI: Hewes) and IBN-0344018 (PI: Hewes)), and the Oklahoma Center for the Advancement of Science and Technology (OCAST) Health Research Project (OHR), (OCAST OHR grant numbers HR06-046 (PI: Hewes) and HR03-048S (PI: Hewes)).

Table of Contents

List of Tables

List of Figures

Abstract

Peptide hormones play important roles in a wide variety of biological processes, such as learning and memory, body weight homeostasis, circadian rhythms, and addiction. In Drosophila, over 20 peptide hormones are produced in the central nervous system (CNS) by distinct groups of specialized neurons, peptidergic neurons. Another important endocrine function is performed by the Inka cell, responsible for the production and secretion of the ecdysis triggering hormone (ETH), which is critical for the ecdysis process of the animal. Although many genes encoding peptide hormones have been identified, our knowledge about factors that regulate the production and secretion of peptide hormones is still very limited. In order to identify more endocrine regulators, we performed an enhancer trap and splice trap screen for genes that are expressed in peptidergic neurons in the CNS and the epitracheal gland, where the ETH-expressing Inka cell is located. From a screen of 545 splice trap lines and 287 enhancer trap lines, we obtained 28 insertions in 25 genes that are expressed in peptidergic neurons of the CNS, and 14 insertions in 14 genes that are expressed in the epitracheal gland. For lines that are expressed in the CNS, we further mapped the expression patterns by immunostaining with antisera to several neuropeptides, including Bursicon, Drosophila insulin-like peptide 2, crustacean cardioactive peptide, and leucokinin, each of which is expressed in distinct groups of neurons. Among the 28 lines identified, the *BG00836* insertion in the gene *alan shepard* (*shep*) was extremely interesting to us because of its restricted reporter gene expression in peptidergic neurons. $shep^{BG00836}$ mutant adults showed defects in wing expansion and decreased resistance to starvation, and these phenotypes were reverted by precise

excision of the *P* element. However, it was later shown that these may be neomorphic phenotypes brought by the combination of the *shep* mutation and unknown factors in the genetic background. Follow-up experiments on *shep* showed that it is involved in the control of neurite outgrowth in the CNS. Therefore, *shep* may function as a general developmental regulator for peptidergic neurons. Lines with reporter gene expression in the epitracheal glands may reveal genes that participate in the regulation of ETH expression or secretion. We examined the functions of the trapped loci by knocking down gene expression specifically in the Inka cells with transgenic RNA interference (RNAi). Expression of *UAS-taiman* $(tai)^{RNAi}$ in the Inka cells led to ecdysis defects and reduced *ETH* expression. TAI is a known ecdysone receptor coactivator, and expression levels of TAI were correlated with the circulating steroid hormone titer. Previous research results in our lab and the Cherbas lab suggested that the basic-leucine zipper transcription factor Cryptocephal (CRC) and the EcR/USP heterodimeric ecdysone receptor together form a complex on the *ETH* promoter and activate the expression of *ETH*. Based on these findings, we propose a model in which a complex of TAI, CRC, and EcR/USP binds to the *ETH* promoter and activates *ETH* transcription.

CHAPTER I

Peptide hormones and hormonally regulated ecdysis behaviors in Drosophila

OVERVIEW

Peptide hormones are a group of peptides produced and secreted by neurosecretory and endocrine cells. Once released into the hemolymph of insects, peptide hormones can initiate a series of coordinated physiological and behavioral processes. Research on many invertebrate neuropeptides and peptide hormones was first concentrated on crustacean and lepidopteran species, primarily because of their large sizes, which enable transplantation, peptide extraction and identification, bioassays to test for the biological activity of the hormones, and physiological recordings. *Drosophila melanogaster* has emerged as an additional model that provides many tools for genetic manipulations to define signaling pathways controlling the expression and secretion of peptide hormones. In addition, because of the high degree of molecular conservation between invertebrates and vertebrates, research results obtained on peptide hormones in Drosophila can shed light on similar processes in mammals.

In Drosophila, major endocrine organs and tissues include: 1) The ring gland, which includes the following three endocrine centers: I. Corpora cardiaca (CC)-the release site for many brain peptides and also a source of adipokinetic hormone (AKH); II. The prothoracic gland (PG), which produces the steroid hormone, ecdysone; III. The corpora allata (CA), the site responsible for the production of juvenile hormone. 2) The central nervous system (CNS) is the production site for a large group of at least 20 neuropeptides (NASSEL 2002), such as the Drosophila insulin like peptides (dILPs), eclosion hormone (EH) and bursicon (BURS). Each peptide is expressed by a distinctive set of neurons, although expression patterns of many different

neuropeptides partially overlap. 3) The midgut: at least six peptides are produced by the endocrine cells of the midgut. They are the allatostatins A, B and C, neuropeptide F, diuretic hormone 31, and the tachykinins. Two other peptides, short neuropeptide F and pigment dispersing factor, are produced in CNS neurons that send projections to the midgut (VEENSTRA *et al.* 2008). 4) The epitracheal glands, which include the endocrine Inka cells. The Inka cells are responsible for the production of the ecdysis triggering hormone (ETH).

In this chapter, I review some recent work on selected peptide hormones secreted from the ring gland, CNS, and the Inka cells, and their involvement in the following biological process: 1) regulation of metabolism, feeding and growth; 2) learning and memory; 3) circadian rhythm; 4) development and ecdysis. The review is focused on the identification, expression patterns and known function of the selected peptide hormones. Ecdysis in Drosophila is a stereotyped biological process regulated by the highly coordinated release of a series of peptide hormones. Therefore, in addition to the peptide hormones, I also review the ecdysis behavior at each developmental stage of Drosophila in this chapter.

The expression of peptide hormone is regulated at each step of their biosynthesis, including transcription, translation, packaging and release. In addition, the morphology of a given peptidergic neuron or endocrine cell can affect its ability to secrete peptide hormones at appropriate locations. With the publication of the Drosophila genome, many genes that encode peptide hormones have been identified. However, we only know a few genes that encode regulators of peptide hormone production and secretion, such as *dimmed* (*dimm*) and the *peptidylglycine*-α-

hydroxylating monooxygenase (*PHM*) (HEWES *et al.* 2006; HEWES *et al.* 2003; JIANG *et al.* 2000). In order to identify more such regulatory factors, in Chapter Two of this dissertation we carried out a splice trap screen to identify genes that are expressed in peptidergic neurons in the CNS and then study their functions as potential neuroendocrine regulators. Chapter Three of this dissertation is focused on an enhancer trap and splice trap screen that we performed to identify regulators of the expression of *ETH*, a critical regulator of ecdysis, in the endocrine Inka cells.

1. PEPTIDE HORMONES IN DROSOPHILA

1.1 Peptides involved in the regulation of metabolism, feeding and growth

Drosophila Insulin Like Peptides (DILPs) are encoded by a family of seven genes, *dilp1-7*. The d*ilp1-5* genes are all located on 67C1-2 of the 3rd chromosome, with *dilp1-4* in a tight cluster. The other two, d*ilp6* and *dilp7* are both located at distinct cytological loci on the X chromosome (BROGIOLO *et al.* 2001). The expression patterns of all the *dilp* genes are restricted. Four of them, *dilp1-3* and *dilp5*, are co-expressed in a group of seven cells in each brain hemisphere, the insulin producing cells (IPCs). The IPCs are the major site for insulin production in larval Drosophila (RULIFSON *et al.* 2002). The IPCs send processes to the lateral protocerebrum and subesophageal ganglion, the corpora cardiaca (CC), and the surface of the heart, where they are released into the hemolymph. The IPCs were defined as functionally analogous to mammalian pancreatic islet β cells (RULIFSON *et al.* 2002). In addition to the IPC site, d*ilp4, 5* and *6* all are expressed in the gut, and

the expression of *dilp7* in larvae is restricted to 10 cells in the ventral nerve cord (BROGIOLO *et al.* 2001; RULIFSON *et al.* 2002).

Of the seven *dilp*s, the functions of dILP2 have been the most intensively studied because it is the most closely related to human insulin (BROGIOLO *et al.* 2001). In Drosophila, the insulin peptides regulate growth, reproduction and aging through a highly conserved pathway that includes a single tyrosine kinase receptor, the insulin receptor, and the receptor substrate, *chico* (BROGIOLO *et al.* 2001; CLANCY *et al.* 2001). IPC ablation or genetic manipulations that block the insulin signaling pathway produce a phenotype reminiscent of mammalian diabetes mellitus, including increased glucose levels in the hemolymph. At the same time, the affected animals also showed retardation in growth rate, a smaller final body size (caused by decreased cell size and cell number), increased lifespan, and increased stress and starvation resistance (BROGIOLO *et al.* 2001; BROUGHTON *et al.* 2005; IKEYA *et al.* 2002; RULIFSON *et al.* 2002). Although ubiquitous DILP2 expression could reverse the phenotypes caused by IPC ablation (RULIFSON *et al.* 2002), reduction of DILP2 alone is not sufficient to produce all the above observed phenotypes (BROUGHTON *et al.* 2008). Knock-down of DILP2 expression by *dilp2*-specific RNAi in the IPCs only led to increased trehalose storage but not extended life span (BROUGHTON *et al.* 2008). Conversely, overexpression of each of the other six *dilps*, *dilp1* and *dilp3-7*, promoted growth in Drosophila (IKEYA *et al.* 2002). These experiments indicate considerable functional redundancy in Drosophila insulin signaling.

Insulin regulates Drosophila development (mainly the growth rate) in part through antagonistic interactions with other factors such as the steroid hormone

ecdysone (COLOMBANI *et al.* 2005; NIJHOUT 2003). For example, increased insulin/insulin growth factor signaling (IIS) within the prothoracic gland led to early onset of metamorphosis, along with the precocious release of ecdysone (COLOMBANI *et al.* 2005; WALKIEWICZ and STERN 2009). The production of juvenile hormone, one of the major hormones that regulates the transition between developmental stages, is under the control of IIS (TU *et al.* 2005). Signaling of other hormones that function in food intake or homeostatic regulation may also interact with IIS. These include adipokinetic hormone (BUCH *et al.* 2008), neuropeptide F (WU *et al.* 2005), and short neuropeptide F (LEE *et al.* 2009; LEE *et al.* 2008), each of which is discussed below.

Adipokinetic Hormone (AKH) is a member of the arthropod RPCH (red-pigment-concentrating hormone)/AKH family. The Drosophila AKH peptide and its coding sequence were identified in the 1990s (NOYES *et al.* 1995; SCHAFFER *et al.* 1990). The peptide has high similarity in sequence and structure to other members of this family, except that the Drosophila AKH contains a charged residue under physiological conditions. At both larval and adult stages, *Akh* is expressed only in the corpora cardiaca (CC) compartment of the ring gland (KIM and RULIFSON 2004; NOYES *et al.* 1995; RULIFSON *et al.* 2002). The *Akh*-expressing CC cells send projections onto the heart and terminated in close proximity to the IPC axons. The heart surface is the major release site for AKH into the blood (KIM and RULIFSON 2004).

AKH regulates energy mobilization during some sustained activities such as flight, and it accelerates the heart rate of Drosophila and other insects (NOYES *et al.* 1995; VAN DER HORST 2003). AKH shares some sequence similarity with human

glucagon, which is secreted by pancreatic α cells. Like glucagon, AKH acts antagonistically with insulin in Drosophila to regulate glucose levels in the hemolymph (KIM and RULIFSON 2004). The gene *target of brain insulin* (*tobi*), an α-1,4-glucosidase, which is expressed in the CC cells, was identified as a target for both insulin- and glucagon-like signaling pathways in Drosophila. Similar to the secretion of mammalian glucagon, expression of *tobi* is regulated oppositely by dietary protein and sugar levels (BUCH *et al.* 2008). This finding is additional evidence in support of the conclusion that the IIS and AKH pathways are antagonistic regulators of blood glucose levels. However, unlike IIS, which affects the development of Drosophila (COLOMBANI *et al.* 2005), AKH does not have any developmental effects (KIM and RULIFSON 2004).

The *Akh*-expressing CC cells act as glucose sensors. Targeted ablation of the CC cells led to decreased hemolymph glucose levels, and this phenotype could be partially reversed by ubiquitous *Akh* expression under heat shock control. Under starvation conditions, CC cell-ablated larvae showed a reduction in circulating glucose that was faster than wild type, implicating that they could not mobilize energy stores normally (KIM and RULIFSON 2004). In addition, under starvation conditions, CC cell-ablated adults had decreased mobility which also reduces energy usage, as a result, CC cell ablation led to increased starvation resistance ability (ISABEL *et al.* 2005; KIM and RULIFSON 2004).

The fat body in Drosophila is functionally analogous to both mammalian adipose tissue and liver (CANAVOSO *et al.* 2001). The *Akh* receptor (*Akhr*) is expressed strongly in the fat body. *Akhr* mutants have increased body fat

accumulation, higher carbohydrate storage, and greater starvation resistance, consistent with a role of AKH in metabolic control (BHARUCHA *et al.* 2008).

Neuropeptide F (NPF) peptides are highly conserved invertebrate homologs of vertebrate neuropeptide Y. All of the identified insect NPFs are 36 amino acid peptides with the consensus (A/L)R(P/L)RF sequence at their C-termini (BROWN *et al.* 1999; HUANG *et al.* 1998; SPITTAELS *et al.* 1996). Drosophila NPF (dNPF) was first detected by radioimmunoassay with an antiserum developed against a gut peptide from the corn earworm, *Helicoverpa zea* (BROWN et al. 1999). dNPF is predominantly expressed in two pairs of cells in the protocerebral region of the brain and in many endocrine cells in the midgut. In larvae, two pairs of dNPF expressing brain neurons arborize extensively throughout the brain lobes and extend into the ventral nerve cord (BROWN *et al.* 1999; SHEN and CAI 2001). The larval dNPF neuronal circuit may be modified by the presence of sugar/sweetener (SHEN and CAI 2001). At the adult stage, *npf* expression is sex- and clock-controlled, and male-specific *npf* expression is downstream of the *transformer* and *fruitless* genes (LEE *et al.* 2006).

NPF function in Drosophila is similar to its mammalian homolog NPY, in that it regulates food intake and food selection (STANLEY and LEIBOWITZ 1985). Overexpression of *npf* or its putative receptor, *npfr1*, led to prolonged feeding, and the larvae were less likely to reject noxious food, while down-regulation of *npf* or *npfr* had the opposite effects (WU *et al.* 2003; WU *et al.* 2005). dNPF and dNPFR1 also regulate the sensitivity to ethanol sedation in Drosophila (WEN *et al.* 2005).

Short Neuropeptide F Peptides (sNPFs): The Drosophila *sNPF* gene was cloned by PCR based on a predicted neuropeptide sequence in the Drosophila genome (HEWES and TAGHERT 2001; LEE *et al.* 2004). In Drosophila, the *sNPF* gene encodes four peptide sequences. Two of them (*sNPF1* and *sNPF2*) share a conserved C-terminal –LRLRFa motif, which is homologous to the sNPFs identified in the Colorado potato beetle. The other two *sNPFs* (*sNPF3* and *sNPF4*) share a C-terminal –RLRWa sequence (CAZZAMALI and GRIMMELIKHUIJZEN 2002; HEWES and TAGHERT 2001; SPITTAELS *et al.* 1996). Sequence analysis showed that Drosophila sNPF does not have a vertebrate homolog. Therefore, dNPF is considered to be the only Drosophila homolog of mammalian NPY (LEE *et al.* 2004).

In situ hybridization and immunostaining revealed that *sNPF* mRNA and the processed peptides, sNPF1 and sNPF2, are all expressed primarily in the nervous system (CNS and sensory neurons in the PNS) throughout development, beginning at embryonic stages 14-16 (JOHARD *et al.* 2009; LEE *et al.* 2009; LEE *et al.* 2004). In feeding larvae, *sNPF* is expressed in selected neurons in the brain lobes, the Kenyon cells in the mushroom bodies, and in neurons in the subesophageal ganglion and the thoracic and abdominal segments of the ventral nerve cord. In adults, strong expression was detected in the medullar neurons and the mushroom body calyx, peduncle, and lobes (JOHARD *et al.* 2009; LEE *et al.* 2004). CNS sNPF-expressing neurons send projections to the midgut, consistent with its role in regulating food intake (VEENSTRA *et al.* 2008).

Research on the functions of the sNPF peptides has focused on their roles in feeding and growth. In both feeding larvae and adults, over-expression of sNPF led to

increased feeding and larger flies. Down-regulation of *sNPF* expression led to decreased feeding. Interestingly, overexpression of sNPF in non-feeding wandering 3rd instar did not lead to prolonged feeding, as was observed following a similar manipulation of dNPF expression, suggesting different roles of sNPF and dNPF in the regulation of larval food intake (LEE *et al.* 2004; WU *et al.* 2003). Recent research suggests linkage of sNPF with the insulin signaling pathway in growth regulation (LEE *et al.* 2009; LEE *et al.* 2008). The sNPF neurons send projections close to the IPCs, which express the sNPF receptor, indicating that the IPCs are likely targets of sNPF. This prediction was supported by neuronal overexpression and down-regulation of sNPF, which increased and decreased *dilp2* levels in the IPCs, respectively. Expression of *dilp1* is also positively regulated by sNPF (LEE *et al.* 2008). Regulation of *dilp* mRNA levels was achieved by mature sNPF1 and sNPF2, the two known active products of pro-sNPF, through extracellular signal-related kinase (ERK)-mediated *dilp* transcription (LEE *et al.* 2009; LEE *et al.* 2008). In Drosophila, a receptor for the sNPFs was identified based on a survey of the G protein-coupled receptors in the Drosophila genome and heterologous expression in the Chinese hamster ovary cells (HEWES and TAGHERT 2001; MERTENS *et al.* 2002). RT-PCR revealed that the receptor was expressed in the brain, consistent with the function of its ligand, sNPF, in regulating feeding behavior (MERTENS *et al.* 2002).

1.2 Peptides controlling learning, memory and addiction

Amnesiac (AMN) was first described in 1979 in a screen for memory mutants in Drosophila (QUINN *et al.* 1979). The *amn*^{1} mutant showed normal learning ability

but defective longer term memory. Later, *amn* was defined as encoding a neuropeptide homologous to vertebrate pituitary adenylyl cyclase-activating peptide (PACAP), which activates the cAMP pathway in vertebrate cells (Feany and Quinn 1995). In addition to its function in memory formation, *amn* is also involved in the control of ethanol sensitivity; the ethanol-sensitive mutation *cheapdate* (*chpd*) is an *amn* allele (MOORE *et al.* 1998). The regulation of adult memory and ethanol sensitivity by *amn* is distinct both temporally or spatially: the reduced ethanol sensitivity in *amn* mutants was reverted by heat-shock inducible (ubiquitous) expression of *amn* (MOORE *et al.* 1998), however, the memory defects could only be rescued by UAS-amn^{+} driven by Gal4 containing P-element (amn^{28A}) and not by heat-shock induced *amn* expression (DEZAZZO *et al.* 1999).

The patterns revealed by immunostaining using antibodies generated specifically to AMN, and also by two other enhancer-trap lines, amn^{chpd} and $amnc^{651}$, showed that AMN is preferentially expressed in two large neurons, the dorsal paired medial (DPM) neurons. The DPM neurons extensively innervate the mushroom bodies (MB), one of the major centers involved in olfactory associated learning. Release of AMN from the NPM neurons is critical for olfactory learning in Drosophila (WADDELL *et al.* 2000).

1.3 Circadian rhythm regulatory peptide

Drosophila pigment dispersing factor (PDF) is one member of the octadecapeptide pigment-dispersing hormone (PDH) family. It was first identified and characterized in the fiddler crab *Uca pugilator* and later in insects (RAO *et al.* 1987;

RAO and RIEHM 1988; RAO *et al.* 1985). In 1993, two separate research groups performed the immunostaining with antiserum raised against the crustacean PDH (β-PDH) in Drosophila and described the distribution of PDF neuronal circuits (HELFRICH-FORSTER and HOMBERG 1993; NASSEL *et al.* 1993). The expression of PDF in Drosophila is strong in eight cells at the anterior base of the medulla, one of the optic lobe neuropiles. A group of four neurons (PDFCa neurons) send processes to the calyces of the mushroom bodies. The other four cells (PDFMe neurons) send processes that are distributed around the medulla and also send axons to the contralateral medulla. Strong PDF expression is also seen in six cells located at the ventral midline of the abdominal ganglia (HELFRICH-FORSTER and HOMBERG 1993; NASSEL *et al.* 1993). The expression pattern of the *Pdf* gene as revealed by anti-Drosophila PDF antiserum, *Pdf*-Gal4 and *in situ* hybridization is very similar to that of anti-β-PDH immunostaining (PARK and HALL 1998; PARK *et al.* 2000; RENN *et al.* 1999).

PDF in Drosophila does not have any known function in pigmentation, and instead functions as an important circadian signal. The four PDFMe neurons are a subpopulation of the major circadian pacemaker, the lateral neurons (LNs), indicating the role of PDF in circadian regulation (NASSEL *et al.* 1993). *Pdf* mutants, or animals in which the PDF neurons were ablated, can be entrained to light-dark cycles but they eventually lose rhythmic activity under constant darkness (LIN *et al.* 2004; RENN *et al.* 1999). The PDF receptor (PDFR, or *groom-of-pdf*) is encoded by CG13758. The mutant phenotype of *Pdfr* mimics that of the *Pdf* mutant (HYUN *et al.* 2005; LEAR *et al.* 2005).

Although PDF has been defined as a major neurotransmitter in circadian regulation, its expression in the cell body does not change throughout the day. Only the axon terminals show oscillating PDF protein levels (PARK and HALL 1998; PARK *et al.* 2000). PDF is a downstream factor of the clock genes, and it is controlled separately by different clock genes. The expression of PDF is controlled by CLOCK and CYCLE at both a transcriptional and translational level only in a subset of the *Pdf* expressing LN neurons, the small LN neurons. Two other clock genes, *period* and *timeless*, only affect PDF oscillation at the axon terminal (PARK and HALL 1998; PARK *et al.* 2000).

1.4 Peptides controlling development and metamorphosis

Prothoracicotropic hormone (PTTH): The existence of prothoracicotropic hormone was noted as early as 1922 as a brain factor that regulates metamorphosis in insects (KOPEC 1922). Seventy years later, PTTH peptide was first isolated from the silkworm, *Bombyx mori*, and its structure was defined as a dimer of two almost identical subunits linked by disulfide bonds (KATAOKA *et al.* 1991). Later on, the functions of PTTH in the control of development and metamorphosis and circadian rhythms were studied extensively in several species of Lepidoptera (KAWAKAMI *et al.* 1990; SAUMAN and REPPERT 1996) .

A Drosophila PTTH-like hormone was purified biochemically and analyzed for its biological activity in activating the release of ecdysteroid from the PG in 1997 (KIM *et al.* 1997). Although the expression pattern of the peptide subunits were similar to Lepidoptera—both are expressed in a pair of central brain neurons that

innervate the ecdysone-producing prothoracic gland (PG) (KAWAKAMI *et al.* 1990; KIM *et al.* 1997)—neither has significant amino acid sequence homology to the lepidopteran PTTH (KIM *et al.* 1997). Ten years later, in 2007, another putative Drosophila PTTH-like hormone was identified based on a homology search of the published Drosophila genomic sequence with the leopidopteran PTTH sequences (MCBRAYER *et al.* 2007). The proposed Drosophila PTTH (DmPTTH) is encoded by *CG13687*, and the predicted peptide product contain conserved residues when compared with the lepidopteran PTTH (MCBRAYER *et al.* 2007). However, a reduced ecdysteroid peak was still observed at the white prepupal stage in *DmPtth* neuron-ablated animals, suggesting the existence of other factors that also contribute to the regulation of ecdysteroid production or release from the PG (MCBRAYER *et al.* 2007). The PTTH-like peptide identified by Kim *et al.* (1997) may be one such factor.

In situ hybridization for *DmPTTH* and enhancer-trap Gal4 *DmPTTH* lines revealed restricted expression in two pairs of brain neurons, similar to the pattern observed for the lepidopteran PTTH (KAWAKAMI *et al.* 1990; MCBRAYER *et al.* 2007). *DmPtth* mRNA expression was detectable at stage 17 in embryos and reached its maximum level in wandering 3rd instar larvae (MCBRAYER *et al.* 2007). PTTH regulates the production and secretion of the steroid hormone ecdysone from the PG (TRUMAN 2006), and targeted ablation of the *DmPtth*-producing neurons caused decreased levels of ecdysteroid, prolonged duration of feeding in larvae, delayed onset of metamorphosis, and in turn, bigger flies (MCBRAYER *et al.* 2007). The receptor for DmPTTH, Torso, is specifically expressed in the larval PG. It was proposed that DmPTTH is released to the PG, where it acts through its receptor Torso, to stimulate

the production of ecdysteroid to coordinate molting, metamorphosis, and other related biological processes (REWITZ *et al.* 2009).

Eclosion hormone (EH) in Drosophila is a 73-amino-acid peptide. It was identified in 1993 by using a probe designed based on the coding sequence of the *Manduca EH* gene (HORODYSKI *et al.* 1993). *In situ* hybridization with a Drosophila *Eh* probe, immunostaining with an antiserum against *Manduca* EH, and later reporter gene expression with an EH promoter-Gal4 transgene, all showed that Drosophila *Eh* is expressed in a single pair of ventromedial cells in the larval brain lobes. The EH neurons send axons to the CC of the ring gland and also through a medial tract along the ventral nerve cord. EH is released into the CNS and into the hemolymph through the terminal projections (HEWES and TRUMAN 1991; HORODYSKI *et al.* 1993; MCNABB *et al.* 1997; SIEGMUND and KORGE 2001).

Targeted ablation of the EH neurons led to ecdysis defects at the larval and adult stages. The EH-ablated animals also were insensitive to treatment with ecdysis-triggering hormone (ETH), another important factor in the regulation of ecdysis behavior (MCNABB *et al.* 1997). However, about a third of the EH neuron-ablated animals developed into normal adults, indicating that EH is important but not absolutely necessary for the initiation of ecdysis. A proportion of the EH cell knockout adults showed defects in post-eclosion events, such as wing expansion and subsequent hardening of the cuticle (MCNABB *et al.* 1997).

Ecdysis triggering hormone (ETH) was first identified and functionally described in *Manduca* (EWER *et al.* 1997; ZITNAN *et al.* 1996). The *Manduca ETH* gene encodes three peptides, preecdysis-triggering hormone (PETH), ETH, and ETH-

associated peptide (ETH-AP) (ZITNAN *et al.* 1999). The Drosophila *ETH* gene was then identified by BLAST searching the Drosophila genomic database with the *Manduca* PETH amino acid sequence. Like its *Manduca* homolog, the Drosophila *ETH* gene also encodes three peptides, DrmETH1, DrmETH2 and DrmETH-AP, but none are homologous to *Manduca* ETH-AP (PARK *et al.* 1999).

Expression of ETH in both Drosophila and *Manduca* is restricted to the Inka cells, which are endocrine cells associated with the trachea (PARK *et al.* 2002; ZITNAN *et al.* 1999). In Drosophila, there are a total of 14 Inka cells located along the two major dorsal trachea trunks, with one cell (on each side) on each of the primary tracheal branches at metamers 1 and 4-9. *ETH* expression is detected in both larval and adult stages (PARK *et al.* 2002), and ETH expression levels fluctuate during development and are correlated with circulating ecdysone levels (GAUTHIER 2008). Immunostaining and labeling of Inka cells with an *ETH*-EGFP transgene showed that peak ETH expression was high in larvae at the double vertical plates (dVP) stage (25-30 minutes prior to ecdysis) and dropped sharply afterwards (10 minutes after dVP), indicating that ETH is depleted immediately prior to ecdysis, consistent with the role in triggering ecdysis behaviors (PARK *et al.* 2002).

To examine functions of ETH genetically in Drosophila, *ETH* mutants were generated by imprecise excision of a *P*-element that was inserted close to the *ETH* gene. Almost all (98%) of the mutants failed to complete normal ecdysis at the 1st to 2nd instar transition (PARK *et al.* 2002). Injection of ETH triggered premature ecdysis behavior in wild-type pharate adults and larvae, and timely injection of ETH into *ETH*

mutants rescued ecdysis behavior (PARK *et al.* 2002; PARK *et al.* 1999). These findings showed that ETH is an essential factor in controlling ecdysis in Drosophila.

CG5911 was identified as the ETH receptor. Cloning of the gene was based first on a survey of G protein-coupled receptors in the Drosophila genome (HEWES and TAGHERT 2001; IVERSEN *et al.* 2002), several of which were then expressed in Chinese hamster ovary (CHO) cells. CHO cells that expressed *CG5911* were stimulated by low concentrations (3.7×10^{-8} M) of ETH (IVERSEN *et al.* 2002).

Crustacean cardioactive peptide (CCAP) is a nonapeptide, that was first identified as a cardioaccelerator from the shore crab *Carcinus maenas* (STANGIER *et al.* 1987). However, before the identification of CCAP in Crustaceae, the peptide was isolated from *Manduca* (but not sequenced) and named as cardioacceleratory peptide 2a (CAP2a) (TUBLITZ and TRUMAN 1985a; TUBLITZ and TRUMAN 1985b). Later, after the amino acid sequence of CAP2a was determined, it was found to be identical to CCAP was therefore re-named as *Manduca* CCAP (CHEUNG *et al.* 1992; STANGIER *et al.* 1987). The *Manduca CCAP* gene was cloned and its expression pattern was characterized in 2001 (LOI *et al.* 2001). Two years later, in 2003, the Drosophila *CCAP* (*DmCCAP*) gene was identified (PARK *et al.* 2003).

Drosophila CCAP is expressed in a restricted pattern in the CNS that was revealed by *in situ* hybridization, immunostaining and the *CCAP*-Gal4 driver, which contains the Gal4 coding sequence under the control of *CCAP* promoter. The CCAP neurons include 2 pairs of neurons in the brain lobes, 3 pairs in the thoracic segments, four pairs with strong signals and seven pairs with weak expression in the abdominal

ganglia. The expression pattern remains unchanged throughout post-embryonic development (PARK *et al.* 2003).

In *Manduca*, CCAP was implicated in the control of ecdysis behavior (GAMMIE and TRUMAN 1997). Drosophila CCAP seems dispensable for larval and adult ecdysis but is essential for pupal ecdysis (PARK *et al.* 2003). When the CCAP neurons were genetically ablated, most of the resulting larvae went through ecdysis successfully, although they displayed extended pre-ecdysis behavior and the duration of the ecdysis process was longer than in control animals (PARK *et al.* 2003). At the pupal stage, however, most of the CCAP neuron-ablated animals died after weak unsuccessful pupal ecdyses, and many failed to initiate pupal ecdysis altogether (PARK *et al.* 2003). The CCAP neuron-ablated adult escapers showed defective post-ecdysis behavior, resulting in unexpanded wings and an external cuticle that failed to be sclerotized and melanized. The adult post-ecdysis defect was later shown to be caused by the failure of these animals to secrete the tanning hormone, bursicon (BURS), into the blood. BURS is expressed by a subset of the CCAP neurons, and ablation of CCAP neurons therefore led to loss of BURS-producing cells (DEWEY *et al.* 2004; PARK *et al.* 2003). In addition to its role in ecdysis control, CCAP in Drosophila also has a cardioactive property, similar to its crustacean homolog (DULCIS *et al.* 2005). *CG6111*, which encodes a G protein-coupled receptor, was identified as the CCAP receptor (CAZZAMALI *et al.* 2003; HEWES and TAGHERT 2001).

Bursicon (BURS) is a hormone that functions after adult ecdysis (eclosion). After adult eclosion is completed, release of BURS into the hemolymph initiates wing expansion behavior and hardens the soft, new cuticle. The peptide was identified in

1965 and was named after its biological function ("tanning" in Greek) (FRAENKEL and HSIAO 1965). The properties of the protein were defined soon after (FRAENKEL *et al.* 1966), but it was many years before the structure was identified. Using a partial BURS peptide sequence identified from the cockroach *Periplaneta americana* by Honegger et al. (HONEGGER *et al.* 2002), a BLAST search of the Drosophila genome led to the identification of the Drosophila *burs* gene, *CG13419* (DEWEY *et al.* 2004), which was later defined the Burs α-subunit (*Bursα*) (MENDIVE *et al.* 2005). Bursα does not have any bursicon bioactivity by itself, indicating that other factors may interact with Bursα to initiate the biological process. Re-examination of previously purified Burs peptide preparations from the cockroach *Periplaneta americana* by Honegger et al. (HONEGGER *et al.* 2002) revealed the existence of partner of BURSα (*pBurs*, a.k.a. *Bursβ*) (encoded by CG15284) (LUO *et al.* 2005; MENDIVE *et al.* 2005). BURSα and pBURS form a bioactive heterodimer (BURS) (LUO *et al.* 2005; MENDIVE *et al.* 2005).

Immunostaining in several species of insects including Drosophila with an antiserum raised against a fragment of the *Periplaneta americana* BURS peptide showed co-localization of BURS and CCAP in selected CNS neurons (HONEGGER *et al.* 2002). BURSα and pBURS coexpression is restricted to the four pairs of bilateral neurons within the VNC BURS pattern (LUO *et al.* 2005). BURS but not pBURS expression is detected at the subesophageal and posterior abdominal neurons (LUO *et al.* 2005). In Drosophila, co-expression of BURSα and CCAP is mainly in the 28 neurons (14 on each side) located in the abdominal ganglia. No BURS (BURSα and pBURS) expression is observed in the CCAP-expressing brain lobe neurons and two

pairs of CCAP neurons in the first thoracic segment. Therefore, targeted CCAP cell ablation led to the disappearance of most of the BURS expressing cells as well (DEWEY *et al.* 2004).

Careful examination of neuronal activity and also studies with genetic mosaics of two different sets of BURS-expressing neurons, the abdominal ganglion (B_{AG}) and the subesophageal ganglion (B_{SEG}) groups, revealed distinct functions: the B_{SEG} neurons project extensively throughout the CNS, and release of BURS from the B_{SEG} initiates post-ecdysis behaviors, such as air ingestion. BURS release from the B_{SEG} also promotes secondary BURS release from the B_{AG} neurons to drive wing expansion and tanning processes (LUAN *et al.* 2006; PEABODY *et al.* 2008). In addition to the post-eclosion processes, BURS release is required for the initiation of apoptosis of the B_{AG} neurons and the wing epithelial cells after successful wing expansion (NATZLE *et al.* 2008; PEABODY *et al.* 2008).

Expression levels of *burs*α, *pburs* and their receptor DLGR2 (encoded by the *rickets* gene) in Drosophila are correlated. All are low during the larval stages and increase during pupal development, with peak expression of all three at the pharate adult stage (BAKER and TRUMAN 2002; LUO *et al.* 2005). BURS is released from axons of the BURS expressing neuons within 1 hour after adult eclosion (ZHAO *et al.* 2008).

2. ECDYSIS BEHAVIOR OF DROSOPHILA

The life cycle of an insect includes several molts, during which a new cuticle is produced underneath each old one. At the end of each molt, the animal has to shed the

remains of the old cuticle and continue the growth in the new cuticle. The process of shedding the old cuticle is called ecdysis. Ecdysis is a stereotyped physiological and behavioral set of events. Initiation of each step of ecdysis is precisely timed and is regulated mainly by the release of peptide hormones, such as EH, ETH, CCAP and BURS.

2.1 Description of the ecdysis process

Larval ecdysis: Park and colleagues carefully examined the sequence of the larval ecdysis events and provided a detailed timeline (PARK *et al*. 2002). At about 1 hr before ecdysis, new mouth hooks form, and about 30 minutes later new vertical plates appear, forming the "double vertical plates" (dVP) stage. Also during this 1 hr, the old tracheal linings separate from the new ones, the old tracheae collapse, and the new tracheae are inflated. Pre-ecdysis behavior starts about 15 minutes after dVP and begins with anterior-posterior contractions, followed later by rolling contractions (squeezing). These series of movements loosen the connections between the old and new cuticles and mouthparts. After this, about 25 minutes after dVP, ecdysis behavior begins. The animal plants the old mouthparts in the food substrate and performs a series of forward and backward thrusts to escape from the old cuticle (PARK *et al.* 2002). The timely onset of each of the above-described events is critical for a successful ecdysis, and disruption can lead to lethality. The dead animals resulting from failed exdyses show a "buttoned-up" phenotype and bear two sets of mouthparts, and the old cuticle and tracheal linings are retained (PARK *et al.* 2002).

Pupal ecdysis: After larval development is completed, larvae stop moving and contract into the shape of a pupa. This is called pupariation, and it is one of the earliest events at the onset of metamorphosis. During this period, adult-specific structures begin a period of rapid development, and several larval tissues, such as the salivary gland and muscles, are destroyed. During the ensuing few hours, another peak of ecdysone triggers the onset of pupal ecdysis (at 12 hours after pupariation), during which the new pupal cuticle is detached from the puparium and the animal takes a more adult shape.

Pupal ecdysis consists of three stages: pre-ecdysis, ecdysis and post-ecdysis. Pre-ecdysis lasts about 10 minutes and is marked by anteriorly directed contractions that separate the new cuticle form the larval cuticle (which later becomes the puparium case). At the onset of ecdysis, the head swings from side to side, and this is accompanied by forward-directed abdominal contractions. Immediately following the onset of ecdysis, the adult head pouch is everted out of the thoracic region (head eversion). This process lasts about 15 minutes. Following this is the post-ecdysis process, which can last up to 1 hour. During post-ecdysis, the abdomen displays peristaltic contractions toward the posterior and the extension of the legs along the abdomen is completed (BAINBRIDGE and BOWNES 1981; KIM *et al.* 2006; WARD *et al.* 2003). The disruption of pupal ecdysis can lead to an incompletely everted head, with the thorax shifted much more to the anterior part of the puparium, the larval mouthparts remaining attached, and the legs and wings only partially extended (PARK *et al.* 2003).

Adult ecdysis and post-ecdysis: Adult ecdysis is also known as eclosion. About 1 hour prior to eclosion, which is called pre-eclosion, the pharate adult moves toward the anterior end of the pupal case. The head and a transitory head structure called the ptilinum are expanded. The ptilinum is pressed against the operculum, the flat part of the puparial case that covers the head, and the resulting pressure forces the operculum to open. After the seam of the operculum opens, ecdysis is initiated. This involves a series of movements including head thrusts, thoracic contractions, and abdominal contractions to make the fly move forward. After the head is out of the pupal case, 6-7 alternated abdominal contractions and body extensions propel the new fly out of the puparium (MCNABB *et al.* 1997). Following a successful adult ecdysis, the newly emerged fly has tightly folded wings and a soft and white cuticle. The animal has to go through a series of post-ecdysis processes, including wing expansion and cuticle tanning, to complete its transformation to a mature adult. During wing expansion, abdominal contractions and air ingestion increase the internal pressure to drive blood into the expanding wings. Wing expansion is usually finalized within 1 hour after adult eclosion. The post-ecdysis process is concluded by tanning, through which the soft cuticle is sclerotized (FRAENKEL *et al.* 1984; PEABODY *et al.* 2008; ZHAO *et al.* 2008).

The phenotypes resulting from defective adult ecdysis include extended pre-ecdysis and ecdysis processes and un-expanded or partially-expended wings. The animals also fail to tan properly, showing a juvenile lighter coloration, sometimes with dimples on the dorsal thorax and crossed postscutellar bristles due to incomplete

thorax expansion and hardening (MCNABB *et al.* 1997; PEABODY *et al.* 2008; ZHAO *et al.* 2008).

2.2 Hormonal control of the ecdysis process:

Based on current understanding, the model of the hormonal regulatory cascade for Drosophila larval ecdysis can be divided into the following five steps (CLARK *et al.* 2004; EWER 2005; EWER *et al.* 1997; EWER and REYNOLDS 2002; KIM *et al.* 2006): Step 1: At the end of each molt, a declining 20HE titer renders the Inka cells competent for ETH secretion and also responsive to molecular or environmental signals. A small amount of ETH is released into the hemolymph at the end of this stage. Step 2: Low levels of circulating ETH turn on the pre-ecdysis program. When the concentration of ETH from this first release reaches a certain level, it activates the release of EH from the ventromedial neurons both within the CNS and into the blood. Step 3: Circulating EH acts on the Inka cells, increasing intracellular levels of cGMP to trigger a massive release of ETH. EH released within the CNS also activates the secretion of CCAP from CNS neurons (into CNS and hemolymph). Step 4: The large amount of ETH released at step 3 will activate programs of late phase pre-ecdysis and together with EH stimulates more secretion of CCAP. Step 5: CCAP then inhibit the pre-ecdysis process and initiates the ecdysis motor program. At this time, the animal escapes from the old cuticle and continues the next cycle of growth.

SUMMARY

As reviewed in this chapter, there are over 20 known peptide hormones that are expressed in the CNS of Drosophila, and they are involved in many important biological processes. One additional peptide hormone, ETH, is expressed by the endocrine Inka cells and is critical for the ecdysis process. Inka cells are located in the isolated epitracheal glands. However, our knowledge about factors that regulate the expression or secretion of each of these peptides is very limited. To identify more endocrine regulatory factors, we performed a splice-trap screen for genes that are expressed in CNS peptidergic neurons as described in Chapter 2. In addition, we showed that the gene *alan shepard* (*shep*) is expressed specifically in peptidergic neurons and involved in metamorphic remodeling of neurites. In chapter 3, I describe an enhancer-trap and splice-trap screen I performed for genes that are expressed in the Inka cells and the epitracheal glands. *Taiman* (*tai*), an ecdysone receptor coactivator, was one of the genes identified, and we showed that *tai* is a key regulator of *ETH* expression.

CHAPTER II

A Drosophila splice trap screen for genes controlling neuroendocrine cell development and function

ABSTRACT

Peptidergic neurons display a suite of specializations that support high-level synthesis and neuroendocrine, or paracrine, secretion of neuropeptides. In an effort to identify novel factors important for the development and function of this class of neurons, we screened a total of 545 splice-trap lines for peptidergic neuron-specific expression. We identified 28 insertions in 25 genes that drive reporter gene expression in a large population of peptidergic neurons that is characterized by high-level expression of the amidation enzyme peptidylglycine-α-hydroxylating monooxygenase (PHM) and the peptidergic neuron differentiation factor *dimmed* (*dimm*). Many of these genes are also expressed in neurons that produce the neuropeptides bursicon, crustacean cardioactive peptide (CCAP), leucokinin, and Drosophila insulin-like peptide 2, and the prohormone convertase furin-1. Four lines, with insertions in the putative mRNA binding factor *alan shepard* (*shep*), the ecdysone response gene *brain tumor*, the metabolic regulatory gene *6-phosphofructo-2-kinase*, and the transcription factor *scribbler*, display broad and peptidergic neuron-restricted expression in the entire CNS or the ventral nerve cord. *BG00836*, an insertion in an intron of *shep*, drives reporter expression almost exclusively in peptidergic neurons in the CNS and in a pattern very similar to that of PHM and *dimm*. A second insertion in *shep* displays a similar pattern but with additional low-level expression throughout the CNS. Homozygous *BG00836* adults showed defects in wing expansion, decreased resistance to starvation, and reduced axon outgrowth during metamorphic remodeling of the CCAP/bursison neurons. However, the wing expansion defects and starvation sensitivity were not observed in *BG00836*/deficiency

hemizygotes nor following RNA interference (RNAi) to *shep*, and were likely the result of genetic background effects. In contrast, the *BG00836* hemizygotes and *shep* RNAi animals displayed markedly reduced outgrowth of the adult CCAP/bursicon peripheral axons. These findings suggest a general role for *shep* in the regulation of the development of peptidergic neurons. Other genes identified in this screen are likely to play additional important roles in peptidergic neuron development and signaling.

INTRODUCTION

Neuropeptides and peptide hormones are short peptide transmitters that regulate many important processes in animals, such as learning and memory, body weight homeostasis, circadian rhythms, and addiction (FEANY 1996; HILLEBRAND *et al.* 2002; NESTLER 2000; RENN *et al.* 1999). They are produced by neurons that are specialized to express neuropeptide pro-hormones, process them through the Golgi apparatus, and package them in secretory granules for regulated secretion. Each of the steps in the neuropeptide secretory pathway is subject to regulation (SOSSIN *et al.* 1989), and defects in these processes can have profound effects on neuropeptide signaling (MILLER *et al.* 2003). In addition, many peptidergic neurons display neuroendocrine characteristics, including the production, storage, and secretion of very large amounts of neuropeptides (HEWES *et al.* 2003). These cellular features are crucial for the operation of neuroendocrine systems, yet we are only beginning to understand how neuropeptidergic cell properties differentiate and are regulated. As a first step toward addressing these questions, it will be important to identify the genes involved.

Drosophila is an excellent genetic model for exploring aspects of peptidergic neuron biology. Many Drosophila neuropeptides share structures and functions with analogous vertebrate neuropeptides. For example, adipokinetic hormone (AKH) is structurally related to mammalian glucagon, and they are both involved in the regulation of blood glucose levels (KIM and RULIFSON 2004; LEE and PARK 2004). Seven *Drosophila* insulin-like peptides (DILPs) have also been identified, and like their vertebrate homologs they regulate growth and glucose metabolism (BROGIOLO *et*

al. 2001; IKEYA *et al.* 2002; ZHANG *et al.* 2009). There is also substantial homology among neuropeptide receptors (HEWES and TAGHERT 2001), in the secretory granule exocytosis machinery (BURGOYNE and MORGAN 2003), and in the enzymes important for neuropeptide processing (SIEKHAUS and FULLER 1999). Thus, the general mechanisms for neuropeptide processing, packaging, secretion and signaling are highly conserved. With the powerful tools available for the manipulation of Drosophila peptidergic neurons (HEWES *et al.* 2006; SHAKIRYANOVA *et al.* 2005; ZHAO *et al.* 2008), these mechanisms are amenable to detailed genetic analysis.

In this study, we utilized a reverse genetics strategy, based on patterns of gene expression, to identify factors important for neuropeptidergic cell development and function. This approach is based on the fact that genes with cell type- or tissue-specific expression often fall into one of two classes. Some act as critical differentiation factors for a specific cell type or tissue. Examples of this class include *MyoD* in skeletal muscle (DAVIS *et al.* 1987; WRIGHT *et al.* 1989) and *eyeless*/*Pax6* in the eye (HALDER *et al.* 1995; HILL *et al.* 1991). The other class of genes (e.g., photoreceptor proteins in the eye) performs tissue-specific functions. Based on this simple rationale, expression-based approaches have aided in the identification of genes with peptidergic cell-specific functions. For example, the *dimmed* (*dimm*) transcription factor was identified based on the expression pattern of the *c929* enhancer trap line (HEWES *et al.* 2003). In the CNS, the *c929* insertion drives reporter gene expression that is restricted to a diverse population of ~300 peptidergic neurons (GAUTHIER and HEWES 2006; HEWES *et al.* 2003; PARK *et al.* 2008b). In larvae, this pattern is an accurate reflection of *dimm* expression (HEWES *et al.* 2003; PARK *et al.* 2008b), and

reverse genetic studies demonstrated a key role for the DIMM transcription factor in controlling the expression of selected neuropeptides and enzymes that are critical for neuropeptide biosynthesis. One notable target is peptidylglycine-α-hydroxylating monooxygenase (PHM), which is essential for the C-terminal amidation of many Drosophila neuropeptides (EIPPER *et al.* 1992; JIANG *et al.* 2000). PHM expression is regulated by DIMM in both differentiating and mature cells (GAUTHIER and HEWES 2006; HEWES *et al.* 2006; HEWES *et al.* 2003; PARK *et al.* 2008a), and consequently, DIMM and PHM are extensively colocalized markers that essentially define a single population of peptidergic neurons. Several other factors with expression patterns that are either enriched for peptidergic neurons or that are exclusively peptidergic include other peptide biosynthetic enzymes, neuropeptide precursors, and transcription factors important for peptidergic neuron differentiation (ALLAN *et al.* 2003; HAYFLICK *et al.* 1992; PARK *et al.* 2004; PARK *et al.* 2008b; SIEKHAUS and FULLER 1999). These findings suggest that there may be additional genes to be identified that display peptidergic neuron-restricted expression and that play key roles in peptidergic cell differentiation, neuropeptide expression and peptidergic cell signaling.

In the present study, we screened through a collection of 545 genomically mapped splice-trap insertions for genes with peptidergic neuron expression. We confirmed peptidergic cell expression for 28 insertions (in 25 genes) by colocalization of reporter gene expression and anti-PHM immunoreactivity. We obtained more detailed mapping of the patterns by double-labeling with more restricted peptidergic markers, including crustacean cardioactive peptide (CCAP), Drosophila insulin-like peptide 2 (DILP2), furin-1, leucokinin (LK), and –Rfamide-containing peptides

(BROGIOLO *et al.* 2001; CHIN *et al.* 1990; HAYFLICK *et al.* 1992; PARK *et al.* 2003). Six insertions produced expression patterns that largely mirrored PHM. One of these, *BG00836*, drove reporter gene expression in a pattern of brain lobe and ventral nerve cord (VNC) neurons that recapitulated the pattern of PHM and *dimm* expression. Although the *BG00836* insertion (in homozygotes) caused defects in wing expansion and resulted in reduced starvation resistance in adults, we did not observe these phenotypes in *shep BG00836*/deficiency transheterozygous or *shep* RNA interference (RNAi) animals, suggesting that these phenotypes may be the result of genetic background effects. However, *shep BG00836*/deficiency and $shep^{RNAi}$ animals displayed markedly reduced outgrowth of adult CCAP/bursicon peripheral axons during metamorphic remodeling. A SHEP::GFP protein trap line revealed ubiquitous CNS expression, and the *BG00836* reporter therefore likely detects only a subset of *shep* transcripts. Therefore, *shep* is a candidate regulator of the post-embryonic remodeling of peptidergic neurons, and possibly many other neuronal cell types, during metamorphosis.

MATERIALS AND METHODS

Fly stocks: Flies were cultured on standard cornmeal-yeast-agar media at 25°C. The splice trap (BG) lines and most other stocks were obtained from the Bloomington Drosophila Stock Center (Indiana University, Bloomington, IN). The *C522* enhancer trap line was kindly provided by K.M. Beckingham (Rice University).

Screening for CNS expression: Each BG line was crossed to *UAS-mCD8::GFP* to reveal the splice trap expression pattern. Third instar larvae were obtained from apple juice–agar egg-collection plates supplemented with yeast paste, washed briefly in saline, mounted under coverslips with 70% glycerol, and then placed at -20˚C for 30 minutes. After subsequent thawing, we observed the whole larvae by compound epifluorescence to detect GFP expression in the CNS. BG>mCD8::GFP larvae from crosses that displayed GFP fluorescence in the CNS were dissected in calcium-free saline [182 mM KCl, 46 mM NaCl, 2.3 mM $MgCl_2.6H_2O$, 10 mM 2-amino-2-(hydroxymethyl) propane-1,3-diol (Tris), pH=7.2], and processed for immunocytochemistry.

Immunocytochemistry: Immunostaining was performed as described (BENVENISTE *et al.* 1998; HEWES *et al.* 2003). After fixation for 1 hr at room temperature (RT) in 4% paraformaldehyde (PFA), 4% paraformaldehyde/7% picric acid (PFA-PA), or Bouin's fixative, primary antisera (rabbit or guinea pig) to the following proteins were used: CCAP (1:4000, PFA-PA) (EWER and TRUMAN 1996), bursicon α-subunit (1:5000, PFA/PA) (LUAN *et al.* 2006), PHM (1:750, Bouin's)

(JIANG *et al.* 2000), LK (1:500, PFA-PA) (NASSEL and LUNDQUIST 1991), DILP2 (1:50, PFA-PA) (Rulifson et al. 2002), Furin-1 (1:1000, Bouin's) (JIANG *et al.* 2000), -RFamide (PT2 antiserum) (1:2000, PFA-PA) (TAGHERT 1999), and DIMM (1:200, PFA-PA) (ALLAN *et al.* 2005). Because fixation with Bouin's destroyed the native mCD8::GFP fluorescence, we performed additional mouse anti-GFP (1:500) (Invitrogen, Carlsbad, CA) staining when Bouin's was used. The secondary antibodies were goat Cy3 or ALEXA 488 conjugates (Jackson ImmunoResearch, West Grove, PA) and were used at a 1:500 dilution. We obtained confocal z-series stacks and 2D projections using an Olympus Fluoview FV500 microscope (Olympus, Center Valley, PA).

Starvation resistance assay: Because males and females differed in their ability to resist starvation, we chose to use only virgin females. Flies were collected and kept in vials with regular food. After two days, the females were transferred onto starvation media (1.5% agar) in vials, to provide moisture but no nutrition (HARBISON *et al.* 2004), and were maintained in an incubator with a tub of water to maintain consistent humidity. We placed 10 female flies in each vial, and 80-120 animals of each genotype were used. Surviving flies were counted every few hours for the ensuing ~3 days. The BG collection was generated using an isogenic w^{1118}*; Iso2A; Iso3A* line as the background genotype (BELLEN *et al.* 2004a), so we used this line as a control for the starvation resistance assays.

RESULTS

Identification of splice-trap lines: From a screen of 545 BG insertion lines, we obtained an initial set of 38 lines that drove CNS expression of mCD8::GFP. After dissection and mounting of the CNS, we found that eight of the patterns were restricted to glial-like cells (Figure II.1), and these lines are discarded. The remaining 30 insertions drove expression in CNS neurons (Figure II.2). To determine whether the CNS expression patterns contained peptidergic cells, we crossed each of the latter 30 lines to *UAS-mCD8::GFP* and immunostained the tissues for PHM and GFP. PHM is required for C-terminal amidation of over 90% of insect neuropeptides (HEWES and TAGHERT 2001; JIANG *et al.* 2000) and therefore served as a general peptidergic cell marker. We found 28 insertions that drove expression in PHM-positive neurons (Table II.1, Figures II.3 and 4). Six of the lines (*BG00836*, *BG01610*, *BG01322*, *BG01850*, *BG02721*, and *BG02836*) all had restricted expression patterns that included many PHM positive neurons (Figure II.3). Notably, *BG00836* (an insertion in *shep*, see below) was expressed in a pattern almost identical to that of PHM (Figure II.3B). Only 8% of the *BG00836*-expressing, and very few if any of the PHM-expressing, neurons lacked expression of the other marker, and the intensities of *BG00836* and anti-PHM immunoreactivity were highly correlated. *BG01322*, an insertion in a different intron of *shep*, produced a similar pattern of reporter gene expression, although it also drove lower-level expression in many other neurons located throughout the CNS. The DIMM transcription factor drives PHM expression, and the DIMM and PHM patterns are highly synchronous (HEWES *et al.* 2003). Similarly, most of the *BG00836*-expressing neurons expressed DIMM (data not

shown). Therefore, with only a few exceptions, *BG00836*, PHM, and DIMM together mark a single population of larval peptidergic neurons. This population is characterized by high-level expression of amidated neuropeptides (HEWES *et al.* 2003; PARK *et al.* 2008a; PARK *et al.* 2008b).

Four lines, *BG01610*, *BG01850*, *BG02721* and *BG02836*, were expressed strongly and selectively in many but not all PHM neurons in the VNC (Figure II.3). *BG02721* only displayed distinct peptidergic neuron expression in the VNC; within the brain lobes, its expression was much more uniform and ubiquitous and included many glial-like cells (Figures II.2 and 3E). *BG02836* displayed strong expression in the abdominal ganglia in a pattern that largely mirrored PHM. In the brain lobes, *BG02836* displayed restricted expression in a cluster of midline protocerebral neurons (IPCs, see below) and strong expression in the mushroom bodies (Figures II.2 and 3F). The *BG01610* line drove stronger expression in many PHM-positive neurons in the VNC but also lower level expression in many midline VNC neurons, the Kenyon cells, and in diffuse neuropilar projections in the brain lobe and VNC (Figure II.3C). *BG01850* labeled the fewest PHM-positive neurons, including a subset of the PHM neurons in the VNC and a few brain neurons (Figure II.3D).

All of the other 22 lines showed co-localization with the PHM expression pattern, and the strength of reporter expression in the PHM cells was variable. Some of the lines produced very broad patterns of reporter gene expression that included most of the PHM neurons. For example, *BG00665* (Figure II.5A-B) and *BG01711* (Figure II.5C-D) were both coexpressed with PHM throughout the brain lobe and the

VNC, but there also was detectable expression in many non-PHM-positive neurons. Other lines (e.g. *BG02222*) had much more restricted expression patterns.

Splice trapped genes: When the BG element is inserted in an intron of a gene, and in the correct orientation, transcription and mRNA splicing leads to the expression of Gal4 in a pattern matching that of the native mRNA (LUKACSOVICH *et al.* 2001). This also occurs when the BG element inserts in the correct orientation in an exon of the trapped gene. Therefore, we analyzed the insertion sites for the 28 lines with expression in PHM-positive neurons (Table II.1). We found 22 lines with insertions in the correct orientation for trapping in an intron or exon of 21 genes; the *BG02820* element is inserted in the introns of two nested genes, and two genes, *alan shepard* (*shep*) and *hipk* each had two insertions. In many cases, the trapped genes display alternative splicing, and the BG element insertions may only report on the expression of a subset of the alternative transcripts (e.g. *BG00836* and *BG01322* are both inserted in *shep*, but *BG01322* labeled many more neurons). Although the expression patterns of the genes must eventually be confirmed—through analysis of mRNA and/or protein expression patterns—these genes are likely to be the source of the splice trap expression patterns for 22 of the 28 PHM-positive lines.

For five lines, we regarded the gene identifications as more tentative, and for one additional line (*BG02222*), we have not identified a candidate source gene for the splice trap expression pattern. Three of the BG insertions, representing two genes (*jim* and *CG13917*), were located in the correct orientation but upstream of the first known exon. In these cases, the splice trap expression patterns may simply reflect the

existence of yet to be identified upstream exons. Finally, we identified two insertions, *BG01610* in an intron of the *scribbler* (*sbb*) gene and *BG00476* only 4 bp upstream of *CG4860*, with unknown orientations at the insertion sites. Although the *BG00476* insertion may actually be inserted within the first exon of some longer *CG4860* transcripts, the confirmation of *CG4860* and *sbb* as the candidate source genes for these expression patterns will require the identification of the insertion orientations for the respective BG insertions.

Together, these lines reveal the putative peptidergic neuron expression patterns of 25 genes. Hereafter, we refer to each insertion as an allele of the candidate trapped gene. The genes include seven transcription factors (*Aef1*, *brat*, *CG13917*, *chif*, *jim*, *sbb*, and *tai*), two of which, *brat* and *tai*, have known roles in the regulation of transcription by the steroid hormone ecdysone (BAI *et al.* 2000; BECKSTEAD *et al.* 2005). An additional five genes (*CG8963*, *cpo*, *Dcp2*, *heph*, and *shep*) are predicted to play roles in mRNA binding and/or processing, and one gene (*ERp60*) regulates disulfide bond formation during oxidative protein folding in the ER. Seven of the genes encode factors involved in signal transduction (*CG11444*, *fz2*, *hipk*, *MYPT-75D*, *PK61C*, and *PKa-C1*), or regulation of neuronal electrical activity (*SKIP*). Two genes (*CG4860* and *Pfrx*) encode enzymes with predicted functions in the regulation of cellular catabolism. Finally, there were three genes encoding proteins of unknown functions (*CG31145*, *CG32306*, and *CG42231*). Together, these 25 genes are predicted to play a variety of roles in the regulation of peptidergic neuron development and function.

Co-expression with other neuropeptides and peptide biosynthetic enzymes: To further characterize the expression patterns of the 28 lines with neuropeptidergic cell expression, we performed double labeling for the mCD8::GFP reporter gene and six selected neuropeptidergic cell markers. These included five neuropeptides, bursicon α-subunit (BURS, Figure II.6), crustacean cardioactive peptide (CCAP, Figure II.7), Drosophila insulin-like peptide 2 (DILP2; Figure II.8), leucokinin (LK; Figure II.9), and RFamide (Figure II.10A-B), and one peptide biosynthetic enzyme, Furin-1 (Figure II.10C-F).

The most commonly co-expressed marker, in 17 lines, was CCAP (Table II.1, Figure II.7). There were varying degrees of overlap with the reporter gene, and the insertions segregated into three groups based on similarities in pattern (Figure II.7). The Group I lines, *CG8963*^{BG00665}, *CG11444*^{BG01894} and two insertions upstream of *CG13917*, *CG13917*^{BG02772} and *CG13917*$^{GT\text{-}000078}$, displayed partial colocalization with CCAP in the brain lobe and VNC (Figure II.7A). In each case, the intensity of the reporter gene expression in CCAP neurons was weak to moderate. The 10 Group II lines were defined based on expression that was restricted within the CCAP pattern to the subset of the CCAP neurons that produce a second hormone, BURS (LUAN *et al.* 2006) (Figure II.7B). These cells are recognizable based on position and the intensity of CCAP immunostaining (LUAN *et al.* 2006; ZHAO *et al.* 2008). However, we confirmed the coexpression with BURS for two of the lines, *shep*^{BG00836} and *BG02222* (Figures II.6B-D). The *BG02222* line displayed particularly notable expression in the VNC that was limited almost exclusively to the BURS neurons and a small cluster of neurons in the posterior VNC in larvae. In pharate adults *BG02222* displayed strong

expression in some non-BURS neurons in the VNC (Figure II.6C). The final set of three lines, Group III, displayed colocalization with CCAP in only a few neurons located in the brain lobes (Figure II.7C).

A total of nine insertions in eight genes displayed expression in seven bilateral pairs of midline protocerebral neurons. The insulin producing cells (IPCs) are in this location and express four out of the seven Drosophila insulin peptide genes, including DILP2, which labels all 14 cells (BROGIOLO *et al.* 2001; RULIFSON *et al.* 2002). We therefore used anti-DILP2 immunostaining to confirm colocalization in the IPCs (Figure II.8) and in the neurites leading to the heart and ring gland (data not shown). Three lines, *shep*^{BG00836}, *Pfrx*^{BG02836}, and *heph*^{BG01850}, displayed expression that was restricted to several brain lobe neurons, including moderate to strong reporter gene expression in all of the IPCs and their neuroendocrine projections (Figures II.8B-D). The *shep*^{BG01322} line also drove IPC expression. Two lines, *brat*^{BG02721} and *CG31145*^{BG00449}, displayed broader expression patterns that included some glia, and both also drove moderately strong transgene expression in the IPCs and their projections (Figures II.8E-F). The *CG31145*^{BG00449} pattern included strong expression in the endocrine prothoracic gland cells. The final three lines (Table II.1; *fz2*^{BG01711}, *jim*^{BG00197}, and *SKIP*^{BG00076}) all drove lower level IPC reporter gene expression.

We chose a subset of the 28 lines for characterization with additional markers. Five lines, *brat*^{BG02721}, *heph*^{BG01850}, *shep*^{BG00836}, *shep*^{BG01322}, and *Pfrx*^{BG02836}, displayed reporter gene expression in lateral abdominal VNC cells in the vicinity of seven pairs of neurons that express LK (CANTERA and NASSEL 1992). Through double labeling, we confirmed that all five of these lines drove transgene expression in the full set of

14 abdominal LK neurons (Figure II.9). Finally, because of the highly peptidergic neuron-specific expression pattern of *shep*^{BG00836}, we chose it (and the other *shep* insertion, *shep*^{BG01322}) for double labeling with an antiserum against the prohormone convertase furin 1 and an antiserum (PT2) that labels RFamide-containing neuropeptides (JIANG *et al.* 2000; TAGHERT 1999). Consistent with their broad peptidergic cell patterns, both insertions drove reporter expression in most RFamide-positive neurons, including the Tv neurons (Figures II.10A-B) and all Furin-1-expressing neurons in the VNC (Figures II.10C-F).

Genomic organization of *shep*: The *shep* gene encodes at least 5 mRNA isoforms that are predicted to produce 5 SHEP proteins through alternative splicing and the use of alternative transcriptional start sites (FLYBASE_CONSORTIUM 2003). Two isoforms, RC and RE, share the same transcriptional start site and the same exons, except that the sixth exon of RC is 33bp shorter than RE due to the use of an alternative splice donor site (Figure II.11). Based on the numbers of published ESTs (from multiple tissue sources and stages), among all the five isoforms, RC and RE are the most abundant (40 ESTs for RC and RE, 5 for RA, 3 for RB and 5 for RD) (FLYBASE_CONSORTIUM 2003).

The two *shep* alleles from this current screen, *shep*^{BG00836} and *shep*^{BG01322}, are inserted in different introns of the gene (Figure II.11). The *shep*^{BG00836} insertion is located within a shared, ~50kb intron of RA, RB and RD and 24bp into the first exon of RC and RE. *shep*^{BG01322} is inserted in the 2nd intron of RA and 1st intron of RD and 14bp 5' of the transcription start site of RB. The different insertion sites for

shep^{BG00836} and *shep*^{BG01322} may lead to splice trapping of distinct transcripts, and this may account for the differences in reporter gene expression in these two lines.

To further examine the expression pattern of *shep*, we obtained the protein trap line *G00261*, which is inserted in the first common intron of all the 5 isoforms of *shep*, 142bp into the first intron of RC and RE (Figure II.11) (MORIN *et al.* 2001). *Shep*^{G00261} expressed ubiquitously and specifically to the CNS neurons, located in the cytoplasm (Figure II.12). Double labeling of *shep*^{G00261} with anti-BURS antiserum showed the colocalization of *shep*^{G00261} neurons and the BRUS expressing neurons (Figure II.12).

Survey for neuropeptide-associated mutant phenotypes: Because splice-trap insertions may disrupt mRNA splicing, they can be used directly for preliminary functional studies of the trapped genes (LUKACSOVICH *et al.* 2001). To determine whether genes identified in this screen play roles in the differentiation of peptidergic neurons or the production of neuropeptides, we tested the lines for recessive lethality (Table II.2), and we examined the effects of selected homozygous insertions on the expression levels of CCAP, DILP2, and PHM in third instar larvae (Table II.2 and data not shown). We did not observe changes in immunostaining for these neuropeptides in any of the tested lines, nor did we detect changes in neuronal morphology at this stage in development (data not shown). However, several of the splice trap lines displayed reporter gene expression in neurons (e.g., CCAP/BURS neurons) known to play important roles in the control of ecdysis-associated behaviors.

Therefore, we also examined the lines for evidence of external morphological defects that are associated with disruptions in late molting events (ZHAO *et al.* 2008).

Seven of the lines were recessive lethal and five additional lines displayed partial lethality (Table II.2). In addition, several lines had other visible phenotypes that may result from the disruption of neuropeptide-controlled behaviors. For example, homozygous *fz2*^{BG01711} animals pupariated abnormally in the food rather than on the sides of the culture vials, suggesting an alteration in wandering behavior or the behaviors associated with the choice of pupariation site. In addition, four alleles displayed phenotypes associated with disruptions in ecdysis or associated developmental events (Table II.2). The *tai*^{BG01746} line had partial larval and pupal lethality. Some of the dead larvae had multiple mouthparts, consistent with a failure to complete larval ecdysis (HEWES *et al.* 2000; PARK *et al.* 2002), and we have determined that the larval *tai* phenotype is the result of reduced peptide hormone gene expression (Chapter 3). At the adult stage, homozygous *shep*^{BG00836} and *shep*^{BG01322} animals each displayed defective tanning or sclerotization of the cuticle (resulting in loss of the normal glossy appearance of the cuticle surface) and/or partially expanded wings. These phenotypes, in addition to the neuropeptidergic cell-enriched *shep* reporter expression patterns, led us to focus further on the functions of *shep* in peptidergic neurons.

Phenotypes similar to the wing expansion and cuticle tanning defects seen in *shep*^{BG00836} or *shep*^{BG01322} homozygotes result from loss of BURS or its receptor or disruption of the CCAP/BURS neurons (BAKER and TRUMAN 2002; LUAN *et al.* 2006; PARK *et al.* 2003; ZHAO *et al.* 2008). Within 1 hr after adult ecdysis (eclosion), the

CCAP/BURS neurons undergo a period of large-scale, episodic neuropeptide release that can be detected by anti-BURS immunostaining (PEABODY *et al.* 2008; ZHAO *et al.* 2008). Each of the splice trap insertions in *shep* displayed expression in BURS-positive neurons (Figures II.6D and 7B). Therefore, to determine whether mutations in *shep* result in defects in the development of the CCAP/BURS neurons, expression of BURS, or the regulation of BURS secretion, we performed anti-BURS immunostaining on abdominal fillet preparations of homozygous $shep^{BG00836}$ adults at eclosion and 1 hr after eclosion. We did not observe any change in the extent of BURS expression or secretion in homozygous $shep^{BG00836}$ adults (data not shown). However, the CCAP/bursicon cell neurites were shorter and had fewer branches, both within the CNS (Figure II.13A-B) and the peripheral axonal arbor (data not shown). In follow-up studies, Dahong Chen has shown that expression of $shep^{RNAi}$ in the CCAP/bursicon neurons led to a similar reduction in neurite length and branching in the CNS (Figure II.13C-D) and periphery (Figure II.13E-F). He obtained the same result with *BG00836*/deficiency transheterozygotes. These findings together with the lack of any change in CCAP/bursicon cell morphology in third instar larvae, indicate that *shep* plays an important role in neurite outgrowth during the metamorphic remodeling of the CCAP/bursicon neurons. The wide expression of *shep* in the CNS neurons suggesting it might be a general regulator for the neurite outgrowth in the CNS, thus it will be important in future studies to examine the metamorphic remodeling of other CNS neurons in *shep* mutants.

Closely-associated genetic background effects: The *shep* gene was first identified in a screen for gravitaxis mutants (ARMSTRONG *et al.* 2005). However, an insertion in *shep* (*shep*^{BG01130}) was also picked up in a prior screen for quantitative trait loci affecting starvation resistance in adults (HARBISON *et al.* 2004). Given the expression of *shep*^{BG00836} and *shep*^{BG01322} in the IPCs and potentially in other peptidergic cell types known to play a role in the regulation of Drosophila metabolism and feeding behaviors (BADER *et al.* 2007; BROGIOLO *et al.* 2001; NASSEL and HOMBERG 2006; SHEN and CAI 2001), we tested both of these *shep* alleles for their effects on starvation resistance.

Homozygous *shep*^{BG00836} and *shep*^{BG01322} adult female flies had a normal life span when raised and maintained on normal food (data not shown). The control genotype, *w*^{1118}*; Iso2A; Iso3A*, was the isogenic genetic background in which the BG insertions were generated (BELLEN *et al.* 2004a). Under starvation conditions, homozygous *shep*^{BG00836} flies died ~10 hours earlier than the controls (Figure II.14A). *shep*^{BG01322}, which is inserted in a different intron (Figure II.11), showed normal starvation resistance (Figure II.14A). The starvation sensitivity phenotype was fully reverted by precise excision of the BG element in the *shep*^{BG00836} line (*shep*^{Rev6B}) (Figure II.14B). Surprisingly, the starvation sensitivity also disappeared after *shep*^{BG00836} was outcrossed for seven generations with *w*^{1118}*; Iso2A; Iso3A*, and hemizygous, outcrossed *shep*^{BG00836}/*deficiency* flies (Figure II.11) showed normal starvation resistance (Figure II.15). Expression of *shep*^{RNAi} in peptidergic neurons using either *386-Gal4* or the *shep*^{BG00836} driver also had no effect on adult starvation resistance (data not shown).

We observed wing expansion defects in both *shep*^{BG00836} and *shep*^{BG01322} adults (Table II.2), and the homozygous *shep*^{Rev6B} adults displayed normal wing expansion (n=34). Outcrossed *shep*^{BG00836} flies also still displayed wing expansion defects. Nevertheless, outcrossed *shep*^{BG00836}/*deficiency* (n=31) and outcrossed *shep*^{BG00836}/*shep*^{BG01322} (n=123) flies all had normal wing expansion (data not shown).

These results suggest that the starvation resistance with *shep*^{BG00836} may be caused by genetic background or by combinatorial interactions between the loss of *shep* and the genetic background, but not by *shep* mutants alone. The rescue of the wing expansion phenotype by the putative precise excision of the *P* element (*shep*^{Rev6B}) indicates that the wing expansion defects observed in both *shep*^{BG00836} and *shep*^{BG01322} may also be caused by combinatorial interactions of *shep* mutations and the genetic background. Alteratively, these phenotype may be caused by mutation of another gene in the vicinity of *shep* by a second, as yet unidentified P-element insertion.

DISCUSSION

Peptidergic neurons are specialized to express large quantities of neuropeptide pro-hormones, process them into mature neuropeptides, package them into secretory granules, and secrete them in response to appropriate cues. In this study, we employed a reverse genetics strategy, based on patterns of gene expression, to identify factors important either for the differentiation of these characteristic features of peptidergic neurons or for signaling by this cell type. We used splice-trap (BG) lines (LUKACSOVICH *et al.* 2001) for our screening for three reasons. First, because the BG construct relies on a donor splice site from a native transcript for expression of Gal4, the pattern of reporter gene expression that results is determined by the promoter of the native gene. Therefore, the splice trap expression patterns are often an accurate reflection of the spatial and temporal expression patterns of tagged transcripts. Second, because a BG insertion may interfere with normal mRNA splicing, each is a strong candidate loss-of-function allele of the targeted gene. Third, the identity of the trapped gene can often be determined unambiguously based on the location of the insertion in an intron or exon (in the correct orientation) of the gene. For most of the 545 BG lines screened in this study, the insertion sites have previously been mapped to precise locations in the *Drosophila* genome (FLYBASE_CONSORTIUM 2003). This greatly facilitated our rapid identification of the trapped genes.

Multiple additional markers define a distinct class of peptidergic neurons: Previous studies have revealed a large and diverse class of peptidergic neurons that display several common properties. The first indication that this class of neurons

existed was the cloning of the *dimm* gene (HEWES *et al.* 2003). *dimm* is essential for high-level expression of many neuropeptides and some peptide biosynthetic enzymes, although many peptidergic neurons continue to express neuropeptides (albeit at lower levels) in the absence of zygotic *dimm* expression (HEWES *et al.* 2003). The neuropeptide amidation enzyme, PHM, is a direct transcriptional target of DIMM (PARK *et al.* 2008a), and these two proteins are therefore expressed in highly congruent patterns (HEWES *et al.* 2006; HEWES *et al.* 2003; PARK *et al.* 2008a; PARK *et al.* 2008b). These and other observations suggest that these markers define a distinctly specialized population of neurons (HEWES *et al.* 2003), for which Park and Taghert coined the term "LEAP cells" for their relatively large somata, evidence at least in some cases of rapid episodic neuropeptide release, and expression of amidated peptides (PARK and TAGHERT 2009). The LEAP cells are also a heterogeneous population, and many different subsets of these cells can be defined by their expression of specific neuropeptides and associated proteins (HEWES *et al.* 2003; PARK *et al.* 2008b). These observations suggest that the features common to LEAP cells are not limited to any specific neuropeptide and instead define more basic cellular properties that are shared by a large and diverse set of peptidergic neurons.

Our discovery of a third marker, $shep^{BG00836}$, that is highly congruent with DIMM and PHM provides further support for the LEAP cell hypothesis. The $shep^{BG00836}$ insertion drives reporter gene expression in a restricted pattern that includes essentially all the PHM-positive cells in the CNS, PNS and corpora cardiaca (CC) (Figure I.1, and data not shown), without expression in other tissues. Conversely, only ~8% of the $shep^{BG00836}$-positive neurons lacked detectable PHM immunostaining.

This may be an underrepresentation of the degree of overlap, since the fixative (PFA-PA) used for double-labeling for GFP and PHM represented a compromise for the two markers, and the resulting PHM staining was much weaker than what can be obtained with Bouin's fixation. In addition, with a few notable exceptions (e.g., a set of neurons in the terminal abdominal ganglia and 4 lateral abdominal neurons on each side), the intensity of the PHM staining was correlated with the intensity of the strength of the *shep*^{BG00836}-driven expression of the reporter gene, and most of the *shep*^{BG00836}-positive and PHM-negative neurons were only weakly *shep*^{BG00836}-positive. Therefore, future work to determine the cellular and molecular functions of the SHEP protein in peptidergic neurons may help to reveal the processes by which LEAP cells differentiate or provide for amplified expression, packaging, and regulated secretion of amidated neuropeptides.

***SHEP* regulates neurite outgrowth through RNA alternative splicing:** The *shep* gene encodes at least 5 mRNA isoforms that are predicted to produce 5 SHEP proteins through alternative splicing and the use of alternative transcriptional start sites. SHEP is a putative RNA binding protein containing two RNA Recognition Motifs (RRM), which are found in many proteins that participate in post-transcriptional gene expression processes, including mRNA splicing, export of RNAs from the nucleus, and the regulation of RNA stability. RRM domains can also be involved in binding to single stranded DNA and proteins (MARIS *et al.* 2005). RNA binding proteins are important cellular regulators, and mutations in these factors are associated with several classes of human disease, including neurologic disorders, muscular atrophies, and

cancer (LUKONG *et al.* 2008). As a RNA binding protein, SHEP may regulate the peptidergic neuron development (neurite outgrowth) through RNA splicing.

The CCAP/bursicon cells system is an excellent model for the study of metamorphic outgrowth because these cells go through metamorphic remodeling. Using this system, our lab has identified several genes that are involved in the metamorphic remodeling (ZHAO *et al.* 2008). Here we report that *shep* regulates the metamorphic outgrowth of CCAP/bursicon cell neurites. The effect of *shep* on the neurite outgrowth of other CNS neurons will be of interest in future studies. For example, our findings suggest that the reported gravitaxis defect in *shep* mutant (ARMSTRONG *et al.* 2005) may be caused by wiring defect of some yet-to-be-identified CNS neurons. In addition, if *shep* functions through alternative mRNA splicing, then it will be important to identify the relevant mRNA targets and their roles in neurite outgrowth.

TABLE II.1

Genes identified in the splice-trap screen with expression in the PHM-positive peptidergic CNS neurons:

Transposon insertion	Gene	location	Transcripts	Gene product	Co-localized neuropeptides and peptide biosynthetic enzymes
BG00076	*Shal K^+ channel interacting protein* (*SKIP*)	338 bp into 1st exon of RB, RE		Ion channel regulating protein	DILP2, PHM, -RFamide peptides
BG00197	*jim*	2343 bp upstream		transcription factor	PHM
BG00449	*CG31145*	Intronic splice trap	RA-RD	novel	PHM, DILP2
BG00476	*CG4860*	Insertion orientation unknown, 4 bp upstream		Short chain acyl-CoA dehydrogenase (SCAD) (metabolism)	PHM
BG00665	*CG8963*	Intronic splice trap	RA-RC	poly(A) binding protein, middle domain of eukaryotic initiation factor 4G (MIF4G) superfamily.	CCAP, PHM
BG00836	*alan shepard (shep)*	Intronic splice trap	RA, RB, RD	RNA binding protein	CCAP, DILP2, DIMM, Furin-1, LK, PHM,

					-RFamide peptides
BG01322	*alan shepard (shep)*	Intronic splice trap	RA, RD	RNA binding protein	CCAP, DILP2, Furin-1, LK, PHM, RFamide
BG00855	*homeodomain interacting protein kinase (hipk)*	Intronic splice trap	RA, RB	serine/threonine kinase	CCAP, PHM
BG02654	*homeodomain interacting protein kinase (hipk)*	Intronic splice trap	RB	serine/threonine kinase	CCAP, PHM
BG01140	*MYPT-75D*	Intronic splice trap	RA	myosin phosphatase regulator	PHM
BG01171	*Adult enhancer factor 1 (Aef1)*	Intronic splice trap	RA, RC	RNA polymerase II transcription factor (C2H2 Zn finger)	CCAP, PHM
BG01610	*scribbler (sbb)*	Intron insertion but orientation unknown	RD-RG	transcription factor	CCAP, PHM
BG01711	*frizzled 2* (*fz2*)	Intronic splice trap	RD	Wnt receptor	CCAP, DILP2, PHM, RFamide
BG01746	*taiman (tai)*	Intronic splice trap	RA	PAS domain transcriptional coactivator, signal transduction	CCAP, PHM

BG01766	*Decapping protein 2 (Dcp2)*	Intronic splice trap	RB	mRNA decapping enzyme 2 (Dcp2p)	PHM
BG01850	*hephaestus (heph)*	Intronic splice trap	RB	RNA recognition motif (RRM), RNA binding protein	CCAP, DILP2, LK, PHM, RFamide
BG01854	*ERp60*	Intronic splice trap	RA	protein disulfide isomerase	PHM
BG01894	*CG11444*	Intronic splice trap	RA	casein kinase substrate, phosphoprotein PP28 superfamily	CCAP, PHM
BG02142	*cAMP-dependent protein kinase 1 (Pka-C1)*	75bp into the 1st exon of RA-RC		Serine/threonine kinase	PHM
BG02222	unknown	45bp upstream of *CG9975*, but in wrong orientation for splice trap			CCAP, DILP2, PHM
BG02427	*CG32306*	Intronic splice trap	RD-RF	novel	CCAP, PHM
BG02721	*brain tumor (brat)*	Intronic splice trap	RA	Zn-finger, B-box (translational regulator)	CCAP, DILP2, LK, PHM
BG02759	*protein kinase 61C (Pk61C)*	Intronic splice trap	RD	serine/threonine kinase	CCAP, PHM
BG02772	*CG13917*	>6 kb upstream		Broad-Complex,	CCAP, PHM

				Tramtrack and Bric a brac (BTB/POZ) domain-containing protein (possible transcription factor)	
GT-000078	*CG13917*	>4 kb upstream		Broad-Complex, Tramtrack and Bric a brac (BTB/POZ) domain-containing protein (possible transcription factor)	CCAP, PHM
BG02810	*couch potato (cpo)*	Intronic splice trap	RA, RE, RG, RJ	RNA recognition motif (RRM), RNA binding	PHM
BG02820[1]	*chiffon (chif)*	Intronic splice trap	RA, RB	Zinc finger in DBF-like protein (ZnF_DBF)	PHM
	CG42231	Intronic splice trap	RA	novel	
BG02836	*6-phosphofructo-2-kinase (Pfrx*)	Intronic splice trap	RA, RI, RF	6-phosphofructo-2-kinase (6PF2K)	DILP2, DIMM, LK, PHM, RFamide

[1], Inserted in two nested genes.

TABLE II. 2

Recessive phenotypes of splice trap lines:

Transposon insertion	Peptidergic markers tested	Viability	Other phenotypes
Aef1^{BG01171}	CCAP	Some pupal lethality, adults normal.	Normal
brat^{BG02721}	CCAP, DILP2	Normal	Normal
CG4860^{BG00476}		Not tested	Normal
CG8963^{BG00665}	CCAP, DILP2, PHM	Homozygous lethal, with death at all larval stages. No multiple mouthparts observed.	Normal
CG9975^{BG02222}	CCAP	Some mid to late pupal lethality.	Normal
CG11444^{BG01894}		Normal	Darkened cuticle in shape of trident on adult dorsal thorax.
CG13917^{BG02772}	CCAP	Normal	Normal
CG13917$^{GT\text{-}000078}$	CCAP	Normal	Normal
CG31145^{BG00449}		Some mid-pupal to pharate adult lethality.	Normal
CG32306^{BG02427}	CCAP	Normal	Normal

chif^{BG02820}		Normal	Normal
cpo^{BG02810}		Homozygous lethal.	Normal
Dcp2^{BG01766}		Homozygous lethal, with early to late pupal lethality.	Normal
ERp60^{BG01854}		Normal	Normal
fz2^{BG01711}		Normal	Pupariation mostly in the food.
heph^{BG01850}		Normal	Normal
hipk^{BG00855}		Homozygous lethal.	Normal
hipk^{BG02654}	CCAP	Normal	Normal
jim^{BG00197}		Homozygous lethal, with mid-pupal lethality.	Normal
MYPT-75D^{BG01140}		Normal	Normal
Pfrx^{BG02836}	DILP2	Normal	Normal
Pk61C^{BG02759}	CCAP	Normal	Normal
Pka-C1^{BG02142}		Homozygous lethal, with mid-pupal lethality.	Normal
sbb^{BG01610}	CCAP, DILP2	Homozygous lethal (no adults or pupae).	Normal

shep^{BG00836}	CCAP, DILP2, PHM	Normal	10% PEW (many also with dimpling and/or darkened cuticle in shape of trident on dorsal thorax), most with loss of the glossy surface finish of the cuticle. 25% adults with ectopic wing vein extending from pcv. 2% of the adults fail to completely eclose and remain stuck halfway out of the pupal case.
shep^{BG01322}	CCAP, PHM	Normal	25% PEW, most with loss of the glossy surface finish of the cuticle.
SKIP^{BG00076}		Some pharate adult lethality.	Normal
tai^{BG01746}	CCAP	Some larval and pupal lethality.	Larval lethality sometimes associated with multiple mouthparts. A small number of adults with dark pigmentation in shape of trident on dorsal thorax and/or loss of the glossy surface finish of the cuticle.

PEW, partially expanded wings (ZHAO *et al.* 2008).

Figure II.1: CNS or ring gland expression of eight splice trap lines in non-peptidergic neurons. These lines drove reporter gene expression within several tissues/cell types. (A-C) *BG00653*, *BG01100* and *BG01273* were all expressed in the ring gland (arrows). *BG01100* also expressed in the kenyon cells (asterisks). (B-E) Four lines, *BG01100*, *BG01273*, *BG01684* and *BG02732*, drove reporter expression in two longitudinal tracts within the ventral nerve cord (unfilled arrowheads). (E-H) Four lines, *BG02732*, *BG02660*, *BG01347*, and *BG00919* were expressed in glial-like cells in CNS. In *BG02660* and *BG02732*, the expression in the brain lobes was in cells that wrapped around small clusters of neuronal somata (filled arrowheads).

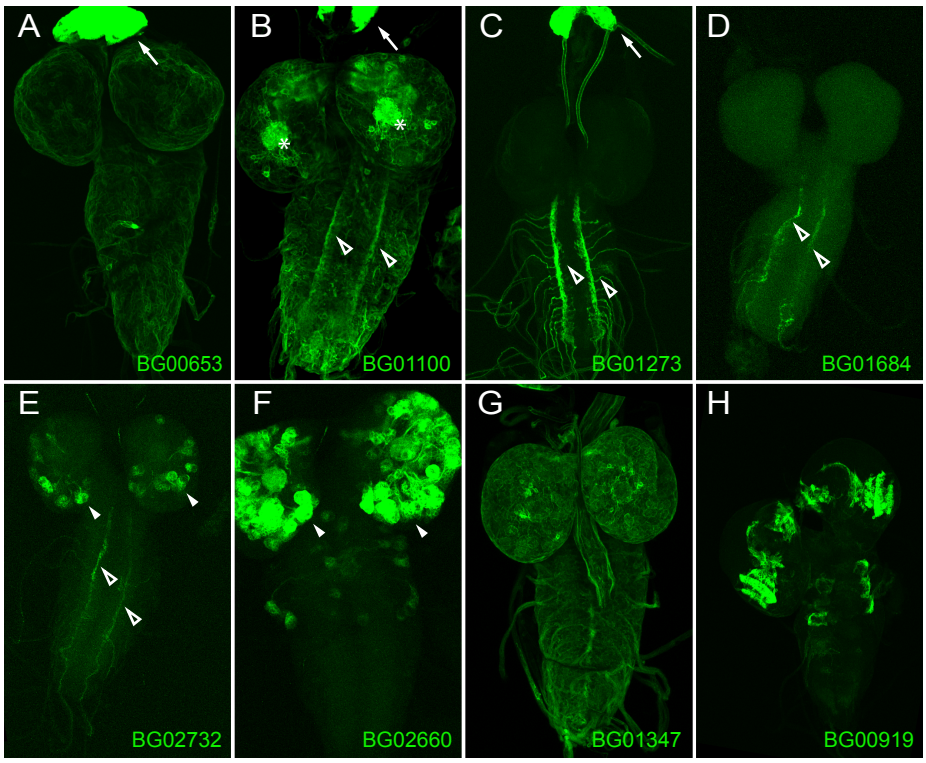
A
BG00653
B
BG01100
C
BG01273
D
BG01684
E
BG02732
F
BG02660
G
BG01347
H
BG00919

Figure II.2: Reporter gene expression patterns for 30 lines with expression in selected CNS neurons. Except for *BG00876* and *BG02083*, all of the 30 lines displayed at least some expression in peptidergic neurons. In addition to selected peptidergic neurons, expression in other tissue/cell types was also observed. Eight lines were expressed in the prothoracic gland (arrows) (*BG00449*, *BG00665*, *BG01171*, *BG01746*, *BG01766*, *BG01894*, *BG02759*, and *BG02820*). Two lines, *BG00836* and *BG02836*, showed expression in the corpora cardiaca (arrowheads). Distinct mushroom body expression (asterisks) was observed in 14 lines: *BG00476*, *BG01171*, *BG01610*, *BG01766*, *BG01894*, *BG02083*, *BG02142*, *BG02222*, *BG02427*, *BG02772*, *BG02810*, *BG02820*, *BG02836* and *GT-000078*.

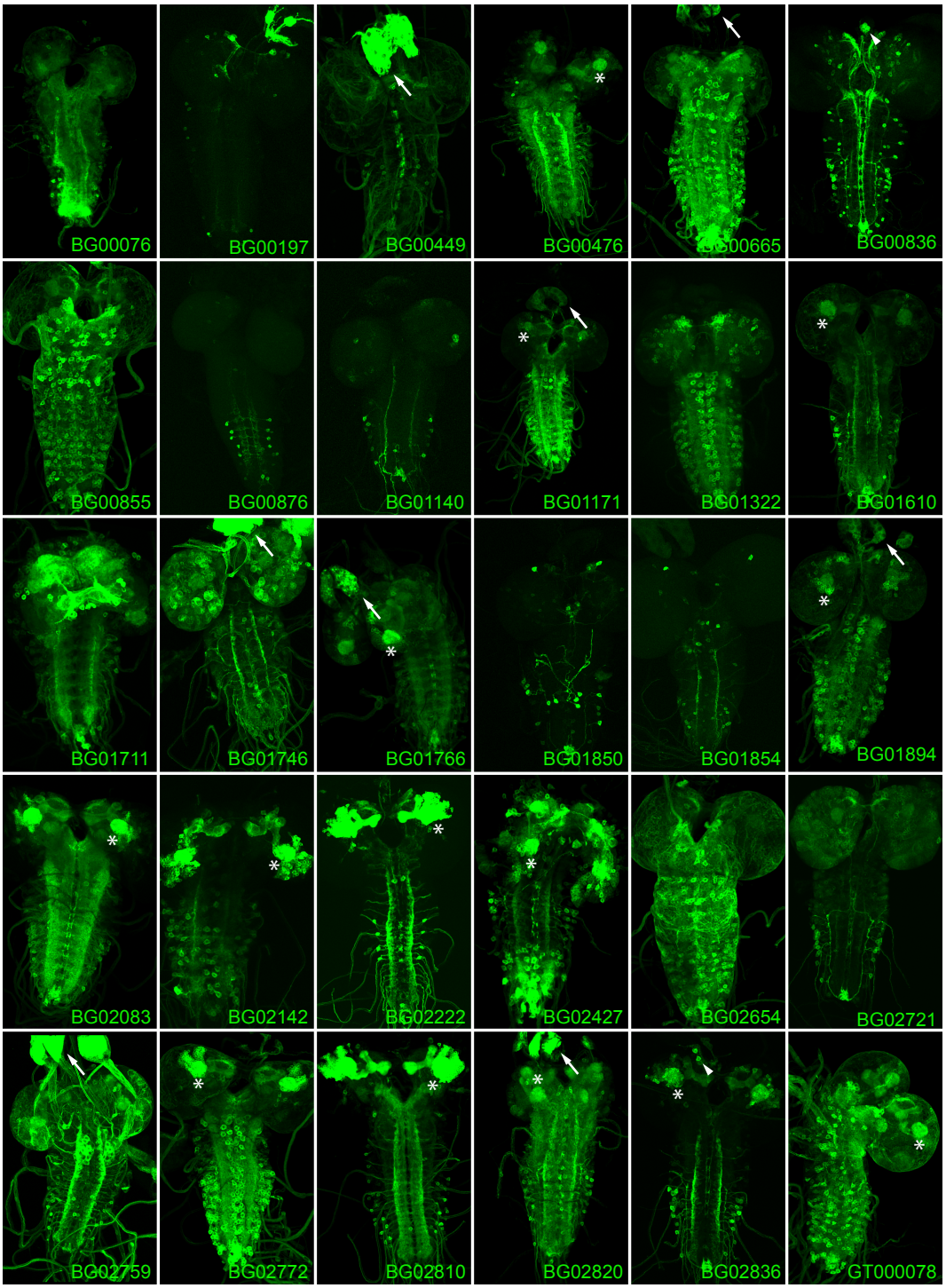
BG00076
BG00197
BG00449
BG00476
BG00665
BG00836
BG00855
BG00876
BG01140
BG01171
BG01322
BG01610
BG01711
BG01746
BG01766
BG01850
BG01854
BG01894
BG02083
BG02142
BG02222
BG02427
BG02654
BG02721
BG02759
BG02772
BG02810
BG02820
BG02836
GT000078

Figure II.3: Colocalization of selected splice-trap expression patterns with PHM. (A) Schematic of prominent cells in the PHM expression pattern. (B) *BG00836* drove UAS-mCD8::GFP (green, 836) expression strongly and specifically in most PHM-positive neurons (magenta, PHM), including the IPC, MP2, d1-d11, Tv and LC cells. (C) *BG01610* (green, 1610) colocalized with PHM (magenta, PHM) in most of the neurons in the brain lobe, and in the LC cells of the VNC. (D) *BG01850* (green, 1850) was expressed in a restricted pattern. It was expressed strongly in some PHM neurons (magenta, PHM) in the brain lobe, including the IPC, and in the LC cells in the VNC. (E) *BG02721* (green, 2721) was expressed in a restricted pattern in the VNC that included the d1-d11 and the LC neurons. (F) *BG02836* (green, 2836) was expressed strongly in the LC cells. Arrows, colocalization of the reporter gene and PHM; arrowheads, reporter gene expression in PHM-negative cells. Abbreviations: d1 and d4, dorsal chain neuron (Ap-let) (PARK *et al.* 2004) 1 and 4; IPC, insulin producing cells (RULIFSON *et al.* 2002); LC3 and LC7, lateral cluster neurons in abdominal segment 3 and 7; MP1 and MP2, medial protocerebrum neurons 1 and 2; PA, posterior abdominal neurons; SE, subesophageal neurons; SP1, superior proto-cerebrum neuron 1; T3va, b, ventral neurons a and b in thoracic segment 3 (TAGHERT 1999); VA, ventral abdominal neurons (O'BRIEN and TAGHERT 1998). Bars: B-E, 50µm; F, 20µm.

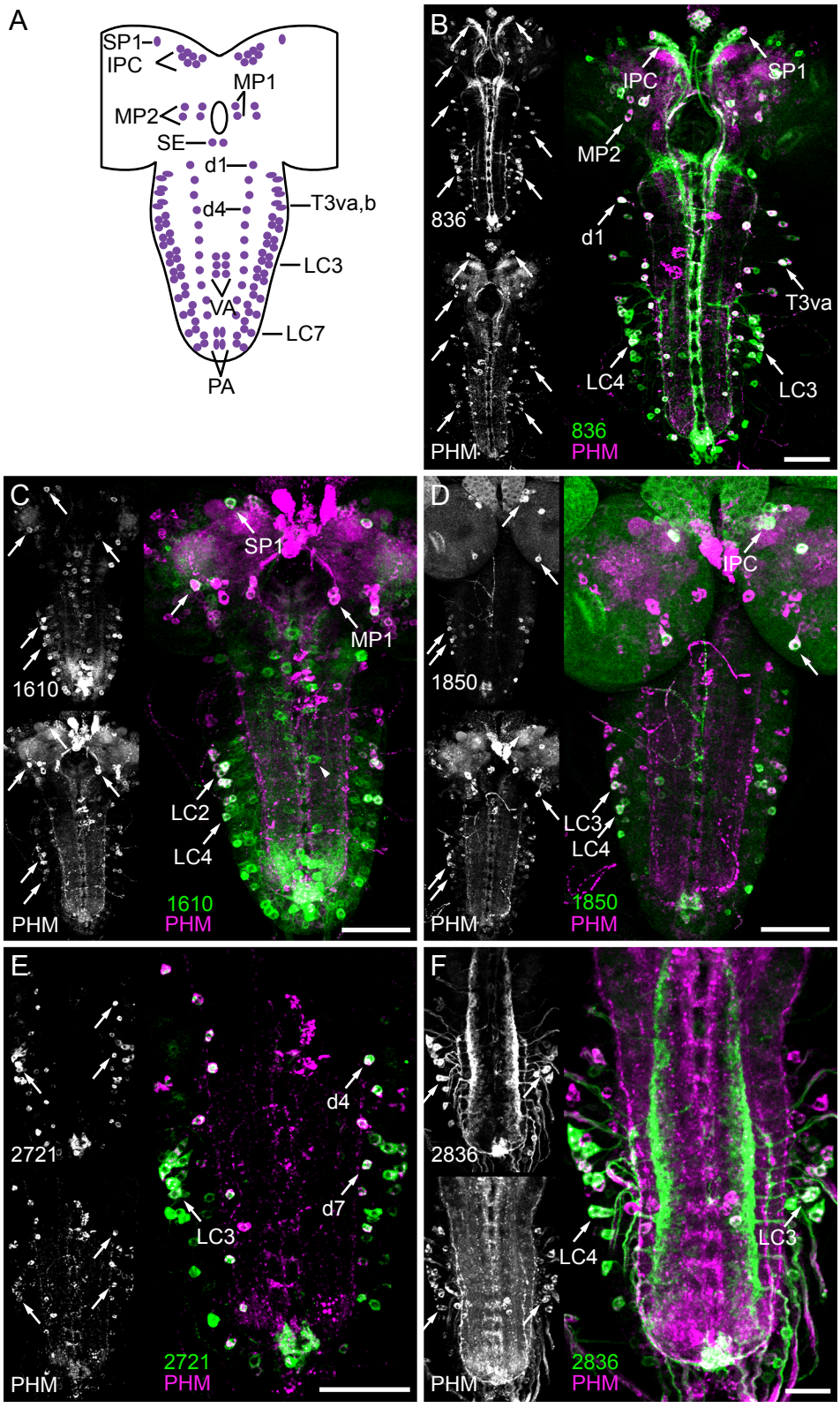
A
SP1
IPC
MP1
MP2
SE
d1
d4
T3va,b
LC3
VA
LC7
PA
B
IPC
SP1
MP2
836
d1
T3va
LC4
LC3
PHM
836
PHM
C
SP1
MP1
1610
LC2
LC4
PHM
1610
PHM
D
IPC
1850
LC3
LC4
PHM
1850
PHM
E
d4
2721
d7
LC3
PHM
2721
PHM
F
2836
LC4
LC3
PHM
2836
PHM

Figure II.4: Schematic representations of splice trap expression patterns in the PHM-positive neurons. PHM neurons indicated in the schematics are neurons with prominent PHM staining. The double labeling of the splice-trap line expression patterns was performed by anti-PHM (JIANG *et al.* 2000) immunostaining on the CNS of BG>UAS-mCD8::GFP wandering third instar larvae. Colocalization and staining intensities were determined based on examination of optical sections within confocal z-series image stacks. Relative reporter intensities are represented as shown in the key.

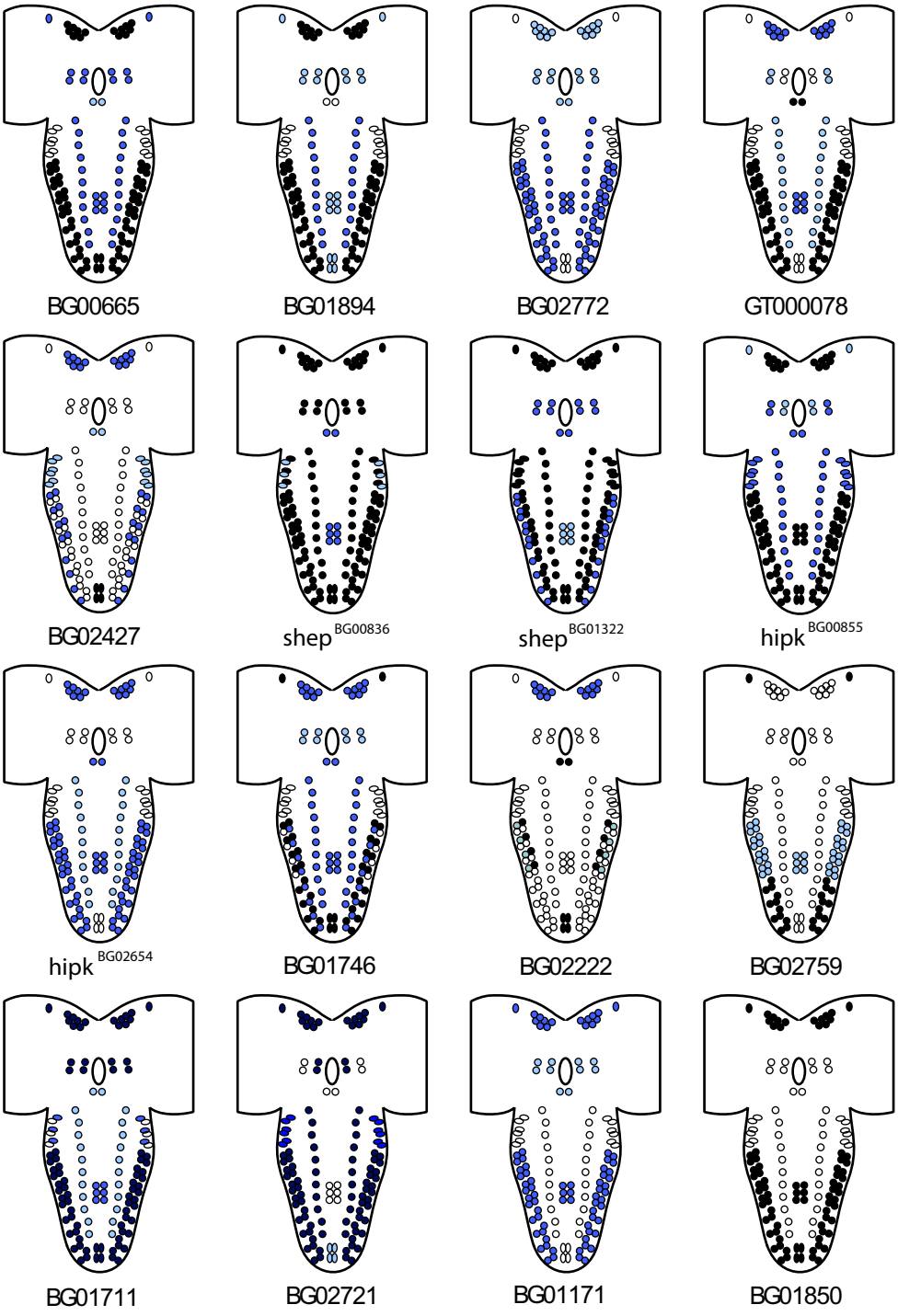
BG00665
BG01894
BG02772
GT000078
BG02427
shep BG00836
shep BG01322
hipk BG00855
hipk BG02654
BG01746
BG02222
BG02759
BG01711
BG02721
BG01171
BG01850

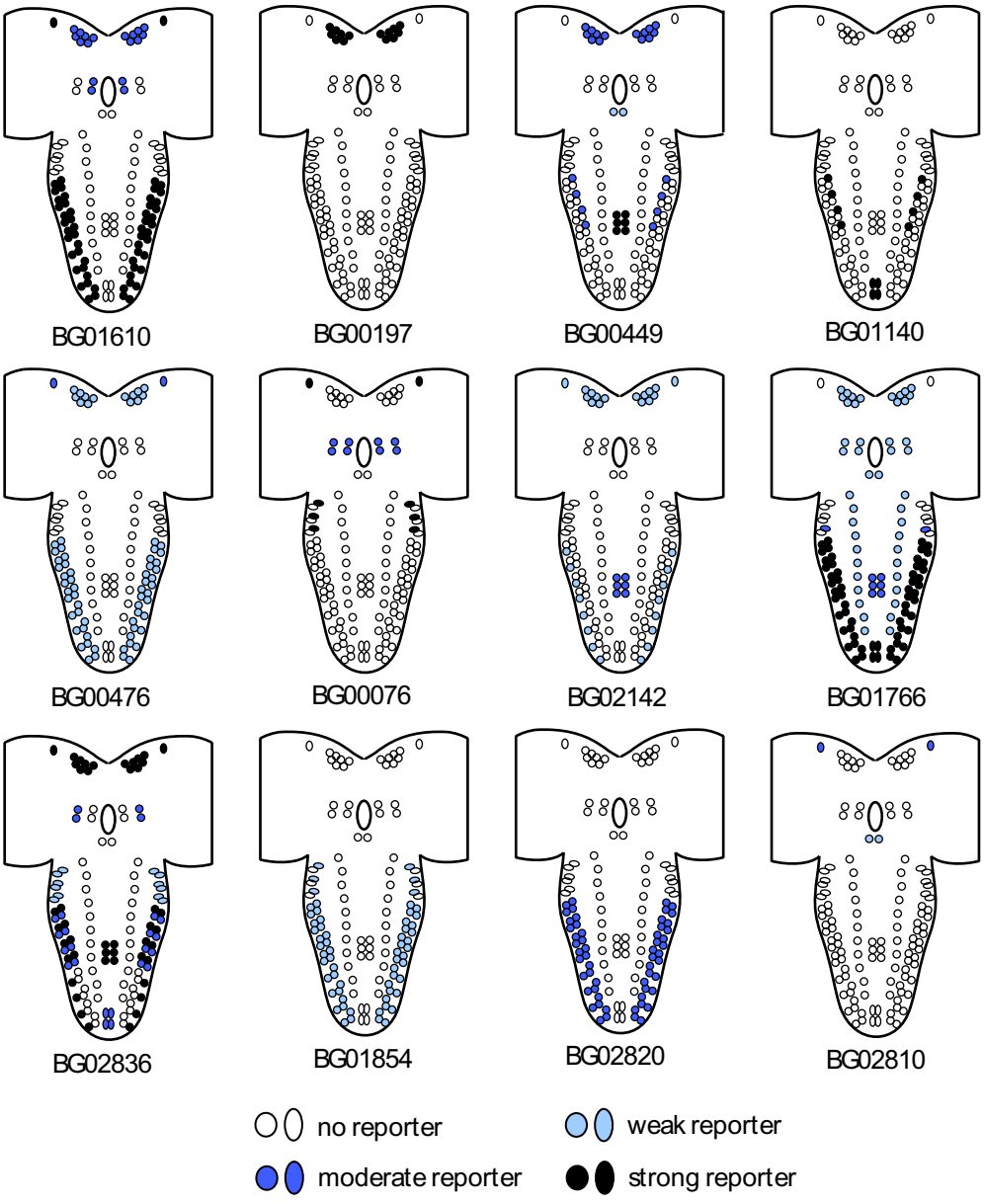
BG01610
BG00197
BG00449
BG01140
BG00476
BG00076
BG02142
BG01766
BG02836
BG01854
BG02820
BG02810
no reporter
weak reporter
moderate reporter
strong reporter

Figure II.5: Expression of *BG00665* and *BG01711* in PHM neurons. Both *BG00665* (green, 665) (A and B) and *BG01711* (green, 1711) (C and D) drove UAS-mCD8::GFP expression widely in CNS neurons. The reporter gene expression in the brain lobes (A and C) and ventral nerve cord (B and D) included most of the PHM-positive neurons (magenta, PHM). Arrows, examples of colocalization of reporter expression and anti-PHM immunostaining in PHM neurons. Arrowheads, reporter expression in non-PHM cells. Bars, 20μm.

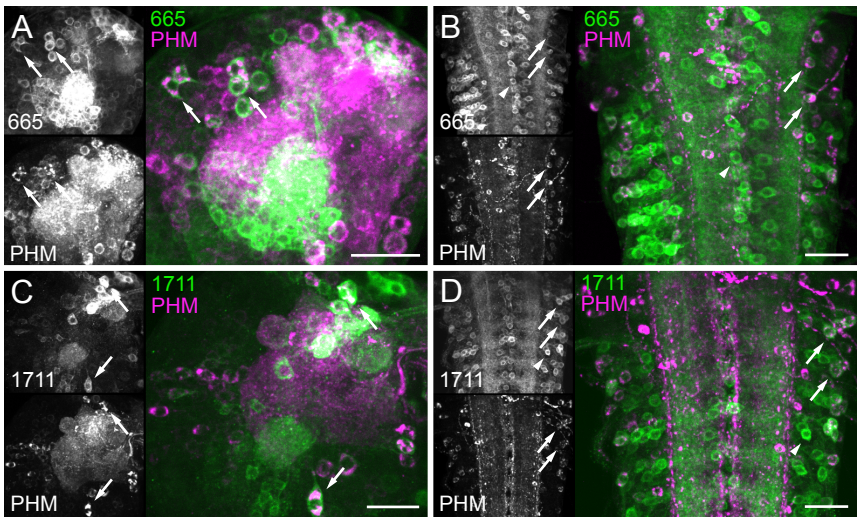
A
665
PHM
665
PHM
B
665
PHM
665
PHM
C
1711
PHM
1711
PHM
D
1711
PHM
1711
PHM

Figure II.6: Expression of selected splice-trap lines in the CCAP/Burs cells. (A) Schematic of the CCAP immunostaining pattern. (B) *BG02222* (green, 2222) drove UAS-mCD8::GFP expression strongly in CCAP/Burs neurons A1a-A4a (magenta, Burs). It also showed strong expression in the mushroom bodies (MB). (C) At the P14 pharate adult stage, *BG02222* (green, 2222) continued to be strongly expressed in the CCAP/Burs neurons (magenta, Burs) (arrows) in the VNC, as well as many additional Burs-negative cells (arrowheads). (D) *BG00836* (green, 836) drove moderate UAS-mCD8::GFP expression in CCAP/Burs neurons (magenta, Burs) (arrows) and strongly in many non-CCAP/Burs neurons (arrowheads). Abbreviations: A (2a and b, A4a and b, 6 and 7), abdominal neurons in indicated segments; LSE1-4, lateral subesophageal neurons 1-4; MPA, midline protocerebral anterior neurons; MSE, midline subesophageal neurons; T (1, 3a and b), neurons on thoracic segments 1 and 3. Bars, 50µm.

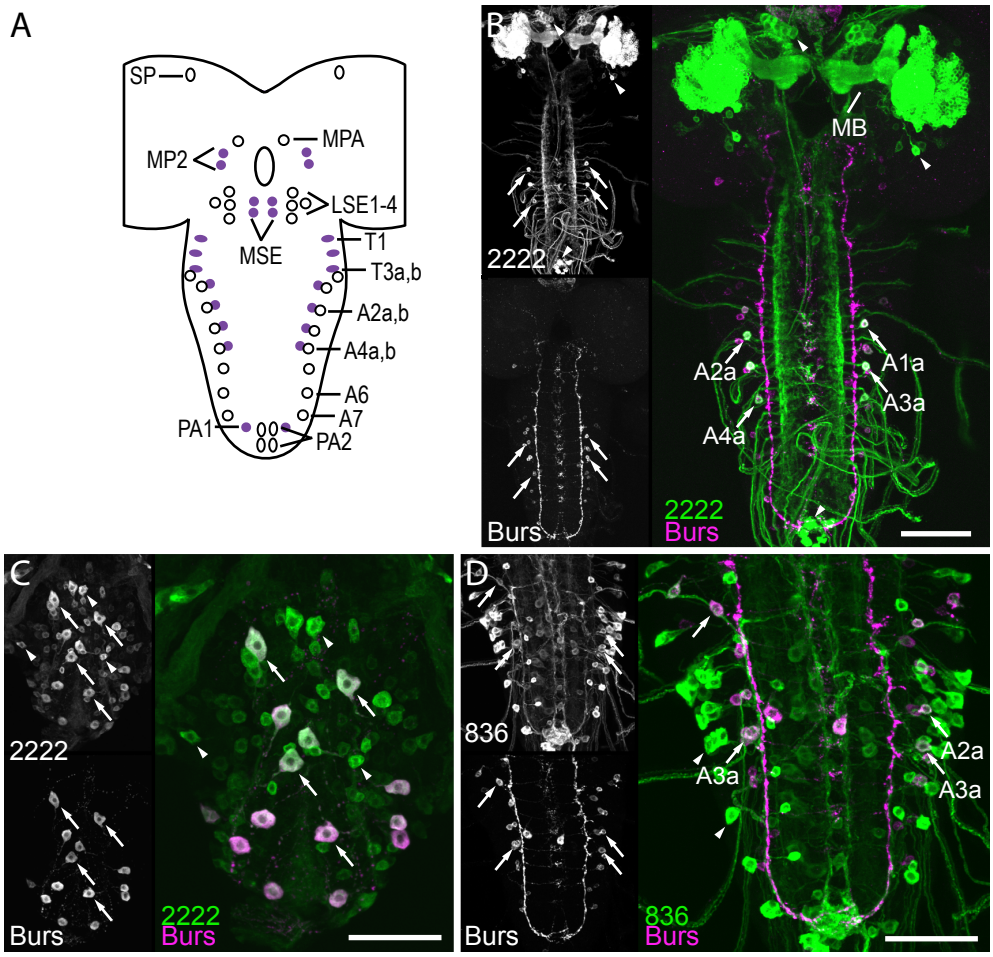
A
SP
MP2
MPA
LSE1-4
MSE
T1
T3a,b
A2a,b
A4a,b
A6
A7
PA1
PA2
B
2222
Burs
MB
A2a
A1a
A3a
A4a
2222
Burs
C
2222
Burs
2222
Burs
D
836
Burs
A3a
A2a
A3a
836
Burs

Figure II.7: Schematic representation of the expression of splice-trap line reporters within CCAP-positive neurons. (A) Four splice-trap lines drove expression in the CCAP neurons in both the brain lobes (or subesophageal ganglia) and the VNC. (B) Ten lines displayed colocalization with the CCAP neurons only in selected cells in the VNC. (C) Three lines drove expression in selected CCAP neurons only in the brain lobes. Colocalization and staining intensities were determined based on examination of optical sections within confocal z-series image stacks. Relative reporter intensities are represented as shown in the key.

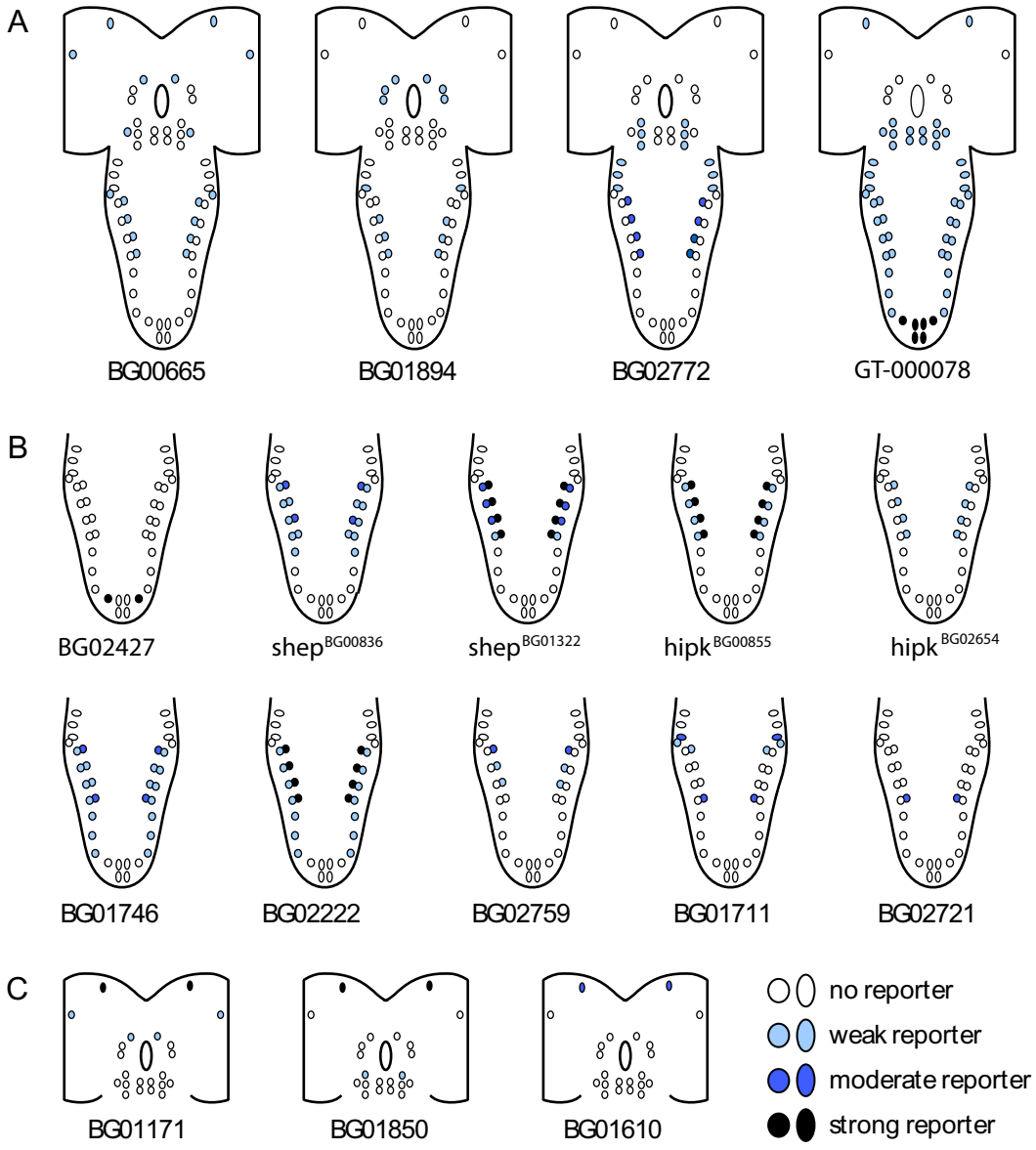
A
BG00665
BG01894
BG02772
GT-000078
B
BG02427
shep BG00836
shep BG01322
hipk BG00855
hipk BG02654
BG01746
BG02222
BG02759
BG01711
BG02721
C
BG01171
BG01850
BG01610
no reporter
weak reporter
moderate reporter
strong reporter

Figure II.8: Colocalization of selected splice trap expression patterns with dILP2. (A) Schematic of anti-dILP2 immunostaining in the third instar larval CNS. Filled (purple) circles, strongly dILP2-immunoreactive cells; purple lines, neurite projections to the ring gland. (B) *BG00836* (green, 836) drove strong UAS-mCD8::GFP expression in all seven dILP2-positive IPCs (magenta, dILP2) in each brain lobe and in many dILP2-negative cells. (C) *BG02836* (green, 2836) was expressed strongly in two of the seven IPCs (magenta, dILP2) and weakly in the others. *BG02836* was also expressed in the mushroom bodies (MB) and some dILP2-negative cells. (D) *BG01850* (green, 1850) was expressed at moderate levels in all the IPCs (magenta, dILP2) and strongly in the SP1 cells, and it was also expressed in many dILP2-negative neurons. (E) *BG02721* (green, 2721) was expressed in all the IPCs (magenta, dILP2) and many brain lobe glia. (F) *BG00449* (green, 449) was expressed in all IPCs (magenta, dILP2) and some brain lobe glia. In addition, *BG00449* displayed very strong expression in the prothoracic gland (PG) cells. Arrows, co-localization of reporter gene expression and anti-dILP2 immunostaining in somata and neurites; arrowheads, reporter gene expression in dILP2-negative cells; asterisks, reporter expression in glial cells. Bars: B, 20µm; C-F, 50µm.

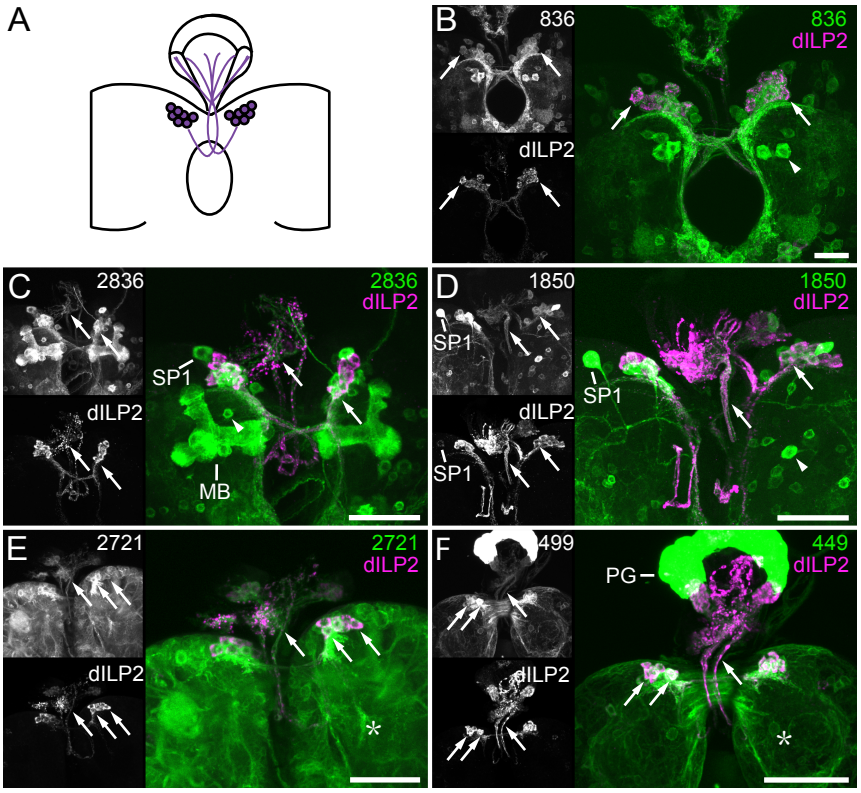
A
B
836
836
dILP2
dILP2
C
2836
2836
dILP2
dILP2
SP1
MB
D
1850
1850
dILP2
SP1
SP1
dILP2
SP1
E
2721
2721
dILP2
dILP2
*
F
499
449
dILP2
PG
dILP2
*

Figure II.9: Colocalization of selected splice-trap lines with LK. Four selected BG insertions drove strong UAS-mCD8::GFP expression (green) in the LK neurons (magenta, LK) in the VNC. In addition to LK neurons, *BG00836* (836) (A), *BG02721* (2721) (C) and *BG02836* (2836) (D) also drove reporter expression in 2-3 adjacent non-LK neurons in each abdominal segment. *BG01850* (1850) (B) expression was more specifically (though not exclusively) restricted to the LK neurons. Arrows, colocalization of reporter and LK. Arrowheads, reporter expression in LK-negative cells. Bars, 50μm.

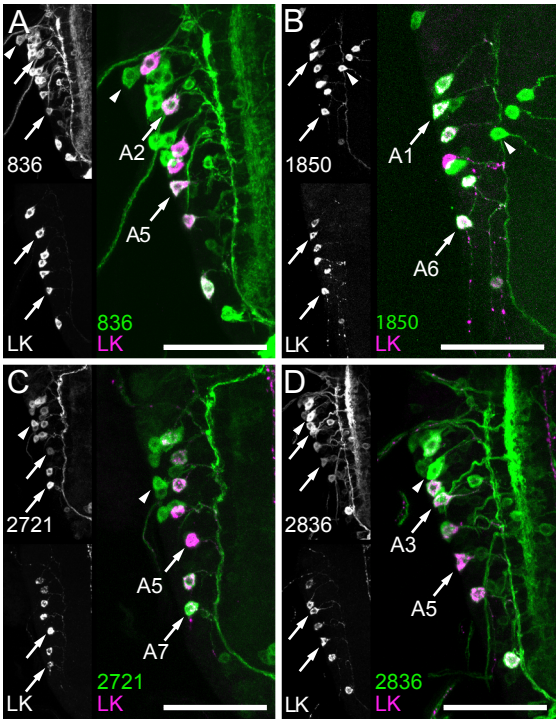
A
836
A2
A5
LK
836
LK
B
1850
A1
A6
LK
1850
LK
C
2721
A5
A7
LK
2721
LK
D
2836
A3
A5
LK
2836
LK

Figure II.10: Expression of *BG00836* and *BG01322* in –RFamide-positive and Furin-1-positive cells. *BG00836* (green, 836) (A) and *BG01322* (green, 1322) (B) both drove UAS-mCD8::GFP expression in the Tv neurons and two –RFamide-positive cells (magenta, PT2) in the superior protocerebrum (SP3). In the brain lobes, *BG00836* is also expressed in lateral protocerebrum neuron (LP1). (C, D) ventral view of the colocalization in the VNC of *BG00836* (C) and *BG01322* (D) with Furin1 (magenta, Furin1) in the Tv and Tvb neurons. (E, F) dorsal view of *BG00836* (E) and *BG01322* (F) expression in the dorsal chain (d1-d11) of Furin1-positive neurons in the VNC. Arrows, colocalization of reporters with neuropeptide markers. Arrowheads, reporter expression in PT2- or Furin1-negative cells. Bars, 50μm.

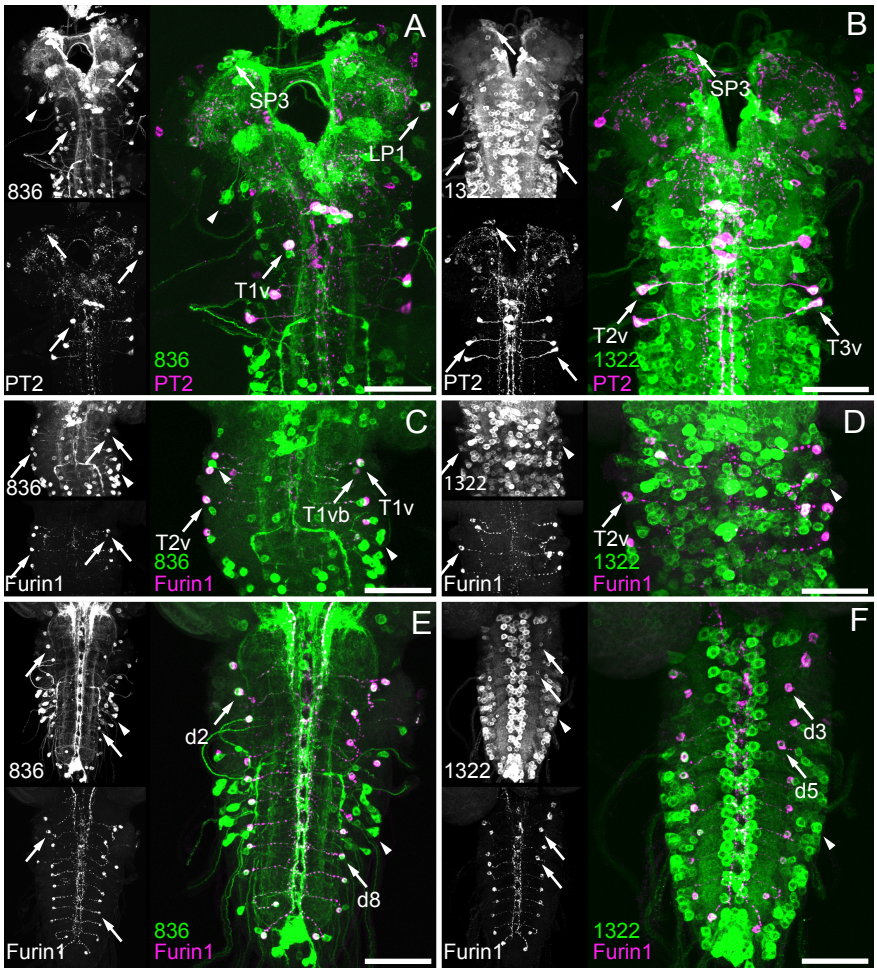
A
SP3
LP1
836
T1v
PT2
836
PT2
B
SP3
1322
T2v
T3v
PT2
1322
PT2
C
836
T1vb
T1v
T2v
Furin1
836
Furin1
D
1322
T2v
Furin1
1322
Furin1
E
836
d2
d8
Furin1
836
Furin1
F
1322
d3
d5
Furin1
1322
Furin1

Figure II.11: Genomic organization of *alan shepard* (*shep*). The *shep* gene encodes five known transcripts, *RA-E*. The start sites for each of the transcripts are indicated with arrows. The 12th exon (asterisk) of *shep* is shared by all five isoforms. However, in *RA* and *RC* exon 12 is 33bp shorter due to the use of an upstream splice donor site. The genome insertion sites for the *BG01322* and *BG00836* splice trap insertions (BELLEN *et al.* 2004b) and the *G00261* protein trap insertion (MORIN *et al.* 2001) are indicated as triangles. The regions deleted by the *Exel6103*, *Exel6104*, and *ED210* deficiencies are indicated with horizontal gray bars below the transcripts, with arrows indicating extension of the deletions beyond the region shown.

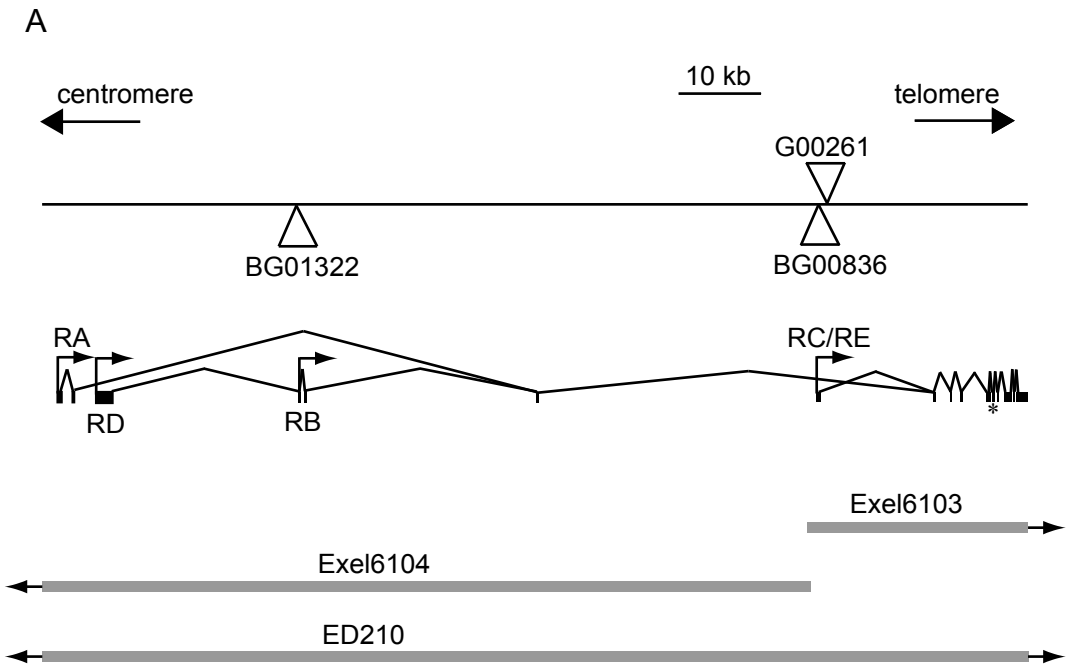
A
centromere
10 kb
telomere
G00261
BG01322
BG00836
RA
RC/RE
RD
RB
*
Exel6103
Exel6104
ED210

Figure II.12: Expression pattern of the protein trap line *shep*^{G00261} in CNS neurons. (A) *shep*^{G00261} (GFP, green) was expressed ubiquitously in CNS neurons. The neuronal expression of *shep*^{G00261} was indicated by the colocalization of the reporter with BURS (BURS antiserum, magenta). (C-D) Higher magnification image of boxed area in (A), showing the expression of *shep*^{G00261} reporter in BURS-positive neurons (arrows). *shep*^{G00261} also drove expression ubiquitously in CNS BURS-negative neurons (arrowheads). Bars: A, 50µm; C-D, 10µm.

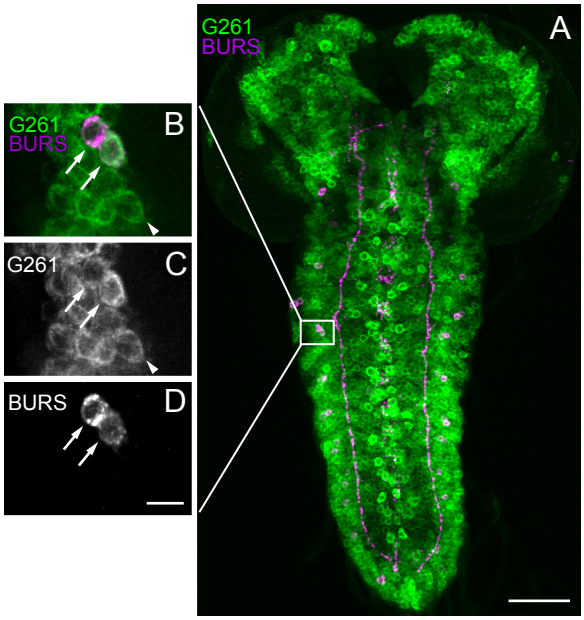
G261
BURS
A
G261
BURS
B
G261
C
BURS
D

Figure II.13: Both *shep*^{BG00836} and CCAP neuron-specific expression of *shep*^{RNAi} led to reduced CNS neurites and reduced extent of the peripheral axonal arbor of BURS-positive neurons. (A) *shep*^{BG00836}/+ animals showed extensive neurite outgrowth at both thoracic segment (arrow) and the longitudinal axonal projections (arrowheads) of BURS-positive neurons (BURS antiserum) in the CNS. (B) The splice trap line *shep*^{BG00836}/*shep*^{BG00836} displayed reduced thoracic arbor. (C-D) CCAP neuron-specific expression of *shep*^{RNAi} (*CCAP-Gal4>UAS-shep*^{RNAi}) (D) led to a reduced neurite arborization (arrows) and more weakly labeled longitudinal projections (arrowheads) compared to the heterozygous controls, *UAS-shep*^{RNAi}/+ (C). (E-F) *CCAP-Gal4>UAS-shep*^{RNAi} (F) animals had a reduced peripheral axon arbor compared to the heterozygous controls, *UAS-shep*^{RNAi}/+ (E). Bars: A-D, 50µm; E and F, 200µm.

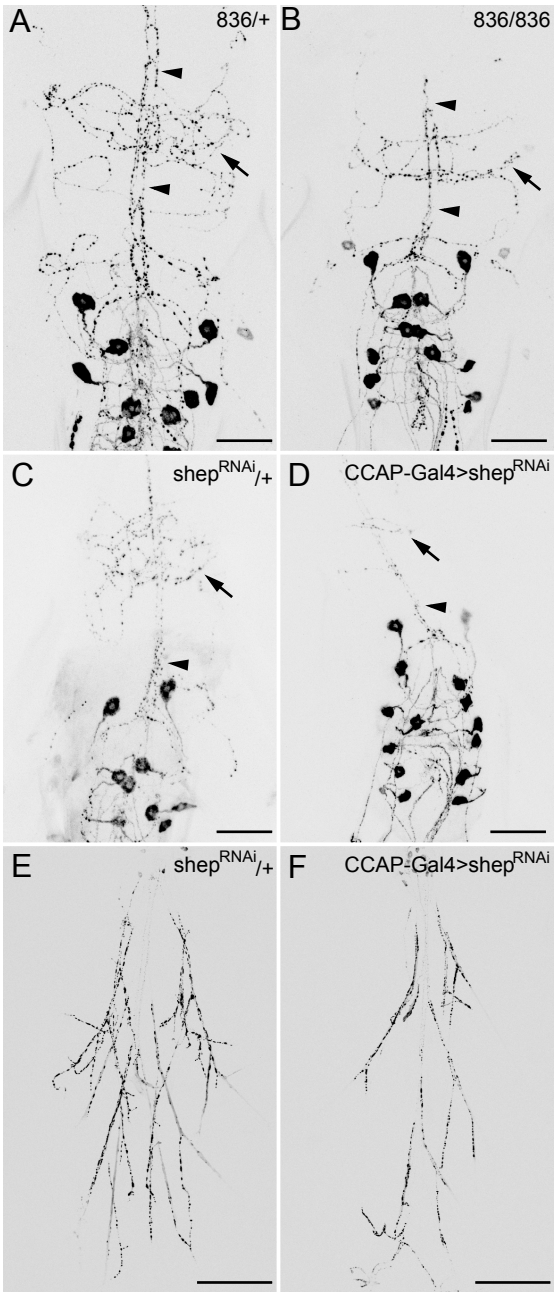
A
836/+
B
836/836
C
shep^RNAi/+
D
CCAP-Gal4>shep^RNAi
E
shep^RNAi/+
F
CCAP-Gal4>shep^RNAi

Figure II.14: <u>*shep*^{BG00836} displayed reduced starvation resistance, and the phenotype was reverted by precise excision of the P-element.</u> 2-day-old females of each genotype were tested for their survival during starvation in vials with 1.5% agar (to provide only moisture but no food). The numbers of surviving flies were counted at 4-hour intervals. (A) *BG00836* (*shep*^{BG00836}) (n=100) showed decreased starvation resistance and died (50% lethality) ~9 hours earlier than *shep*^{BG01322} (n=110) and the control *w*^{1118}*;Iso2A; Iso3A* (n=110) flies. (B) Removal of the *BG00836* insertion rescued the mutant phenotype. *shep*^{Rev6}, which is a precise excision of the *BG00836* P-element, showed normal starvation resistance. *shep*^{BG00836} adults (n=80) died (50% lethality) at around 22 hours after starvation, while 50% of the *shep*^{Rev6} animals (n=60) died at 38 hours after starvation. All other control genotypes, *shep*^{BG00836} */TM3, Ser, Act-GFP* (n=110), *shep*^{BG00836}*/Rev6* (n=110), and *Rev6*/*TM3, Ser, Act-GFP* (n=110) died at 39-41 hours after starvation. The data in (A) and (B) were collected at different times and are not directly comparable to each other.

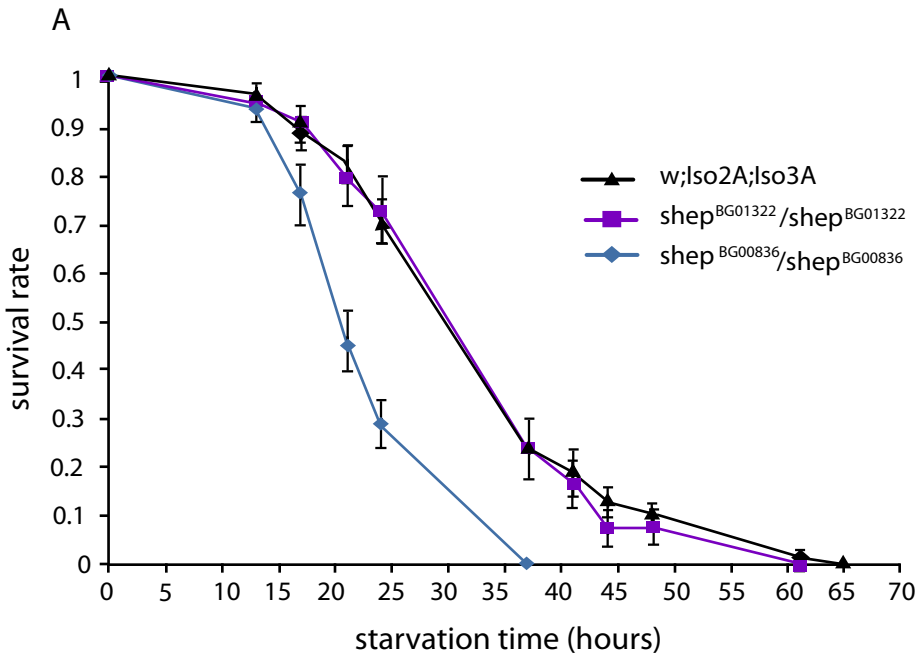
A
survival rate
starvation time (hours)
w;Iso2A;Iso3A
shep BG01322 /shep BG01322
shep BG00836 /shep BG00836

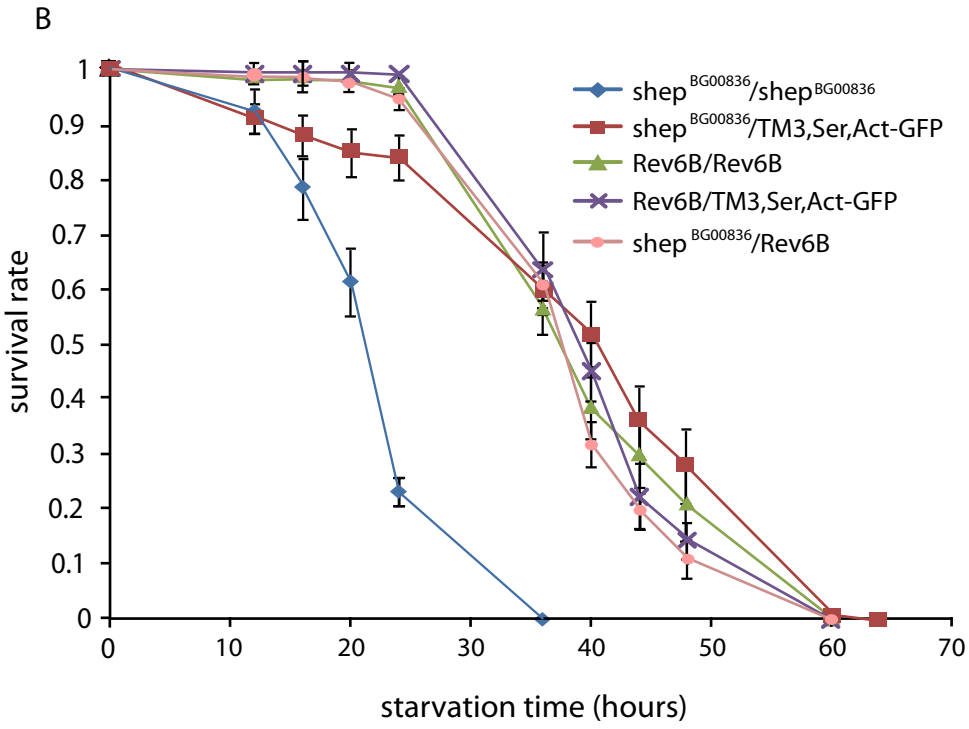
B
survival rate
starvation time (hours)
shep BG00836 /shep BG00836
shep BG00836 /TM3,Ser,Act-GFP
Rev6B/Rev6B
Rev6B/TM3,Ser,Act-GFP
shep BG00836 /Rev6B

Figure II.15: The starvation resistance phenotype of *shep*^{BG00836} was closely linked to the genetic background. The starvation resistance defect of the original *shep*^{BG00836} (n=123) persisted in this experiment (50% lethality at 30 hr after starvation). However, after seven generations of outcrossing of the *shep*^{BG00836} flies with the *w; Iso2A; Iso3A* flies, the outcrossed *shep*^{BG00836} (*shep*^{BG00836OX}/*shep*^{BG00836OX}) adults (n=18) showed almost normal starvation resistance (50% lethality at 66 hr after starvation) that was equivalent to that of the *w; Iso2A; Iso3A* control flies (n=139) (50% of lethality at 70 hr after starvation) and much greater than that of the *shep*^{BG00836}/*shep*^{BG00836} flies. In addition, the times at which we observed 50% lethality of transheterozygote *shep*^{BG00836OX} /deficiency flies [*shep*^{BG00836OX}/*ED210* (n=21), *shep*^{BG00836OX}/*Exel6103* (n=39), and *shep*^{BG00836OX}/*Exel6104* (n=38)] were all within the range of 66-72 hr. The *Rev6B*/*shep*^{BG00836OX} adults (n=63) displayed the strongest starvation resistance (50% lethality at 82 hr after starvation).

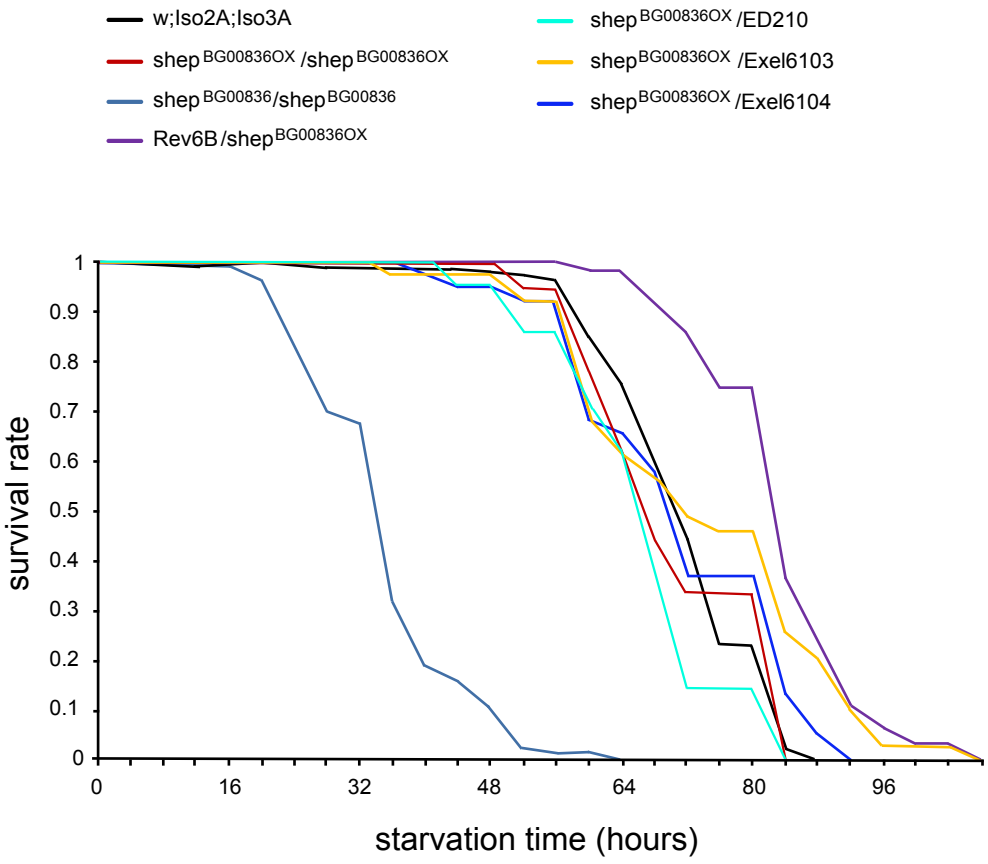
w;Iso2A;Iso3A
shep BG00836OX /shep BG00836OX
shep BG00836/shep BG00836
Rev6B/shep BG00836OX
shep BG00836OX /ED210
shep BG00836OX /Exel6103
shep BG00836OX /Exel6104
survival rate
1
0.9
0.8
0.7
0.6
0.5
0.4
0.3
0.2
0.1
0
0
16
32
48
64
80
96
starvation time (hours)

Chapter III

A Drosophila enhancer trap and splice trap screen for endocrine regulators of ETH expression

ABSTRACT

Each ecdysis in the insect life cycle is coordinated by the hierarchical secretion of neuropeptides and peptide hormones in response to the declining titer of circulating 20-hydroxyecdysone (20HE). The synthesis and release of one of these peptides, ecdysis triggering hormone (ETH), from the endocrine Inka cells of the epitracheal glands is crucial to the initiation of molting behavior. To identify genes contributing to 20HE regulation of ETH synthesis and secretion, we screened through 267 enhancer trap and 545 splice trap lines for genes with Inka cell expression in Drosophila. We also screened for expression in the other three epitracheal gland cells. Six of the enhancer trap lines and 8 splice trap lines displayed expression in the Inka cells or other cells of the epitracheal gland. One of the identified genes with Inka cell expression encodes taiman (TAI), an EcR transcriptional coactivator. Inka cell-targeted RNA interference (RNAi) for *tai* resulted in markedly reduced levels of ETH transcripts and ETH protein. In contrast, secretory granule exocytosis was essentially normal following tai^{RNAi}, since we observed the depletion of anti-peptidylglycine-α-hydroxylating monooxygenase (PHM) immunoreactivity in >90% of the Inka cells at pupal ecdysis. The levels of TAI protein during the first 12 hours of metamorphic development tracked the 20HE titer. Based on these and other findings, we propose a model in which the ecdysone receptor, TAI, the basic-leucine zipper transcription factor cryptocephal, and ultraspiracle form a complex on the promoter region of *ETH* gene to activate *ETH* transcription.

INTRODUCTION

During their life cycle, insects must go through several molts in order to grow in size. During this process, a new, bigger cuticle grows underneath the old one. The inner layer of the old cuticle is then partially digested and reabsorbed. At the end of each molt, the animal then sheds the old cuticle through a set of stereotyped behaviors which is called ecdysis. Successful ecdysis is critical for the survival of the animal (EWER and REYNOLDS 2002). In Chapter 1 of this dissertation, I reviewed the behavioral processes and hormonal regulatory cascade at ecdysis. Here I focus on some of the molecular mechanisms of ecdysis regulation through the control of ETH expression and secretion from the Inka cells.

Molting in insects is initiated by rising levels of steroid hormones, the ecdysteroids, which is produced and secreted from the prothoracic gland. One of the metabolites of ecdysone, 20-hydroxyecdysone (20HE), is the major active form of ecdysteroid involved in the controlling of the molting process (RIDDIFORD 1993). The late behavioral events in the molt are coordinated by 20HE-dependent secretion of neuropeptides and peptide hormones (peptide transmitters). The hierarchical release of a series of peptide transmitters is critical to timely initiation of each step of the ecdysis process. Known and well-studied peptide transmitters that are involved in the regulation of ecdysis are corazonin (KIM *et al.* 2004), eclosion hormone (EH) (HORODYSKI *et al.* 1993), pre-ecdysis triggering hormone (PETH), ecdysis triggering hormone (ETH) (PARK *et al.* 2002), and crustacean cardioactive peptide (CCAP) (PARK *et al.* 2003).

Although all of the above mentioned peptides can stimulate ecdysis or pre-ecdysis in various insects, some are dispensable. For example, targeted ablation in Drosophila CCAP neurons (PARK *et al.* 2003) has little or no effect on ecdysis at some stages and only modest effects on others, suggesting that other complementary or parallel signals exist. However, one peptide hormone, ETH, is critical for ecdysis (PARK *et al.* 2002). It is therefore important to understand the regulation of ETH signaling. The endocrine cells that produce and secrete ETH, the Inka cells, are experimentally accessible. There are only 14 Inka cells, and each is located in an isolated epitracheal gland (EG) situated on the surface of the tracheae. Thus, the Inka cells are an excellent model for understanding the regulation of peptide hormone signaling through the coordinated actions of steroids and other inputs.

Currently, we know that in the tobacco hawkmoth, *Manduca sexta,* the Inka cells respond to 20HE titer in two ways. A high 20HE titer, during the early stages of a molt, signals to the Inka cells to stimulate the synthesis and storage of ETH (ZITNAN *et al.* 1999; ZITNANOVA *et al.* 2001). The declining titer of 20HE later in the molt renders the Inka cells competent to secrete ETH in response to other signals such as peptide transmitters or perhaps local conditions of the cuticle (EWER *et al.* 1997; KINGAN and ADAMS 2000; KINGAN *et al.* 1997; ZITNAN *et al.* 1999). In Drosophila, genetic evidence supports the above model of 20HE-regulated *ETH* expression. Mutants of the ecdysone receptor (EcR) isoforms B1 and B2 (BENDER *et al.* 1997; SCHUBIGER *et al.* 1998), *ultraspiracle* (*USP*) mutants (ORO *et al.* 1992; PERRIMON *et al.* 1985), and larvae with ecdysteroid synthesis defects (FREEMAN *et al.* 1999; VENKATESH and HASAN 1997) all display ecdysis defects. However, we do not know

whether these ecdysis defects are directly related to ETH signaling, and we have little information about the cellular and molecular mechanisms controlling ETH synthesis and secretion.

Previous work in our lab showed that the basic-leucine zipper (bZIP) transcription factor, *cryptocephal* (*crc*), is required for normal *ETH* expression in the Inka cells (GAUTHIER and HEWES 2006). *crc* mutant larvae showed markedly decreased *ETH* mRNA and protein levels, and ecdysis-associated morphological defects were observed in *crc* mutants at both the larval and pupal stages (GAUTHIER and HEWES 2006; HEWES *et al.* 2000). Sequence analysis of the *ETH* promoter region revealed a conserved, putative binding site for CRC and a putative ecdysone responsive element (DR4), which may be a binding site for EcR and its heterodimeric partner USP (GAUTHIER and HEWES 2006; PARK *et al.* 1999). The CRC binding site and DR4 elements in the *ETH* promoter partially overlap, suggesting that CRC and EcR/USP may compete or may form a complex on the *ETH* promoter (GAUTHIER and HEWES 2006).

Recent yeast two hybridization, co-immunoprecipitation, and genetic interaction results suggest a direct interaction between CRC and EcR-B2 (GAUTHIER 2008). This interaction requires the leucine zipper of CRC and the N-terminal, isoform-specific activation function 1 (AF1) of EcR-B2. These findings implicate CRC and EcR in the control of *ETH* transcription. However, the precise molecular mechanisms for the regulation of *ETH* expression remain unclear.

In an effort to identify more factors that might function in controlling ETH synthesis or ETH secretion from the Inka cells, including possible regulatory factors

involving the associated EG cells, we performed an enhancer trap and splice trap screen for genes with expression in the Inka cell and other cells of the EG. We screened through 545 splice-trap and 267 enhancer trap lines and identified 6 enhancer trap lines and 8 splice trap lines with Inka or other EG cell expression. We confirmed Inka cell expression by anti-PETH immunostaining (ZITNAN *et al.* 1999). One of the other three EG cells, PMa, expresses the 36Y-Gla4 marker, and we confirmed expression in the PMa cell by crossing the lines to 36Y-Gal4 (GAUTHIER 2008; O'BRIEN and TAGHERT 1998). One of the insertion lines, *BG01746*, which is inserted in the EcR coactivator *taiman* (*tai*), showed mild larval ecdysis and adult wing expansion defects. We obtained Inka cell specific expression of *UAS-tai*^{RNAi} using a second line identified in our screen, *BG00690*. The *tai*^{RNAi} resulted in ecdysis defects and decreased *ETH* mRNA and ETH protein expression in larvae. Our current data, in combination with other recent research results (BAI *et al.* 2000; GAUTHIER 2008; GAUTHIER and HEWES 2006), support a model in which TAI, EcR, USP, and CRC form a complex together, perhaps on the conserved sequences in the *ETH* promoter, to activate *ETH* expression.

MATERIALS AND METHODS

Fly stocks: Flies were cultured on standard cornmeal-yeast-agar media at 25°C. The splice trap (prefix "BG") lines (LUKACSOVICH *et al.* 2001), enhancer-trap (prefix "PL") lines (HORN *et al.* 2003b) and most other stocks were obtained from the Bloomington Drosophila Stock Center (Indiana University, Bloomington, IN). *UAS-RNAi* lines were obtained from the Vienna Drosophila RNAi Center (VDRC, Vienna, Austria).

Screening for EG expression: Each BG line was crossed to *UAS-mCD8::GFP*, and each PL line was crossed to *UAS-DsRed* to reveal the splice trap or enhancer trap pattern. Third instar larvae were collected from apple juice–agar egg-collection plates supplemented with yeast paste, washed briefly in saline, mounted under coverslips with 70% glycerol, and then placed at -20^{o}C for about 30 minutes. After subsequent thawing, we observed the whole larvae by compound epifluorescence to detect GFP or DsRed expression in the EG. *BG>mCD8::GFP* or *PL>DsRed* larvae obtained from crosses with fluorescence in the epitracheal gland were fillet dissected in calcium-free saline [182 mM KCl, 46 mM NaCl, 2.3 mM $MgCl_2 \cdot 6H_2O$, 10 mM 2-amino-2-(hydroxymethyl)propane-1,3-diol (Tris), pH=7.2] and processed for immunocytochemistry.

Immunocytochemistry: Immunostaining was performed as described (BENVENISTE *et al.* 1998; HEWES *et al.* 2003). We fixed the tissues for 1 hr at room temperature (RT) in 4% paraformaldehyde (PFA), 4% paraformaldehyde/7% picric

acid (PFA-PA), or Bouin's fixative. Primary rabbit antisera (or mouse, as indicated) to the following proteins were used: PETH (1:2000, PFA) (PARK *et al.* 2002; ZITNAN *et al.* 1999), TAI (1:500, PFA) (BAI *et al.* 2000), PHM (1:750, Bouin's) (JIANG *et al.* 2000), and GFP (mouse 1:500) (Invitrogen, Carlsbad, CA). The secondary antibodies were goat Cy3 or Alexa 488 conjugates (Jackson ImmunoResearch, West Grove, PA) and were used at a 1:500 dilution. We obtained confocal z-series projections using an Olympus Fluoview FV500 microscope (Olympus, Center Valley, PA).

***In situ* hybridization:** An ETH cDNA probe was synthesized previously in our lab (GAUTHIER and HEWES 2006). Whole mount larval *in situ* hybridization was performed as described (HEWES *et al.* 2003). Brightfield images were obtained using an Olympus BX51 microscope (Olympus, Center Valley, PA) and an Olympus DP70 camera (Olympus, Center Valley, PA).

Lethal phase analysis: Hatchlings, newly ecdysed small 2nd instar larvae and small 3rd instar larvae were transferred onto new egg plates (1st and 2nd instar larvae) (150 larvae per plate) or into vials (3rd instar larvae, 50 larvae per vial). After growth, we counted the numbers of animals that successfully made it into the next developmental stage. The vials containing the 3rd instar larvae were also used to assay for pupal and adult ecdysis defects.

RESULTS

Identification of lines with EG expression: To screen for genes that are expressed in the EG, we crossed 545 *P{GT1}* insertions (prefix "BG") (LUKACSOVICH *et al.* 2001) to *yw; UAS-mCD8::GFP* flies, and crossed 267 *PBac{GAL4D,EYFP}* insertions (prefix "PL") (HORN *et al.* 2003a) to *w,UAS-DsRed; UAS-DsRed; UAS-DsRed* flies. We used DsRed to reveal the PL expression patterns because of the constitutive expression of EYFP that is driven by the PL element (HORN *et al.* 2000; HORN *et al.* 2003a). Although we didn't observe EYFP signals in the EGs with the PL lines, the DsRed facilitated a more complete description of each reporter expression pattern.

We identified 6 PL and 8 BG lines that drive expression in the Inka cells and/or the other cells in the EG (Table III.1). In addition to the Inka cell and PMa, we found two other cells in each gland, which we named PMb and PMc (Figure III.1). We confirmed expression in the Inka cells with an antiserum directed against *Manduca sexta* pre-ecdysis triggering hormone (PETH) which specifically labels amidated Drosophila ETH (PARK *et al.* 2002; ZITNAN *et al.* 1999). Expression in the PMa cell was confirmed by crossing the BG or PL lines with *yw, UAS-ANF::GFP;; 36Y* flies, which drive reporter gene expression (RAO *et al.* 2001) in both the PMa and Inka cell (O'BRIEN and TAGHERT 1998). If a line had expression in PMb and PMc, then we expected to see more than two ANF::GFP-positive cells with the two Gal4 drivers together. Three reporters, *BG00690*, *PL00407* and *PL00571*, were expressed only in the Inka cells within the EG (Table III.1). Expression of *PL00407* and *PL00571* in other tissues was not recorded because of the wide EYFP expression

driven by the 3XP3 promoter in the PL insertions. EYFP expression was observed in multiple tissue including the Bolwig organ, CNS, PNS, hindgut and anal plates (HORN *et al.* 2000) and the EYFP signal is observable under our current filter settings for DsRed detection. *BG00690* was expressed exclusively in the Inka cells (Figure III.1A). In fillets of third instar *CG10133*^{BG00690}*>UAS-mCD8::GFP* larvae, no other tissues or cell types showed detectable reporter gene expression with *CG10133*^{BG00690}, so we used it as an Inka cell-specific driver in subsequent experiments.

Expression of two lines, *BG01100* and *BG02781* (Figure III.1B) was restricted in the EG to the PMa cell. Five insertions, *BG01746*, *BG02820*, *PL00112*, *PL00408*, *PL00467*, and *PL00571* were expressed in both the Inka cell and PMa (Figure III.1C and Table III.1). *BG00665*, *BG01673*, and *BG02759* were expressed in all four of the EG cells (Figure III.1D and Table III.1). In addition, *BG02759* was also expressed in tracheal cells. The finding of a total of 4 EG cells is consistent with an ultrastructural study in the gypsy moth, *Lymantria dispar* (KLEIN *et al.* 1999), and another recent study in Drosophila (CHANG *et al.* 2009).

In addition to the expression in the EG, *BG00665*, *BG01100*, and *BG01673* were expressed in many other tissues, including the epidermis, central nervous system (CNS), peripheral nervous system (PNS), heart, trachea, muscle, and fat body; *BG02781* was expressed in muscle and epidermis (data not shown). *BG02820* was expressed in the CNS and PNS. *BG01746* was expressed in the CNS, salivary gland, heart, and oenocytes.

Genes that are affected by the splice or enhancer trap insertions: As described in chapter II, when a BG element is inserted inside the intron or exon of a

gene, and also in the correct orientation, the Gal4 expression pattern usually matches that of the native transcript(s) (LUKACSOVICH *et al.* 2001). We analyzed the insertion sites for the 8 BG lines with EG expression. Six lines (*BG00665*, *BG01100*, *BG01746*, *BG01673*, *BG02759*, and *BG02820*) are inserted in the correct orientation in the intron of individual genes (Table III.1).

For two other lines (*BG00690* and *BG02781*), our identification of the affected genes is tentative. Presumably due to problems with the *BG00690* insertion site determination, this is the only BG insertion that is not reported on FlyBase. Although the reported 5' flanking sequence showed that it might be in right orientation for a splice trap of *CG10133* (it is 1539bp 5' of *CG10133*), this site is also immediately upstream (3-47bp) of the EH receptor (HER) encoded by *CG10738* (CHANG *et al.* 2009). *BG02781* is inserted in the 1st exon (5' UTR) of *relative of woc* (*row*), but it is in the wrong orientation for a splice trap insertion.

Enhancer-trapped reporter expression is under the influence of the regulatory sequence of the genes in the vicinity of the insertion, so the expression pattern revealed by the enhancer trap very likely represents the expression of one or more nearby enhancers (BELLEN *et al.* 1989; BRAND and PERRIMON 1993; O'KANE and GEHRING 1987). Five of the PL insertions (*PL00407*, *PL00408*, *PL00467*, *PL00566* and *PL00571*) that displayed EG expression were inserted in introns of a gene (CG2246, *Tyramine receptor* (*TyR*), CG42268, *Furin 1*, *Guanylyl cyclase* β*-subunit at 100B* (*Gyc*β*100B*), respectively) (Table III.1), so these genes were tentatively identified as the trapped loci. One insertion, *PL00112*, was inserted between

annotated genes, so we choose the closest gene (*CG14910*, ~19kb from the insertion) as the candidate trapped gene (Table III.1).

Together, the splice trap and enhancer trap insertions appear to report on the expression of a group of 16 genes in the EGs.

Analysis of ecdysis: ETH is the only known peptide hormone that is expressed in the EG. Disruption of ETH production usually leads to ecdysis defects and lethality in Drosophila (PARK *et al.* 2002). We reasoned that genes that are expressed in the Inka cell or the other three cells in the EGs may have direct or indirect effects on ETH expression. Therefore, mutants of those genes may produce ecdysis defects. Because BG splice trap-element insertions can interrupt normal gene splicing and therefore gene function (LUKACSOVICH *et al.* 2001), we surveyed homozygous insertion animals for ecdysis defects or other mutant phenotypes (Table III.2). Enhancer trap insertions can also disrupt trapped genes (HORN *et al.* 2003a), albeit with less efficiency, and we examined these as well. Of the 14 lines, 10 showed some lethality. One, $tai^{BG01746}$, produced dead larvae (1%) with a "buttoned-up" phenotype (PARK *et al.* 2002), in which animals retained mouthparts and external cuticles from the previous stage. Many of the surviving $tai^{BG01746}$ adults had partially expanded wings (16%) and tanning defects (10%). Adult $row^{BG02781}$ homozygotes also had defects in wing expansion and tanning.

Inka cell knock-down of *tai* led to ecdysis defects: To test for possible functions of the identified genes in the regulation of ETH expression or secretion, we

obtained *UAS-RNAi* lines from the Vienna Drosophila Stock Center (Vienna, Austria) for eight of the genes: *CG10133*, *CG32044*, *chif*, *fur1*, *row*, *tai*, *tara*, and *tyr*. These genes were selected based on their expression patterns and in some cases on predicted functions in *ETH* regulation (see discussion). We used *BG00690* as the Gal4 driver to obtain Inka cell-restricted RNAi, and we examined whole animal phenotypes at all developmental stages. In addition, we used *yw, UAS-ANF::GFP;;36Y-Gal4* to drive *UAS-row*^{RNAi} in both the Inka and PMa cells, since *row*^{BG02781} showed PMa expression. The Inka- or PMa-targeted RNAi for seven out of the eight genes did not produce any observable mutant phenotypes. In contrast, *tai*^{RNAi} produced 37% lethality (Figure III.2A). Most of the *BG00690>tai*^{RNAi} animals completed larval ecdysis, although 1% died at the 1st to 2nd instar ecdysis (n=150), and 6% died at the 2nd to 3rd instar ecdysis (n=150), most with a buttoned-up phenotype (Figure III.2B). Another 6.5% of 3rd instar larvae died prior to pupariation (n=200). Of the animals that pupariated (n=187), 37% died, many with uneverted or partially everted head structures, shortened legs and wings, and a more anterior position of the legs and wings than wild type. These pupal defects result from failures to complete head eversion (HEWES *et al.* 2000; PARK *et al.* 2003; ZHAO *et al.* 2008) (Figure III.2C). All of the surviving adults expanded their wings and tanned normally. These findings revealed a role for TAI in the Inka cells in controlling processes important for the successful completion of larval and pupal ecdysis.

***Tai* regulates ETH expression**: ETH is expressed in the Inka cells and is essential for the completion of each ecdysis in Drosophila. To determine if the ecdysis

defects observed in Inka cell-specific *tai* RNAi animals were due to low ETH levels, we examined the expression of ETH by *in situ* hybridization and immunostaining. Using an *ETH* antisense cDNA probe (GAUTHIER and HEWES 2006), we performed *in situ* hybridization in *BG00690/+* (n=9), *UAS-tai*^{RNAi}/+ (n=7), and *BG00690>UAS-tai*^{RNAi} small 3rd instar larvae (Figure III.3A). The *BG00690>UAS-tai*^{RNAi} larvae were split into two groups based on whether they displayed the buttoned-up phenotype (n=6) or had completed the ecdysis to the 3rd instar (n=7). The *ETH in situ* staining intensity following Inka-cell-targeted *tai* RNAi was substantially decreased, but not eliminated, in both groups of *BG00690>UAS-tai*^{RNAi} larvae. The remaining *ETH* mRNA may have been enough to permit ecdysis in some of the larvae, since the ecdysis defects were not fully penetrant (see above). Anti-PETH immunostaining (PARK *et al.* 2002; ZITNAN *et al.* 2003) in *BG00690>UAS-tai*^{RNAi} animals (8 with multiple mouth-parts and 7 that had completed ecdysis) also showed a substantial reduction in the ETH protein level (Figure III.3B). These results indicate that TAI regulates *ETH* transcription or *ETH* mRNA stability, although we cannot rule out an additional, direct effect on ETH protein levels.

The pattern of *tai*^{BG01746} included expression in several tissues in 3rd instar larvae (see above). To characterize the pattern of TAI expression more fully, we performed anti-TAI immunostaining (BAI *et al.* 2000) at this stage. We found that TAI was ubiquitous in almost all tissues. The protein was restricted to nuclei in most cells. The Inka cells, however, were a notable exception and displayed moderate nuclear and strong cytoplasmic TAI immunoreactivity (Figure III.4). To determine the subcellular localization of the cytoplasmic TAI signal in Inka cells, we performed

anti-TAI immunostaining on cells labeled with 36Y-Gal4-ANF::GFP and confocal imaging. ANF::GFP is a marker that is packaged and transported as a neurosecretory protein (RAO *et al.* 2001). At high magnification, the cytoplasmic TAI signal was heterogenous and strongly colocalized with ANF::GFP (Figure III.4). Therefore, the cytoplasmic TAI staining may reflect cross-reactivity with an unrelated epitope (possibly ETH itself) in the secretory compartment of the Inka cells.

To confirm the specificity of the RNAi for *tai*, we crossed *yw;UAS-mCD8::GFP; 386-Gal4* flies with *w; UAS-tai*^{RNAi} and then performed anti-TAI immunostaining on small 3rd instar larvae. The 386-Gal4 line expresses CD8::GFP strongly in the Inka cells, but it does not drive detectable transgene expression in the other EG cells or neighboring tracheal cells. The cytoplasmic anti-TAI signal in the Inka cells was reduced by *tai* RNAi (data not shown), consistent with cross-reactivity of this antiserum with ETH or another secreted protein. To exclude the cytoplasmic signal, we obtained single confocal sections through the center of the Inka cell nucleus and through neighboring EG cell nuclei as an internal control. Following the *tai* RNAi, the TAI signal in the Inka cell nuclei was reduced by 68% and 70% (n=7), compared to control animals with either *386-Gal4* (n=9) or *UAS-tai*^{RNAi} (n=4) alone (Figure III.5). However, there was also a 29-30% reduction in the TAI signal in the nuclei of the neighboring EG cells, suggesting some leaky expression of the transgene.

***Tai* RNAi did not block ETH release:** TAI has been defined as an ecdysone receptor coactivator (BAI *et al.* 2000). Both ETH transcription and the competence to secrete ETH are regulated by 20HE. Therefore, we asked whether ETH secretion was

disrupted in *BG00690>UAS-tai*^{RNAi} animals. However, because of the marked reduction in ETH protein levels in *BG00690>UAS-tai*^{RNAi} animals, it was necessary to monitor the secretion of an independent secretory marker, PHM. PHM is expressed in the Inka cells and is presumably required for the amidation of ETH (JIANG *et al.* 2000; O'BRIEN and TAGHERT 1998; PARK *et al.* 2004). PHM is also depleted from the Inka cells along with other secretory peptides at ecdysis (O'BRIEN and TAGHERT 1998). Double labeling of the Inka cells with anti-PETH and anti-PHM antiserum showed strong co-localization of the two proteins within the cytoplasm of Inka cells (Figure III.6A). Thus, PHM is likely to be packed together with ETH in secretory granules, as is expected based on studies of the vertebrate homolog (EIPPER *et al.* 1992).

The Inka cells display a rapid and substantial release of PHM and ETH within 30-60 minutes prior to pupal ecdysis (head eversion), about 12 hours after pupariation (O'BRIEN and TAGHERT 1998). Therefore, to assay secretion, we performed anti-PETH immunostaining on fillet preparations staged at 2 hours before and 2 hours after pupal ecdysis. We quantified PHM depletion from the Inka cells by counting the number of visible PHM-positive cells per trachea hemimetamere (per EG) (Figure III.6B) and by measuring the relative staining intensities of the remaining visible Inka cells (Figure III.6C). Most of the Inka cells showed PHM depletion after pupal ecdysis and this was unaffected by *tai* RNAi (Figure III.6B). However, the PHM staining intensity in the remaining, visible Inka cells was higher in *tai* RNAi animals after pupal ecdysis than in controls (Figure III.6C). TAI may play a small role in controlling the extent of PHM depletion. However, these experiments show that TAI

was not essential for the bulk of the PHM release from the Inka cells prior to the pupal ecdysis.

Levels of TAI in Inka cell are correlated with the circulating 20HE titer: In Manduca, at the end of each molt, higher circulating 20HE levels trigger the synthesis of ETH in the Inka cell. Levels of EcR expression in the Inka cells also increase along with the increasing 20HE level and remain at high even when 20HE level begins to subsequently decline (ZITNAN *et al.* 1999). Here, we examined whether levels of the EcR cocativator TAI were also correlated with changes in the 20HE titer. In Drosophila, there are two pulses of 20HE at the onset of metamorphosis, one at puparium formation and a second at head eversion (RIDDIFORD 1993). To determine whether TAI levels fluctuated in the Inka cells during this period, we performed anti-TAI immunostaining at 0hr, 6hr, 9hr, and 12hr APF (Figure III.7). We quantified TAI staining intensity in the nuclei of the Inka cells and neighboring EG cells. In both cells, TAI was at high levels at 0hr APF. By 6 hours APF, TAI levels were much lower and then they increased from 6 to 12 hours APF. Thus, the levels of TAI protein were correlated with the 20HE (RIDDIFORD 1993), suggesting that TAI expression during this period may be steroid-dependent.

Genetic interaction between *tai* and *EcR*: Given that TAI is a transcription coactivator for EcR and the fact that TAI and EcR are both required in the Inka cells for full *ETH* expression, we predicted that mutant alleles for *tai* and *EcR* might display dominant interactions (in transheterozygous animals). We used two EcR alleles, the

EcR-B1/B2 specific EcR^{31} allele and the null EcR^{m554fs} allele. For *tai*, two null *tai* alleles, $tai^{61G1}$and tai^{01351}, and one *tai* deficiency line, *ED678*, were used. Each of the *EcR* alleles was crossed with each of the *tai* alleles to score for lethality. Of all the transheterozygous offspring produced, only EcR^{m554fs}*/ED678* showed mild lethality (data not shown). 67% of EcR^{m554fs}*/ED678* animals died at larval and early pupal stages, with 28% of dead larvae showing a buttoned-up phenotype. To determine whether the buttoned-up phenotype in the EcR^{m554fs}*/ED678* animals resulted from reduced ETH, we performed anti-PETH immunostaining on small 3rd instar larval fillets of EcR^{m554fs}*/ED678* animals and EcR^{m554fs}*/CyO, Ubi-GFP* and *ED678/CyO, Ubi-GFP* controls. We did not observe any difference in PETH staining intensity (data not shown). Therefore, within the Inka cells, the 50% reduction of *EcR* and *tai* gene dosage was insufficient to disrupt ETH expression. However, because EcR and TAI are both widely expressed, the ecdysis defect in these animals may have been the result of other, more dosage-sensitive targets in other locations (e.g. the CNS).

DISCUSSION

Tools for studying cells in the EG: The EG in the gypsy moth, *Lymantria dispar*, consists four cells (KLEIN *et al.* 1999): one big endocrine cell—the Inka cell, one small endocrine cell, one exocrine cell and one duct cell connected to the exocrine cell. It was recently reported that in the oriental fruit fly, *Bactrocera dorsalis*, there are also four cells (Inka cell and three other cells) located in the EG (CHANG *et al.* 2009). With the lines that were identified in our screen, we observed four cells, including the Inka cell, situated in the EG of Drosophila. To our knowledge, our result is the first time that showed the EG in Drosophila also contains four cells, suggesting developmental and functional conservation of the EG.

Of the four EG cells, the Inka cell is the most intensively studied because it is responsible for the production of ETH, a key peptide hormone controlling ecdysis behavior. The PMa cell in Drosophila was also previously identified in *36y-Gal4* (36y) larvae, which have reporter expression in both the Inka and PMa cells (O'BRIEN and TAGHERT 1998). We named the other two cells next to Inka as PMb and PMc, although we do not have markers yet to distinguish these two cells. The functions of PMa, PMb and PMc cells are also unknown.

The PMa and Inka cells: PMa cell expression of the 36y reporter persists during the larval stages and disappears at pupal ecdysis (O'BRIEN and TAGHERT 1998). However, whether the PMa cell itself still exists at this stage remained unclear. By crossing the BG and PL lines that have EG expression with 36y, followed by immunostaining with antiserum to Manduca PETH, we successfully identified 6 (2 BG and 4 PL insertions) lines that were expressed in the both the Inka and the PMa

cell, and two lines (*CG16708*^{BG01100} and *row*^{BG02781}) that were expressed only in the PMa cell within the EG (Table III.1). During our initial analysis, *row*^{BG02781} animals displayed severe (90%) lethality at larval and early pupal stages, and surviving adults displayed wing expansion and tanning defects (Table III.2). We also observed that ~1% of dead *row*^{BG02781} larvae showed a "buttoned-up" phenotypes and we found a correlation between the strength of *row*^{BG02781} reporter expression in the PMa cells and the level of PETH immunostaining level in the adjacent Inka cells (data not shown). This was a repeatable phenotype, but it disappeared for unknown reasons in follow up experiments, and we were unable to pin down the responsible gene(s). We do not know what led to the phenotypic change, but there remains a possibility that the PMa and Inka cells may interact with each other through some unidentified signals. In addition, the identification of the two PMa specific (in the EG) reporter lines: *CG16708*^{BG01100} and *row*^{BG02781}, should provide tools for testing for a possible interaction between the Inka and PMa cells.

PMb and PMc cells: In our screen, we also identified three lines (*CG8963*^{BG00665}, *tara*^{BG01673}, and *PK61C*^{BG02759}) that are expressed in all four of the EG cells. However, we did not observe any lines that had reporter expression in either PMb or PMc, or both, without concurrent reporter expression in the other two cells (Inka and PMa) (Table III.1).

Genes with possible functions in ETH release or synthesis: In Manduca, the bulk of ETH release is triggered by EH (EWER *et al.* 1997; KIM *et al.* 2004; KINGAN *et al.* 1997). Experiments on Drosophila also support such a model (CLARK

et al. 2004; KIM *et al.* 2006). In Manduca, EH acts on the Inka cells and leads to elevated cGMP levels within the cells (KINGAN *et al.* 2001). The increase of cGMP could be a result of the activation of a guanylyl cyclase, either soluble or membrane bound form (LUCAS *et al.* 2000). Research in Manduca supports a model that a soluble guanylyl cyclase is activated by EH and activates a downstream signaling pathway responsible for triggering the major ETH release event (MORTON and SIMPSON 2002). A recent research paper on the oriental fruitfly, *Bactrocera dorsalis*, identified a membrane-bound guanylyl cyclase, BdmGC-1, that acts as a high affinity EH receptor (CHANG *et al.* 2009). Interestingly, we identified two guanylyl cyclase genes that their expression within the EG were only in the Inka cell: one soluble guanylyl cyclase, *Gycβ100B* (reported by insertion *PL00571*), and a membrane-bound guanylyl cyclase, encoded by CG10738 (possibly reported by *BG00690*, see note for table III.1). CG10738 is homologous to the *Bactrocera dorsalis BdmGC-1* gene (CHANG *et al.* 2009). The identification of both soluble and membrane bound guanylyl cyclase in the Inka cell suggests the possibility that EH may act through either Gycβ100B or CG10738, or both in parallel, to initiate the release of ETH from Inka cells. While the targets of cGMP in the Inka cells have not been identified, cGMP is predicted to function through stimulation of a cGMP-dependent protein kinase (PKG) (MORTON and TRUMAN 1988a; MORTON and TRUMAN 1988b).

Interestingly, a second gene that might be reported by *BG00690* insertion, CG10133, encodes a protein orthologous to a vertebrate phospholipase A2 (PLA2G4B). One of the sites of highest PLA2G4B expression in humans is in the pancreas (PICKARD *et al.* 1999), suggesting a conserved endocrine function. However,

because of unknown insertion orientation of the *BG00690* insertion, the expression of *CG10738* or *CG10133* within the Inka cell needs to be confirmed.

We also identified two genes that are candidate regulators of ETH synthesis, the peptide hormone biosynthetic enzyme *Fur1*, and a transcriptional coactivator of EcR, *tai* (BAI et al. 2000; MCDONALD et al. 2003). *Fur1* is a member of the Kex2 family of endoproteases, which cleaves polypeptides at -Lys (K)-Arg (R)- or -R-R- doublets (HAYFLICK *et al.* 1992; ROEBROEK *et al.* 1991). The ETH pro-peptide contains three canonical endoprotease cleavage and amidation sites: GKR, GR and GRR (PARK *et al.* 1999). These sites are potential targets for Fur1 cleavage. *Fur1* is expressed in a specific subset of peptidergic neurons in the CNS (HAYFLICK *et al.* 1992), but a previous report did not find *Fur1* expression in the Inka cells by immunostaining (PARK *et al.* 2004). These conflicting results reflect a difference in sensitivity between these particular markers. Interestingly, there is also uncertainty with regard to the evidence for the expression of *amontillado* (*amon*) (CG6438) in the Inka cells. *amon* is the Drosophila homologue of the vertebrate neuropeptide-processing enzyme PC2 (SIEKHAUS and FULLER 1999). At embryonic stages, *amon* expression was detected in the Inka cells by *in situ* hybridization (SIEKHAUS and FULLER 1999). The 386-Gal4 driver, which is a reporter for *amon* (TAGHERT *et al.* 2001), is expressed in the Inka cells during the larval stages. However, immunostaining with antisera to vertebrate PC2 and Amon did not reveal positive signals in the Inka cells in larvae (PARK *et al.* 2004; RAYBURN *et al.* 2009). This raises the question of whether these subtilisin proteases may function at low

concentrations that are difficult to detect with some markers, and the possible involvement of Fur1 and Amon in ETH processing deserves additional study.

Tai may regulate ETH expression by binding to the EcR/USP complex: The expression of ETH in Inka cell is upregulated by circulating 20HE (GAUTHIER 2008). In Drosophila, the 382-base pair upstream promoter region of *ETH* gene, which contains a putative ecdysteroid responsive element, DR4 (direct repeat 4), is sufficient for activation of *ETH* expression (GAUTHIER and HEWES 2006; PARK *et al.* 2002; PARK *et al.* 1999). However, we do not know the molecular details such as whether there are other factors involved and how the complex functions in the initiation of *ETH* transcription from the promoter. Previous work in our lab showed that the bZIP transcription factor, CRC, is also required for high-level *ETH* expression in the Inka cells (GAUTHIER and HEWES 2006). Sequence analysis of the *ETH* promoter region revealed a conserved, putative binding site for CRC (GAUTHIER and HEWES 2006). The partial overlap of the putative CRC binding site and DR4 elements in the *ETH* promoter suggests that CRC and EcR/USP may compete or form a complex on the *ETH* promoter (GAUTHIER and HEWES 2006). In addition, yeast two hybridization, co-immunoprecipitation, and genetic interaction results suggest a direct interaction between the leucine zipper of CRC and the AF1 domain of EcR-B2 (S.A. Gauthier, L. Cherbas, E. VanHaaften, C. Qu, P. Cherbas, and R.S. Hewes, in prep). Therefore, we propose a model in which CRC and EcR/USP bind as a complex on the *ETH* promoter to control 20E-dependent regulation of *ETH* transcription.

Here, we identified an ecdysone receptor coactivator, TAI, and showed TAI expression in the Inka cells was necessary for elevated *ETH* expression. Immunostaining with an antiserum to TAI (BAI *et al.* 2000) revealed that TAI expression is ubiquitous and includes the Inka cells. Down-regulation of *tai* expression by UAS-RNAi led to reduced *ETH* transcript and ETH protein levels. However, the release of ETH was essentially normal. These results suggest that TAI regulates *ETH* expression at a transcriptional level. TAI and EcR interact directly through the LXXLL domain of TAI and the AF2 domain of EcR, in a ligand (20HE) dependent manner (BAI *et al.* 2000), and this interaction is supported by genetic studies (L. Cherbas, personal communication).

These results lead us to include TAI into the working model for *ETH* transcriptional regulation. In this model, upon the binding of 20HE to the EcR-B2/USP complex, the LXXLL domain of TAI binds to the AF2 domain of EcR-B2 to mediate transcriptional activation at the *ETH* promoter. The leucine zipper of CRC binds to the AF1 domain of EcR-B2, and this may help to stabilize the complex (Figure III.8). Further tests of this model will need to examine whether the complex directly binds to the promoter region of *ETH* gene, and whether these proteins bind or leave the proposed complex in a particular order. In addition, it will be of interest to test whether CRC and TAI are important for isoform-specific actions of EcR-B2 in other tissues.

TABLE III.1

Genes identified in the enhancer and splice trap screen with expression in the epitracheal gland:

Transposon insertion	Gene	Location	Transcripts	Gene product	EG expression
BG00690	*CG10133*	1539bp 5' of the gene (ZHAI *et al.* 2003)		Vertebrate phospholipase A2, group IVB	Inka
PL00407	*CG2246*	Intron	A-M	ribose-phosphate diphosphokinase	Inka
PL00571	*Guanylyl cyclase* β-*subunit at 100B* (*Gyc*β*100B*)	Intron	A	cGMP biosynthesis enzyme	Inka
BG01746	*Taiman (tai)*	Intronic splice trap	A	Ecdysone receptor coactivator,	Inka, PMa

BG02820	*chiffon (chif)*	Intronic splice trap	A, B	Zinc finger in DBF-like proteins (ZnF-DBF)	Inka, PMa
PL00112	*CG14910*	Intergenic, 18.99kb 5' of gene		novel	Inka, PMa
PL00408	*Tyramine receptor (TyrR)*	Intron	A, B	Tyramine receptor	Inka, PMa
PL00467	*CG42268*	Intron	H	novel	Inka, PMa
PL00566	*Furin 1* (*Fur1*)	Intron	A-F	serine-type endopeptidase	Inka, PMa
BG00665	*CG8963*	Intron	A-C	eukaryotic initiation factor 4G (eIF4G)	Inka, PMa-c
BG01673	*taranis (tara)*	Intronic splice trap	A, B	novel trithorax group member	Inka, PMa-c
BG02759	*Protein kinase 61C (Pk61C)*	Intronic splice trap	D	serine/threonine kinase	Inka, PMa-c

BG01100	CG16708	Intronic splice trap	A	Diacylglycerol kinase catalytic domain (DAGKc)	PMa
BG02781	*relative of woc* (*row*)	5' UTR of *row* but in wrong orientation for splice trap insertion	A, B	C2H2 Zn-finger transcription factor	PMa

Note: Except *BG00690*, the insertion sites for all the BG lines are from Lukacosvich et al. (LUKACSOVICH *et al.* 2001).

Insertion site for BG00690 was determined by Zhai et al. (ZHAI *et al.* 2003).

The insertion sites for the PL lines are from Horn et al. (HORN *et al.* 2003a).

TABLE III.2

Whole animal phenotypes of identified lines:

Transposon insertion	Viability	Other phenotypes
CG8963^{BG00665}	Homozygous lethal, with death at all larval stages. No multiple mouthparts observed.	
CG10133^{BG00690}	Normal	
CG16708^{BG01100}	Homozygous lethal, with death embryonic stage.	
tara^{BG01673}	Homozygous lethal, with death at larval or embryonic stages.	
tai^{BG01746}	Some larval (1%) and pupal lethality.	Larval lethality sometimes associated with multiple mouthparts. 16% of adults with PEW. 10% of adults with dark pigmentation in shape of trident on dorsal thorax and/or loss of the glossy surface finish of the cuticle.
Pk61C^{BG02759}	Some larval and pupal lethality at all stages. No	

	multiple mouthparts observed.	
row^{BG02781}	~90% homozygous lethal with larval and late pupal lethality. 1% dead larvae with multiple mouthparts.	100% of survived adults with PEW, with dark pigmentation in shape of trident on dorsal thorax and/or loss of the glossy surface finish of the cuticle.
chif ^{BG02820}	Normal	
CG14910^{PL00112}	Homozygous larval and paharate adult lethality. No multiple mouthparts observed.	
CG2246^{PL00407}	Some mid-pupal to pharate adult lethality.	
TyrR^{PL00408}	Some pharate adult lethality	
CG32044^{PL00467}	Normal	
Fur1^{PL00566}	Normal	
Gyc β*100B*^{PL00571}	Mostly homozygous lethal, with mid-pupal to pharate adult lethality	

Figure III.1: Expression patterns of selected lines in the epitracheal gland. (A) *BG00690* (mCD8::GFP) is expressed specifically in the ETH expressing Inka cell (anti-PETH, magenta). (B) *BG02781* (mCD8::GFP) is expressed only in the PMa cell (arrow), which is next to the Inka cell (anti-PETH, magenta). (C) *BG01746* (mCD8::GFP) is expressed in both the Inka cell (anti-PETH, magenta) and the PMa cell (arrow). (D) In addition to the ETH-expressing Inka cell (anti-PETH, magenta) and the PMa cell, *BG00665* (mCD8::GFP) is also expressed in two other cells in the epitracheal gland. The PMa cell can't be identified from the rest two cells in the EG, arrowheads were used to indicate all three other cells next to the Inka cell in (D). Bars: 10 µm.

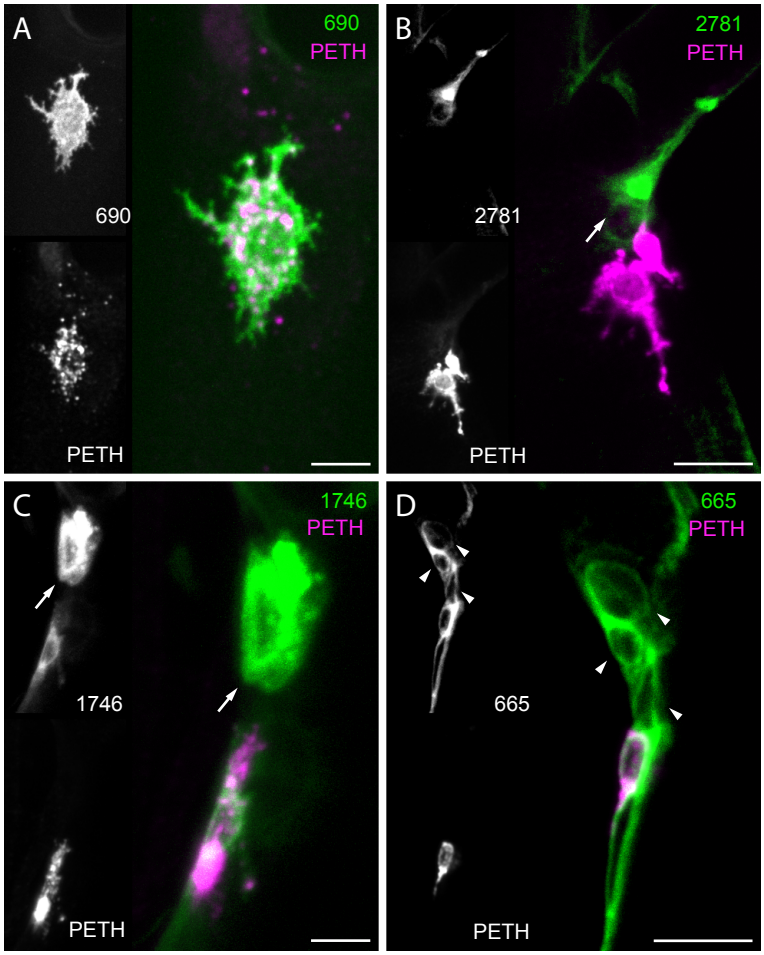
A
690
PETH
690
PETH
B
2781
PETH
2781
PETH
C
1746
PETH
1746
PETH
D
665
PETH
665
PETH

Figure III.2: Inka-specific knock-down of *tai* expression led to ecdysis defects. (A) Use of the Inka-specific driver *BG00690* to drive *UAS-tai*^{RNAi} expression in the Inka cell led to lethality at different developmental stages. The lethality during the 1st, 2nd, 3rd instar and pupal stage was quantified in *BG00690>UAS-tai*^{RNAi} animals (n= 300 for each of the larval stages, n=187 for pupal stage). The control animals were *UAS-tai*^{RNAi}/+ (n=300 for each of the larval stages, n=188 for pupal stage) and *BG00690*/+ (n=300 for each of the larval stages, n=193 for pupa stage). (B) Phenotype of larval ecdysis defect. We observed that 6.5% of *BG00690>UAS-tai*^{RNAi} larvae (right image) died at 2nd to 3rd instar ecdysis. Dead larvae still have mouthparts (arrow) and mouth hooks (arrowhead) from the previous developmental stage. Wild type larvae (left image) only had one set of mouthparts and mouth hooks at this stage. (C) *BG00690>UAS-tai*^{RNAi} pupa (right figure) died at pupal ecdysis with head located within the thoracic segment (arrow) and with legs that were not fully extended (arrowhead).

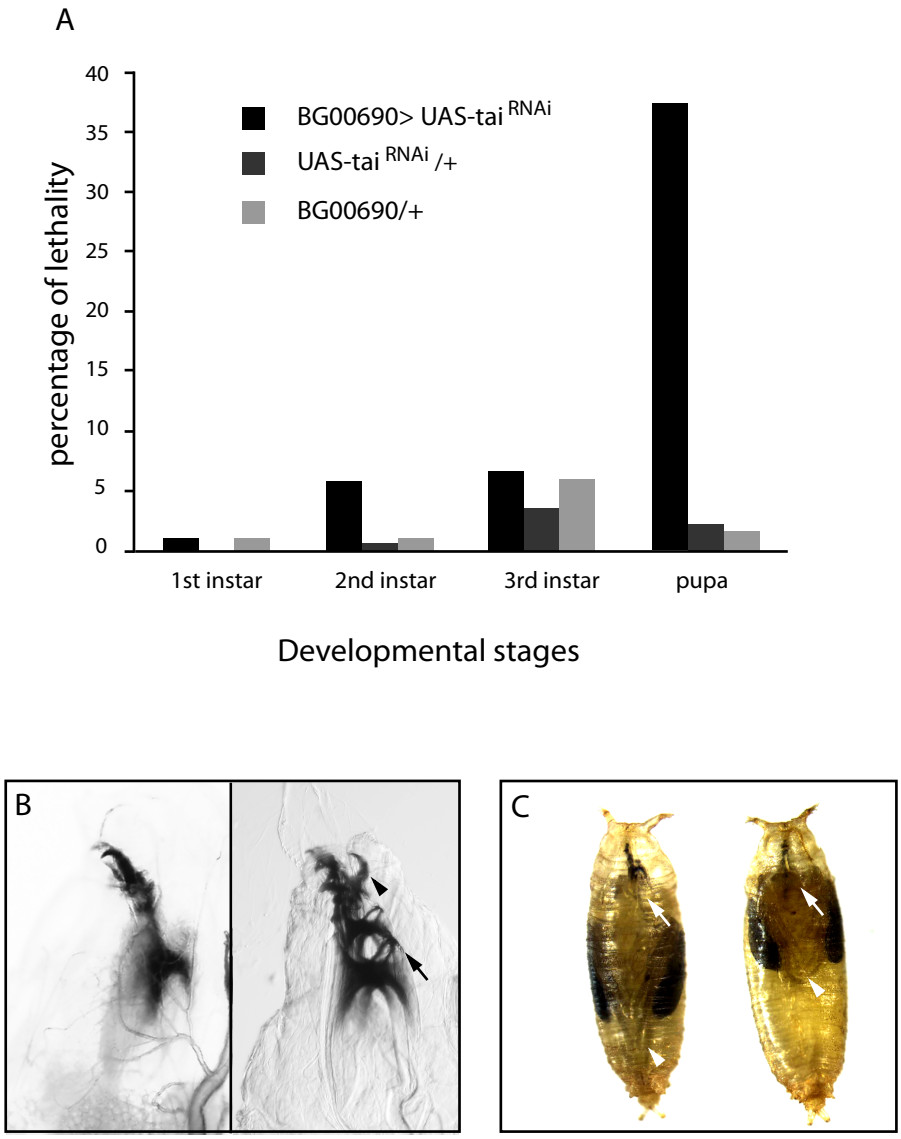
A
40
35
30
25
20
15
10
5
0
percentage of lethality
BG00690> UAS-tai RNAi
UAS-tai RNAi /+
BG00690/+
1st instar
2nd instar
3rd instar
pupa
Developmental stages
B
C

Figure III.3 Knock-down of *tai* expression in Inka cells caused reduced *ETH* transcription and translation. *In situ* hybridization of *ETH* (A) and immunostaining with anti-PETH in size-matched small 3rd instar larvae of tai^{RNAi}/+ (N=7-8), *BG00690/+* (N=8-9), and *BG00690>*tai^{RNAi} that successfully went through ecdysis (N=6-7), or that had multiple mouthparts (**BG00690>*tai^{RNAi}) (N=7-8). *BG00690>*tai^{RNAi} larvae showed substantially reduced *ETH* mRNA (A) and protein (B) levels. Images below the histogram are representative examples of TM5 of each group. Bars: A, 10 µm; B, 2 µm.

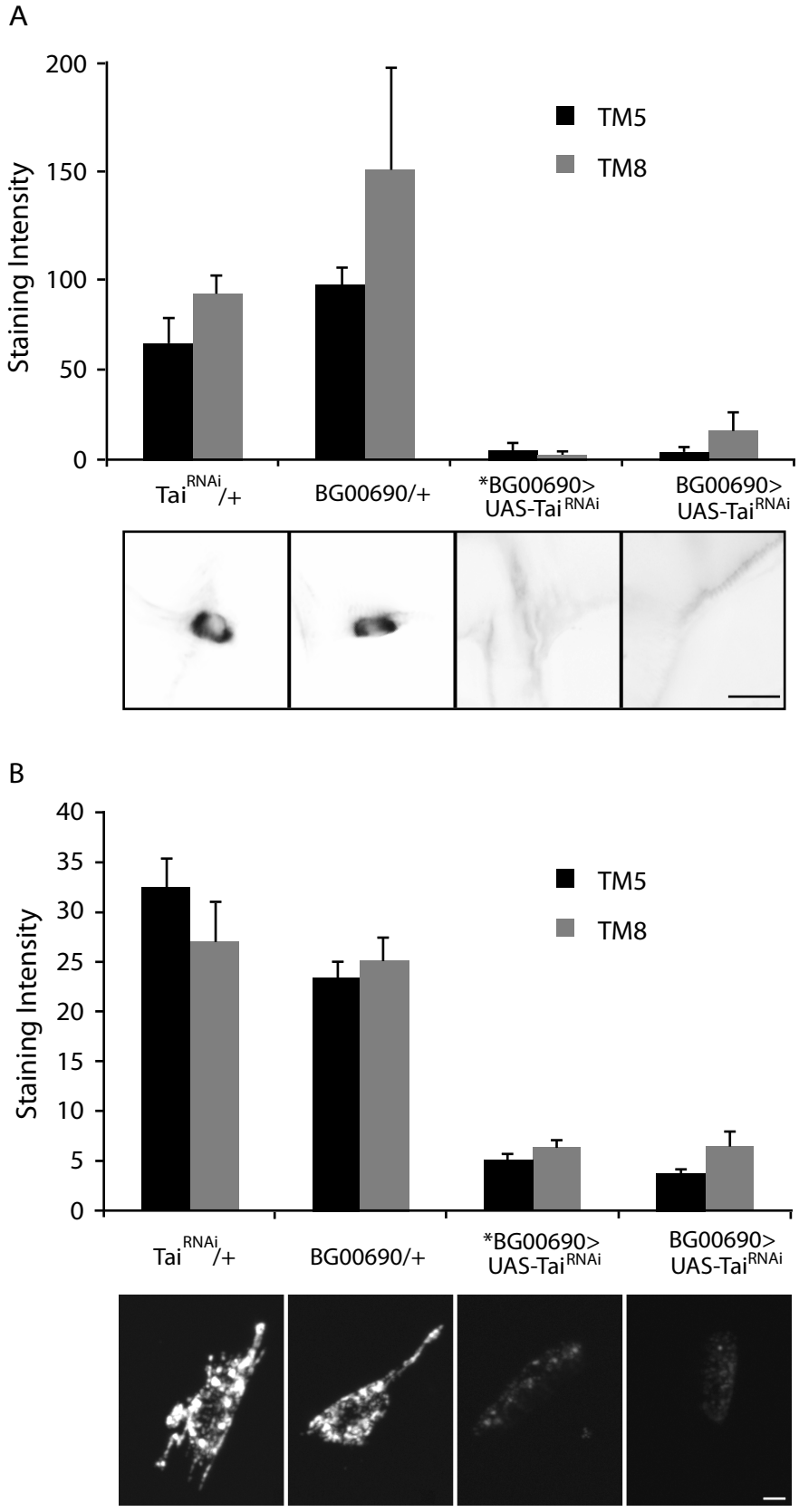
A
200
150
100
50
0
Staining Intensity
TM5
TM8
Tai RNAi /+
BG00690/+
*BG00690> UAS-Tai RNAi
BG00690> UAS-Tai RNAi
B
40
35
30
25
20
15
10
5
0
Staining Intensity
TM5
TM8
Tai RNAi /+
BG00690/+
*BG00690> UAS-Tai RNAi
BG00690> UAS-Tai RNAi

Figure III.4: TAI immunostaining in the Inka cell cytoplasm and nucleus. (A) Immunostaining with an anti-TAI antiserum (magenta) in a 3rd instar fillet of a 36Y-Gal4-ANF::GFP (anti-GFP, green) animal showed moderate TAI staining in the nuclei of all local cell types, including the tracheal cells (arrowheads). The Inka cells have moderate TAI staining in the nuclei, but also have strong staining in the cytoplasm. The cytoplasmic TAI staining showed the same subcellular distribution as the ANF::GFP signal (arrows), suggesting that the cytoplasmic TAI signal was distributed in the secretory compartment and thus may be caused by cross-reactivity between the TAI antiserum and other secretory proteins (possibly ETH). (B) Expression of 36Y-Gal4-ANF::GFP in the Inka cell. (C) Anti-TAI staining in the nuclei of tracheal cells (arrowheads) and in both the nuclear and the cytoplasm (arrows) of the Inka cell. Bars: 5μm.

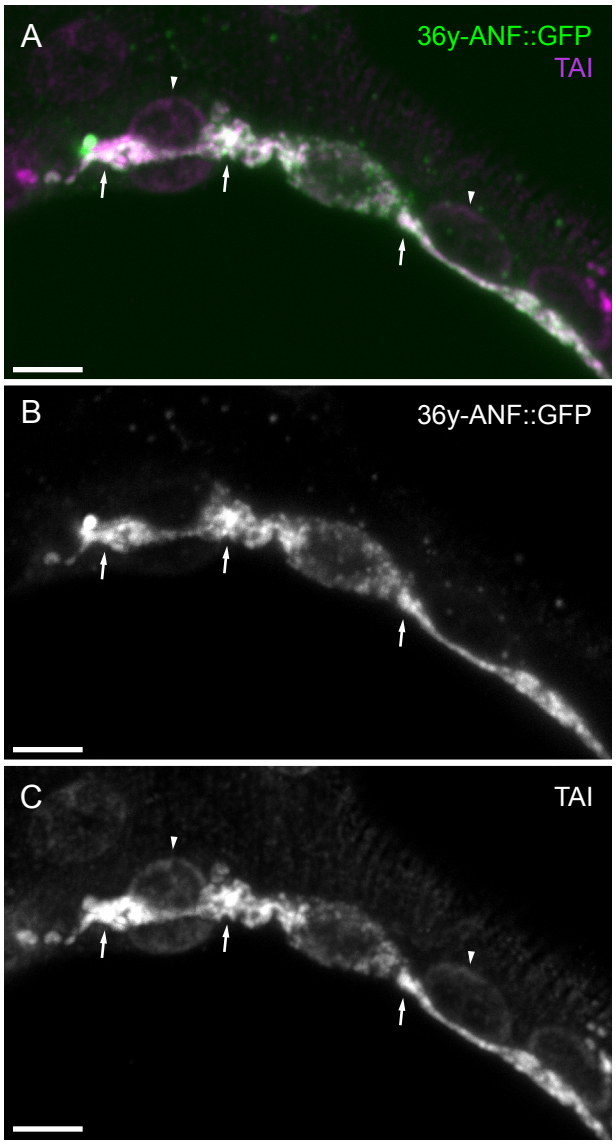
A
36y-ANF::GFP
TAI
B
36y-ANF::GFP
C
TAI

Figure III.5: *UAS-tai*^{RNAi} successfully knocked-down TAI protein levels in the Inka cell. We used *386-Gal4, UAS-mCD8::GFP* to drive *UAS-tai*^{RNAi} expression in the Inka cell. Anti-TAI immunostaining was performed on *386-Gal4, UAS-mCD8::GFP>UAS-tai*^{RNAi} (386>*UAS-tai*^{RNAi}) (n=7), *UAS-tai*^{RNAi}/+ (n=4) and *386-Gal4, UAS-mCD8::GFP* (386/+) (n=9) 3rd instar larvae. TAI staining in the nuclei of the Inka cell (gray bar) and a neighboring cell (black bar) was quantified. One-way ANOVA (Inka cell, p=0.000; neighbor cell, p=0.028) with Bonferroni *post-hoc* test. Genotypes not sharing a common letter have statistically different TAI staining intensities in the nuclei (Inka cell, capital letters; neighbor cell, lower case letters).

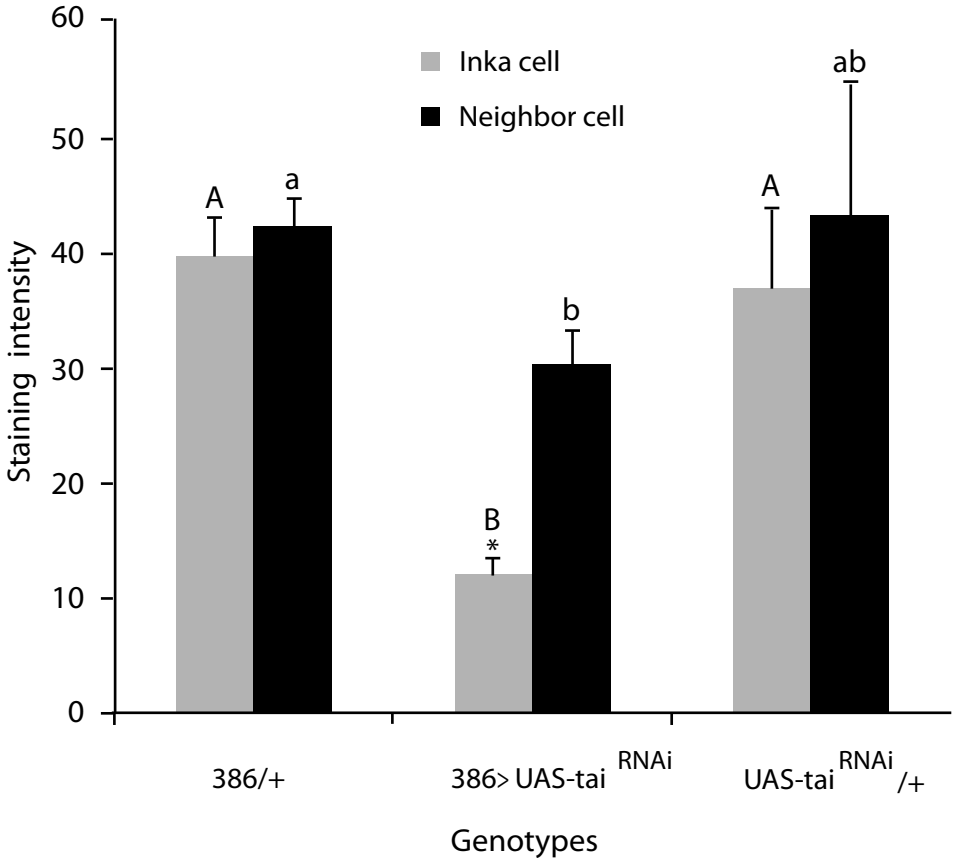
60
50
40
30
20
10
0
Staining intensity
Inka cell
Neighbor cell
A
a
B
*
b
A
ab
386/+
386> UAS-tai RNAi
UAS-tai RNAi /+
Genotypes

Figure III.6: ETH secretion at the pupal ecdysis was essentially normal following Inka cell-specific knock-down of *tai*. (A) ETH (anti-PETH, magenta) and PHM (anti-PHM, green) were colocalized with similar subcellular distributions in Inka cell. Figures to the left showed the PHM and PETH staining separately of the part within the dashed box. Bar, 5μm. (B) The release of PHM was quantified based on the number of visible PHM-positive (anti-PHM) Inka cells in *BG00690/+*, *UAS-tai*^{RNAi}*/+* and *BG00690>UAS-tai*^{RNAi} pupae at 10hr APF (n=7 for each genotype) (black bar) and 14hr APF (n=6, 7, 11, respectively) (gray bar). (C) The staining intensity of all the visible PHM-positive (anti-PHM) Inka cells were quantified in the same animals used in (B) to assess the level of PHM release at 10hr APF (black bar) and 14hr APF (gray bar). One-way ANOVA with Bonferroni *post-hoc* test; *, $p<0.001$. Genotypes not sharing a common letter have statistically different number of visible Inka cells (B) or PHM staining intensities in the nuclei of the Inka cells (C) (10h APF, capital letters; 14h APF, lower case letters).

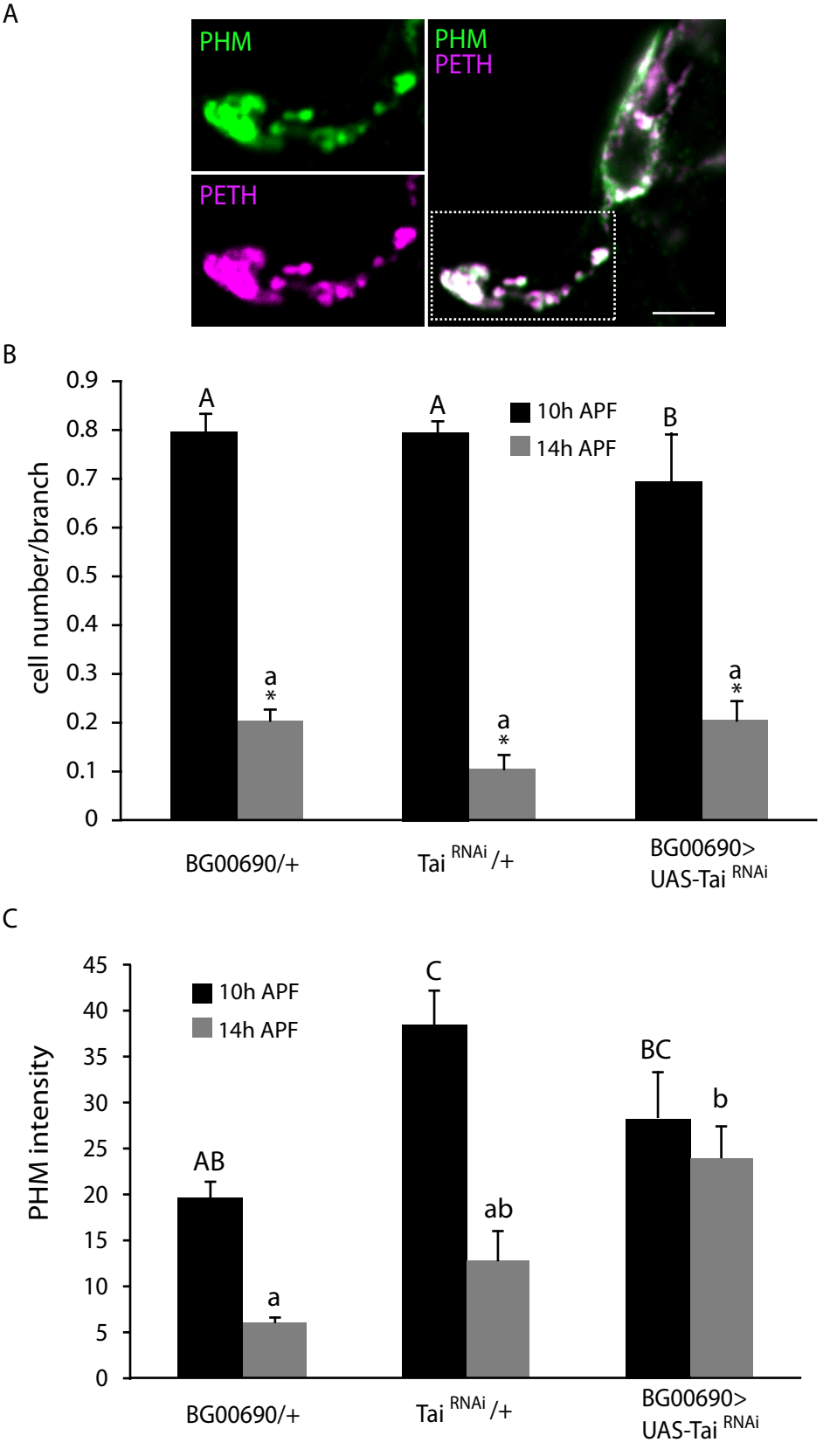
A
PHM
PETH
PHM
PETH
B
cell number/branch
0.9
0.8
0.7
0.6
0.5
0.4
0.3
0.2
0.1
0
10h APF
14h APF
A
a
*
A
a
*
B
a
*
BG00690/+
Tai RNAi /+
BG00690>
UAS-Tai RNAi
C
PHM intensity
45
40
35
30
25
20
15
10
5
0
10h APF
14h APF
AB
a
C
ab
BC
b
BG00690/+
Tai RNAi /+
BG00690>
UAS-Tai RNAi

Figure III.7: Levels fo TAI protein and circulating 20HE were correlated in prepupae. The staining intensity for TAI (anti-TAI) in OregonR flies was quantified in the nuclei of the Inka cell (black bar) and a neighboring EG cell (gray bar) located in TM5 of each main trachea branch. Animals were dissected and stained at 0hr APF (n=7), 6hr APF (n=7), 9hr APF (n=6) and 12hr APF (n=6). The circulating 20HE level at corresponding developmental stages (RIDDIFORD 1993) is shown by the curved line.

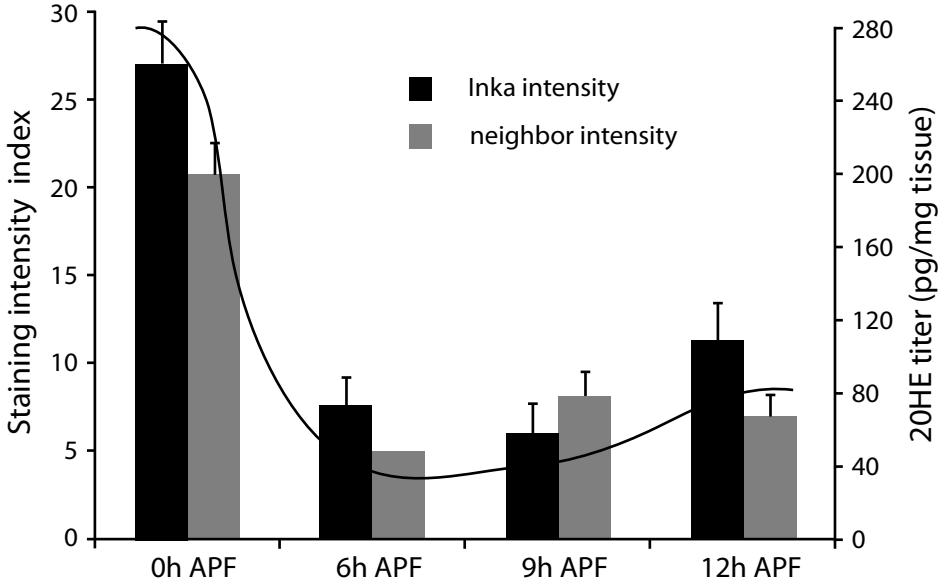
Staining intensity index
20HE titer (pg/mg tissue)
Inka intensity
neighbor intensity
0
5
10
15
20
25
30
0
40
80
120
160
200
240
280
0h APF
6h APF
9h APF
12h APF

Figure III.8: Proposed model for the regulation of *ETH* expression. The promoter region of *ETH* contains DNA sequences that are possible binding sites for the DNA binding domain (DBD) of CRC (filled black bar, CRC-BD) and EcR-B2/USP [gray bar, direct repeat (DR4)]. The bZIP domain of the basic-leucine transcription factor CRC interacts with the AF1 domain of EcR-B2. In the presence of 20HE, the LXXLL domain of the EcR cofactor TAI interacts with the AF2 domain of EcR-B2. USP is the heterodimeric partner for EcR-B2.

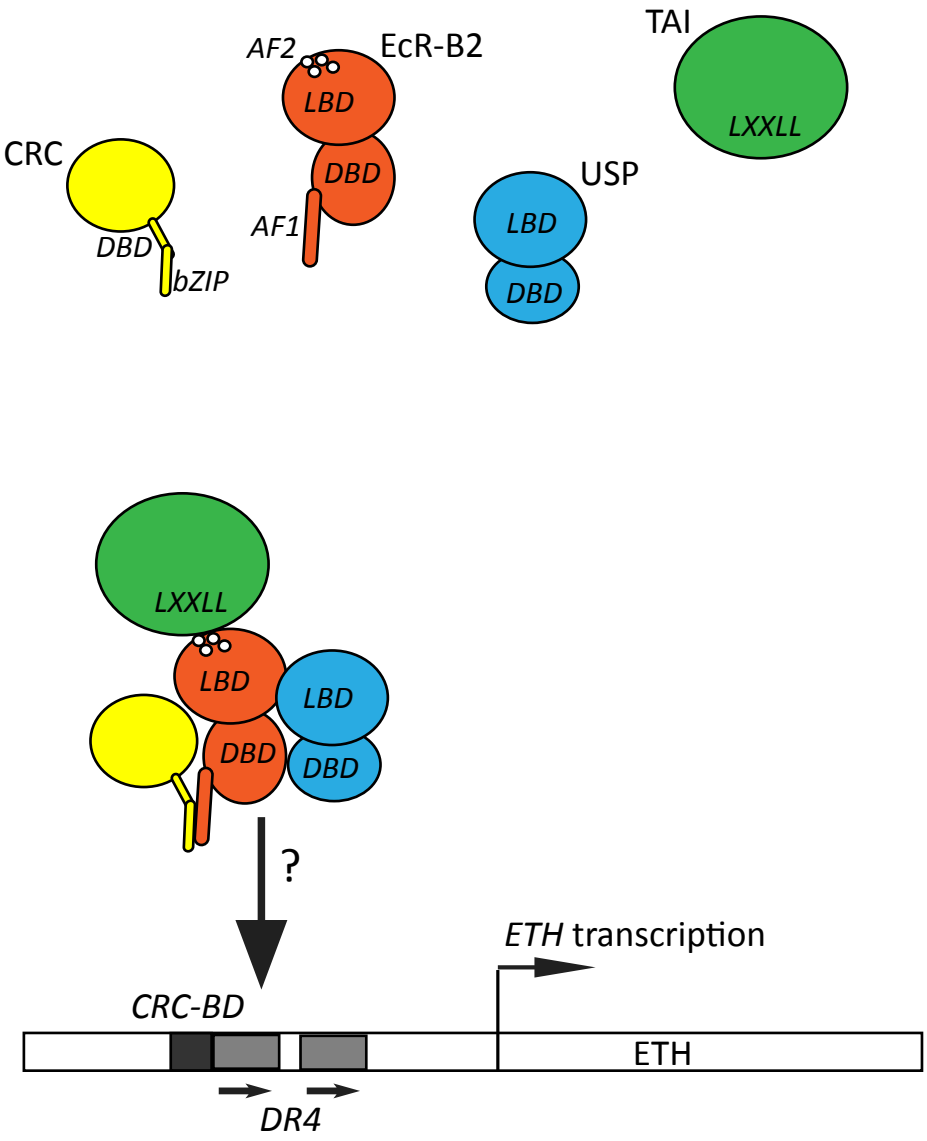
AF2
EcR-B2
TAI
LBD
LXXLL
CRC
DBD
USP
AF1
LBD
DBD
DBD
bZIP
LXXLL
LBD
LBD
DBD
DBD
?
ETH transcription
CRC-BD
ETH
DR4

References

ALLAN, D. W., D. PARK, S. E. ST PIERRE, P. H. TAGHERT and S. THOR, 2005 Regulators acting in combinatorial codes also act independently in single differentiating neurons. Neuron **45:** 689-700.

ALLAN, D. W., S. E. PIERRE, I. MIGUEL-ALIAGA and S. THOR, 2003 Specification of neuropeptide cell identity by the integration of retrograde BMP signaling and a combinatorial transcription factor code. Cell **113:** 73-86.

ARMSTRONG, J. D., M. J. TEXADA, R. MUNJAAL, D. A. BAKER and K. M. BECKINGHAM, 2005 Gravitaxis in Drosophila melanogaster: a forward genetic screen. Genes, Brain and Behavior **5:** 222-239.

BAI, J., Y. UEHARA and D. J. MONTELL, 2000 Regulation of invasive cell behavior by taiman, a Drosophila protein related to AIB1, a steroid receptor coactivator amplified in breast cancer. Cell **103:** 1047-1058.

BAINBRIDGE, S. P., and M. BOWNES, 1981 Staging the metamorphosis of Drosophila melanogaster. J Embryol Exp Morphol **66:** 57-80.

BAKER, J. D., and J. W. TRUMAN, 2002 Mutations in the Drosophila glycoprotein hormone receptor, *rickets*, eliminate neuropeptide-induced tanning and selectively block a stereotyped behavioral program. J Exp Biol **205:** 2555-2565.

BELLEN, H. J., R. W. LEVIS, G. LIAO, Y. HE, J. W. CARLSON *et al.*, 2004a The BDGP gene disruption project: single transposon insertions associated with 40% of Drosophila genes. Genetics **167:** 761-781.

BELLEN, H. J., R. W. LEVIS, G. LIAO, Y. HE, J. W. CARLSON *et al.*, 2004b The BDGP gene disruption project: single transposon insertions associated with 40% of Drosophila genes. Genetics **167:** 761-781.

BELLEN, H. J., C. J. O'KANE, C. WILSON, U. GROSSNIKLAUS, R. K. PEARSON *et al.*, 1989 P-element-mediated enhancer detection: a versatile method to study development in Drosophila. Genes Dev **3:** 1288-1300.

BENDER, M., F. B. IMAM, W. S. TALBOT, B. GANETZKY and D. S. HOGNESS, 1997 Drosophila ecdysone receptor mutations reveal functional differences among receptor isoforms. Cell **91:** 777-788.

BHARUCHA, K. N., P. TARR and S. L. ZIPURSKY, 2008 A glucagon-like endocrine pathway in Drosophila modulates both lipid and carbohydrate homeostasis. J Exp Biol **211:** 3103-3110.

BRAND, A. H., and N. PERRIMON, 1993 Targeted gene expression as a means of altering cell fates and generating dominant phenotypes. Development **118:** 401-415.

BROGIOLO, W., H. STOCKER, T. IKEYA, F. RINTELEN, R. FERNANDEZ *et al.*, 2001 An evolutionarily conserved function of the Drosophila insulin receptor and insulin-like peptides in growth control. Curr Biol **11:** 213-221.

BROWN, M. R., J. W. CRIM, R. C. ARATA, H. N. CAI, C. CHUN *et al.*, 1999 Identification of a Drosophila brain-gut peptide related to the neuropeptide Y family. Peptides **20:** 1035-1042.

BURGOYNE, R. D., and A. MORGAN, 2003 Secretory granule exocytosis. Physiol Rev **83:** 581-632.

CANAVOSO, L. E., Z. E. JOUNI, K. J. KARNAS, J. E. PENNINGTON and M. A. WELLS, 2001 Fat metabolism in insects. Annu Rev Nutr **21:** 23-46.

CANTERA, R., and D. R. NASSEL, 1992 Segmental peptidergic innervation of abdominal targets in larval and adult dipteran insects revealed with an antiserum against leucokinin I. Cell Tissue Res **269:** 459-471.

CHANG, J. C., R. B. YANG, M. E. ADAMS and K. H. LU, 2009 Receptor guanylyl cyclases in Inka cells targeted by eclosion hormone. Proc Natl Acad Sci U S A **106:** 13371-13376.

COLOMBANI, J., L. BIANCHINI, S. LAYALLE, E. PONDEVILLE, C. DAUPHIN-VILLEMANT *et al.*, 2005 Antagonistic actions of ecdysone and insulins determine final size in Drosophila. Science **310:** 667-670.

DAVIS, R. L., H. WEINTRAUB and A. B. LASSAR, 1987 Expression of a single transfected cDNA converts fibroblasts to myoblasts. Cell **51:** 987-1000.

DEWEY, E. M., S. L. MCNABB, J. EWER, G. R. KUO, C. L. TAKANISHI *et al.*, 2004 Identification of the gene encoding bursicon, an insect neuropeptide responsible for cuticle sclerotization and wing spreading. Curr Biol **14:** 1208-1213.

DEZAZZO, J., S. XIA, J. CHRISTENSEN, K. VELINZON and T. TULLY, 1999 Developmental expression of an amn(+) transgene rescues the mutant memory defect of amnesiac adults. J Neurosci **19:** 8740-8746.

DULCIS, D., R. B. LEVINE and J. EWER, 2005 Role of the neuropeptide CCAP in Drosophila cardiac function. J Neurobiol **64:** 259-274.

EIPPER, B. A., D. A. STOFFERS and R. E. MAINS, 1992 The biosynthesis of neuropeptides: peptide alpha-amidation. Annu Rev Neurosci **15:** 57-85.

EWER, J., and S. E. REYNOLDS, 2002 Neuropeptide control of molting in insects, pp. 1-92 in *Hormones, Brain and Behavior in Invertebrats.*, edited by A. P. A. D. W. PFAFF, A. M. ETGEN, S. E. FAHRBACH AND R. T. RUBIN. Academic Press, New York.

EWER, J., and J. W. TRUMAN, 1996 Increases in cyclic 3', 5'-guanosine monophosphate (cGMP) occur at ecdysis in an evolutionarily conserved crustacean cardioactive peptide-immunoreactive insect neuronal network. J Comp Neurol **370:** 330-341.

FEANY, M. B., and W. G. QUINN, 1995 A neuropeptide gene defined by the Drosophila memory mutant amnesiac. Science **268:** 869-873.

FLYBASE_CONSORTIUM, 2003 The FlyBase database of the Drosophila genome projects and community literature. Nucleic Acids Research **31:** 172-175 http://flybase.org/.

FRAENKEL, G., and C. HSIAO, 1965 Bursicon, a hormone which mediates tanning of the cuticle in the adult fly and other insects. J Insect Physiol **11:** 513-556.

FRAENKEL, G., C. HSIAO and M. SELIGMAN, 1966 Properties of bursicon: an insect protein hormone that controls cuticular tanning. Science **151:** 91-93.

FREEMAN, M. R., A. DOBRITSA, P. GAINES, W. A. SEGRAVES and J. R. CARLSON, 1999 The dare gene: steroid hormone production, olfactory behavior, and neural degeneration in Drosophila. Development **126:** 4591-4602.

GAUTHIER, S. A., 2008 Initiation of ecdysis: ecdysteriods and a specific cofactor for ecsysone receptor B2 shape the Inka cell into a peptide hormone factory, pp. in *Department of Zoology*. University of Oklahoma, Norman.

GAUTHIER, S. A., and R. S. HEWES, 2006 Transcriptional regulation of neuropeptide and peptide hormone expression by the Drosophila dimmed and cryptocephal genes. J Exp Biol **209:** 1803-1815.

HALDER, G., P. CALLAERTS and W. J. GEHRING, 1995 Induction of ectopic eyes by targeted expression of the eyeless gene in Drosophila. Science **267:** 1788-1792.

HARBISON, S. T., A. H. YAMAMOTO, J. J. FANARA, K. K. NORGA and T. F. MACKAY, 2004 Quantitative trait loci affecting starvation resistance in Drosophila melanogaster. Genetics **166:** 1807-1823.

HAYFLICK, J. S., W. J. WOLFGANG, M. A. FORTE and G. THOMAS, 1992 A unique Kex2-like endoprotease from Drosophila melanogaster is expressed in the central nervous system during early embryogenesis. J Neurosci **12:** 705-717.

HEWES, R. S., D. PARK, S. A. GAUTHIER, A. M. SCHAEFER and P. H. TAGHERT, 2003 The bHLH protein Dimmed controls neuroendocrine cell differentiation in Drosophila. Development **130:** 1771-1781.

HEWES, R. S., and P. H. TAGHERT, 2001 Neuropeptides and neuropeptide receptors in the Drosophila melanogaster genome. Genome Res **11:** 1126-1142.

HILL, R. E., J. FAVOR, B. L. HOGAN, C. C. TON, G. F. SAUNDERS *et al.*, 1991 Mouse small eye results from mutations in a paired-like homeobox-containing gene. Nature **354:** 522-525.

HONEGGER, H. W., D. MARKET, L. A. PIERCE, E. M. DEWEY, B. KOSTRON *et al.*, 2002 Cellular localization of bursicon using antisera against partial peptide sequences of this insect cuticle-sclerotizing neurohormone. J Comp Neurol **452:** 163-177.

HORN, C., B. JAUNICH and E. A. WIMMER, 2000 Highly sensitive, fluorescent transformation marker for Drosophila transgenesis. Dev Genes Evol **210:** 623-629.

HORN, C., N. OFFEN, S. NYSTEDT, U. HACKER and E. A. WIMMER, 2003a piggyBac-based insertional mutagenesis and enhancer detection as a tool for functional insect genomics. Genetics **163:** 647-661.

HORN, C., N. OFFEN, S. NYSTEDT, U. HACKER and E. A. WIMMER (Editors), 2003b *piggyBac-based insertional mutagenesis and enhancer detection as a tool for functional insect genomics.*

HORODYSKI, F. M., J. EWER, L. M. RIDDIFORD and J. W. TRUMAN, 1993 Isolation, characterization and expression of the eclosion hormone gene of Drosophila melanogaster. Eur J Biochem **215:** 221-228.

HYUN, S., Y. LEE, S. T. HONG, S. BANG, D. PAIK *et al.*, 2005 Drosophila GPCR Han is a receptor for the circadian clock neuropeptide PDF. Neuron **48:** 267-278.

IKEYA, T., M. GALIC, P. BELAWAT, K. NAIRZ and E. HAFEN, 2002 Nutrient-dependent expression of insulin-like peptides from neuroendocrine cells in the CNS contributes to growth regulation in Drosophila. Curr Biol **12:** 1293-1300.

IVERSEN, A., G. CAZZAMALI, M. WILLIAMSON, F. HAUSER and C. J. GRIMMELIKHUIJZEN, 2002 Molecular identification of the first insect ecdysis triggering hormone receptors. Biochem Biophys Res Commun **299:** 924-931.

JIANG, N., A. S. KOLHEKAR, P. S. JACOBS, R. E. MAINS, B. A. EIPPER *et al.*, 2000 PHM is required for normal developmental transitions and for biosynthesis of secretory peptides in Drosophila. Dev Biol **226:** 118-136.

KATAOKA, H., H. NAGASAWA, A. ISOGAI, H. ISHIZAKI and A. SUZUKI, 1991 Prothoracicotropic hormone of the silkworm, Bombyx mori: amino acid sequence and dimeric structure. Agric Biol Chem **55:** 73-86.

KIM, A. J., G. H. CHA, K. KIM, L. I. GILBERT and C. C. LEE, 1997 Purification and characterization of the prothoracicotropic hormone of Drosophila melanogaster. Proc Natl Acad Sci U S A **94:** 1130-1135.

KIM, S. K., and E. J. RULIFSON, 2004 Conserved mechanisms of glucose sensing and regulation by Drosophila corpora cardiaca cells. Nature **431:** 316-320.

KIM, Y. J., I. SPALOVSKA-VALACHOVA, K. H. CHO, I. ZITNANOVA, Y. PARK *et al.*, 2004 Corazonin receptor signaling in ecdysis initiation. Proc Natl Acad Sci U S A **101:** 6704-6709.

KIM, Y. J., D. ZITNAN, C. G. GALIZIA, K. H. CHO and M. E. ADAMS, 2006 A command chemical triggers an innate behavior by sequential activation of multiple peptidergic ensembles. Curr Biol **16:** 1395-1407.

KINGAN, T. G., R. A. CARDULLO and M. E. ADAMS, 2001 Signal transduction in eclosion hormone-induced secretion of ecdysis-triggering hormone. J Biol Chem **276:** 25136-25142.

KLEIN, C., G. K. H and C. RADLICKI, 1999 The 'Inka cell' and its associated cells: ultrastructure of the epitracheal glands in the gypsy moth, Lymantria dispar. J Insect Physiol **45:** 65-73.

KOPEC, S., 1922 Studies on the necessity of the brain for the inception of insect metamorphosis. Biol. Bull. **42:** 323-342.

LEAR, B. C., C. E. MERRILL, J. M. LIN, A. SCHROEDER, L. ZHANG *et al.*, 2005 A G protein-coupled receptor, groom-of-PDF, is required for PDF neuron action in circadian behavior. Neuron **48:** 221-227.

LEE, G., J. H. BAHN and J. H. PARK, 2006 Sex- and clock-controlled expression of the neuropeptide F gene in Drosophila. Proc Natl Acad Sci U S A **103:** 12580-12585.

LEE, G., and J. H. PARK, 2004 Hemolymph sugar homeostasis and starvation-induced hyperactivity affected by genetic manipulations of the adipokinetic hormone-encoding gene in Drosophila melanogaster. Genetics **167:** 311-323.

LIN, Y., G. D. STORMO and P. H. TAGHERT, 2004 The neuropeptide pigment-dispersing factor coordinates pacemaker interactions in the Drosophila circadian system. J Neurosci **24:** 7951-7957.

LOI, P. K., S. A. EMMAL, Y. PARK and N. J. TUBLITZ, 2001 Identification, sequence and expression of a crustacean cardioactive peptide (CCAP) gene in the moth Manduca sexta. J Exp Biol **204:** 2803-2816.

LUAN, H., W. C. LEMON, N. C. PEABODY, J. B. POHL, P. K. ZELENSKY *et al.*, 2006 Functional dissection of a neuronal network required for cuticle tanning and wing expansion in Drosophila. J Neurosci **26:** 573-584.

LUCAS, K. A., G. M. PITARI, S. KAZEROUNIAN, I. RUIZ-STEWART, J. PARK *et al.*, 2000 Guanylyl cyclases and signaling by cyclic GMP. Pharmacol Rev **52:** 375-414.

LUKACSOVICH, T., Z. ASZTALOS, W. AWANO, K. BABA, S. KONDO *et al.*, 2001 Dual-tagging gene trap of novel genes in Drosophila melanogaster. Genetics **157:** 727-742.

LUKONG, K. E., K. W. CHANG, E. W. KHANDJIAN and S. RICHARD, 2008 RNA-binding proteins in human genetic disease. Trends Genet **24:** 416-425.

LUO, C. W., E. M. DEWEY, S. SUDO, J. EWER, S. Y. HSU *et al.*, 2005 Bursicon, the insect cuticle-hardening hormone, is a heterodimeric cystine knot protein that activates G protein-coupled receptor LGR2. Proc Natl Acad Sci U S A **102:** 2820-2825.

MARIS, C., C. DOMINGUEZ and F. H. ALLAIN, 2005 The RNA recognition motif, a plastic RNA-binding platform to regulate post-transcriptional gene expression. Febs J **272:** 2118-2131.

MCBRAYER, Z., H. ONO, M. SHIMELL, J. P. PARVY, R. B. BECKSTEAD *et al.*, 2007 Prothoracicotropic hormone regulates developmental timing and body size in Drosophila. Dev Cell **13:** 857-871.

MCNABB, S. L., J. D. BAKER, J. AGAPITE, H. STELLER, L. M. RIDDIFORD *et al.*, 1997 Disruption of a behavioral sequence by targeted death of peptidergic neurons in Drosophila. Neuron **19:** 813-823.

MENDIVE, F. M., T. VAN LOY, S. CLAEYSEN, J. POELS, M. WILLIAMSON *et al.*, 2005 Drosophila molting neurohormone bursicon is a heterodimer and the natural agonist of the orphan receptor DLGR2. FEBS Lett **579:** 2171-2176.

MERTENS, I., T. MEEUSEN, R. HUYBRECHTS, A. DE LOOF and L. SCHOOFS, 2002 Characterization of the short neuropeptide F receptor from Drosophila melanogaster. Biochem Biophys Res Commun **297:** 1140-1148.

MILLER, R., T. TONEFF, D. VISHNUVARDHAN, M. BEINFELD and V. Y. HOOK, 2003 Selective roles for the PC2 processing enzyme in the regulation of peptide neurotransmitter levels in brain and peripheral neuroendocrine tissues of PC2 deficient mice. Neuropeptides **37:** 140-148.

MORIN, X., R. DANEMAN, M. ZAVORTINK and W. CHIA, 2001 A protein trap strategy to detect GFP-tagged proteins expressed from their endogenous loci in Drosophila. Proc Natl Acad Sci U S A **98:** 15050-15055.

MORTON, D. B., and P. J. SIMPSON, 2002 Cellular signaling in eclosion hormone action. J Insect Physiol **48:** 1-13.

NASSEL, D. R., 2002 Neuropeptides in the nervous system of Drosophila and other insects: multiple roles as neuromodulators and neurohormones. Prog Neurobiol **68:** 1-84.

NASSEL, D. R., and C. T. LUNDQUIST, 1991 Insect tachykinin-like peptide: distribution of leucokinin immunoreactive neurons in the cockroach and blowfly brains. Neurosci Lett **130:** 225-228.

NASSEL, D. R., S. SHIGA, C. J. MOHRHERR and K. R. RAO, 1993 Pigment-dispersing hormone-like peptide in the nervous system of the flies Phormia and Drosophila: immunocytochemistry and partial characterization. J Comp Neurol **331:** 183-198.

O'BRIEN, M. A., and P. H. TAGHERT, 1998 A peritracheal neuropeptide system in insects: release of myomodulin-like peptides at ecdysis. J Exp Biol **201:** 193-209.

O'KANE, C. J., and W. J. GEHRING, 1987 Detection in situ of genomic regulatory elements in Drosophila. Proc Natl Acad Sci U S A **84:** 9123-9127.

ORO, A. E., M. MCKEOWN and R. M. EVANS, 1992 The Drosophila retinoid X receptor homolog ultraspiracle functions in both female reproduction and eye morphogenesis. Development **115:** 449-462.

PARK, D., M. HAN, Y. C. KIM, K. A. HAN and P. H. TAGHERT, 2004 Ap-let neurons--a peptidergic circuit potentially controlling ecdysial behavior in Drosophila. Dev Biol **269:** 95-108.

PARK, D., O. T. SHAFER, S. P. SHEPHERD, H. SUH, J. S. TRIGG *et al.*, 2008a The Drosophila basic helix-loop-helix protein DIMMED directly activates PHM, a gene encoding a neuropeptide-amidating enzyme. Mol Cell Biol **28:** 410-421.

PARK, D., and P. H. TAGHERT, 2009 Peptidergic neurosecretory cells in insects: organization and control by the bHLH protein DIMMED. Gen Comp Endocrinol **162:** 2-7.

PARK, D., J. A. VEENSTRA, J. H. PARK and P. H. TAGHERT, 2008b Mapping peptidergic cells in Drosophila: where DIMM fits in. PLoS One **3:** e1896.

PARK, J. H., and J. C. HALL, 1998 Isolation and chronobiological analysis of a neuropeptide pigment-dispersing factor gene in Drosophila melanogaster. J Biol Rhythms **13:** 219-228.

PARK, J. H., C. HELFRICH-FORSTER, G. LEE, L. LIU, M. ROSBASH *et al.*, 2000 Differential regulation of circadian pacemaker output by separate clock genes in Drosophila. Proc Natl Acad Sci U S A **97:** 3608-3613.

PARK, J. H., A. J. SCHROEDER, C. HELFRICH-FORSTER, F. R. JACKSON and J. EWER, 2003 Targeted ablation of CCAP neuropeptide-containing neurons of Drosophila causes specific defects in execution and circadian timing of ecdysis behavior. Development **130:** 2645-2656.

PARK, Y., V. FILIPPOV, S. S. GILL and M. E. ADAMS, 2002 Deletion of the ecdysis-triggering hormone gene leads to lethal ecdysis deficiency. Development **129:** 493-503.

PARK, Y., D. ZITNAN, S. S. GILL and M. E. ADAMS, 1999 Molecular cloning and biological activity of ecdysis-triggering hormones in Drosophila melanogaster. FEBS Lett **463:** 133-138.

PEABODY, N. C., F. DIAO, H. LUAN, H. WANG, E. M. DEWEY *et al.*, 2008 Bursicon functions within the Drosophila CNS to modulate wing expansion behavior, hormone secretion, and cell death. J Neurosci **28:** 14379-14391.

PERRIMON, N., L. ENGSTROM and A. P. MAHOWALD, 1985 Developmental genetics of the 2C-D region of the Drosophila X chromosome. Genetics **111:** 23-41.

PICKARD, R. T., B. A. STRIFLER, R. M. KRAMER and J. D. SHARP, 1999 Molecular cloning of two new human paralogs of 85-kDa cytosolic phospholipase A2. J Biol Chem **274:** 8823-8831.

QUINN, W. G., P. P. SZIBER and R. BOOKER, 1979 The Drosophila memory mutant amnesiac. Nature **277:** 212-214.

RAO, K. R., C. J. MOHRHERR, J. P. RIEHM, C. A. ZAHNOW, S. NORTON *et al.*, 1987 Primary structure of an analog of crustacean pigment-dispersing hormone from the lubber grasshopper Romalea microptera. J Biol Chem **262:** 2672-2675.

RAO, K. R., and J. P. RIEHM, 1988 Pigment-dispersing hormones: a novel family of neuropeptides from arthropods. Peptides **9 Suppl 1:** 153-159.

RAO, K. R., J. P. RIEHM, C. A. ZAHNOW, L. H. KLEINHOLZ, G. E. TARR *et al.*, 1985 Characterization of a pigment-dispersing hormone in eyestalks of the fiddler crab Uca pugilator. Proc Natl Acad Sci U S A **82:** 5319-5322.

RAO, S., C. LANG, E. S. LEVITAN and D. L. DEITCHER, 2001 Visualization of neuropeptide expression, transport, and exocytosis in Drosophila melanogaster. J Neurobiol **49:** 159-172.

RAYBURN, L. Y., J. RHEA, S. R. JOCOY and M. BENDER, 2009 The proprotein convertase amontillado (amon) is required during Drosophila pupal development. Dev Biol **333:** 48-56.

RENN, S. C., J. H. PARK, M. ROSBASH, J. C. HALL and P. H. TAGHERT, 1999 A pdf neuropeptide gene mutation and ablation of PDF neurons each cause severe abnormalities of behavioral circadian rhythms in Drosophila. Cell **99:** 791-802.

RIDDIFORD, L. M., 1993 Hormones and Drosophila development, pp. 899-939 in *The Development of Drosophila melanogaster*, edited by M. BATE and A. M. ARIAS. Cold Spring Harbor Laboratory Press.

ROEBROEK, A. J., I. G. PAULI, Y. ZHANG and W. J. VAN DE VEN, 1991 cDNA sequence of a Drosophila melanogaster gene, Dfur1, encoding a protein structurally related to the subtilisin-like proprotein processing enzyme furin. FEBS Lett **289:** 133-137.

RULIFSON, E. J., S. K. KIM and R. NUSSE, 2002 Ablation of insulin-producing neurons in flies: growth and diabetic phenotypes. Science **296:** 1118-1120.

SCHUBIGER, M., A. A. WADE, G. E. CARNEY, J. W. TRUMAN and M. BENDER, 1998 Drosophila EcR-B ecdysone receptor isoforms are required for larval molting and for neuron remodeling during metamorphosis. Development **125:** 2053-2062.

SHEN, P., and H. N. CAI, 2001 Drosophila neuropeptide F mediates integration of chemosensory stimulation and conditioning of the nervous system by food. J Neurobiol **47:** 16-25.

SIEKHAUS, D. E., and R. S. FULLER, 1999 A role for amontillado, the Drosophila homolog of the neuropeptide precursor processing protease PC2, in triggering hatching behavior. J Neurosci **19:** 6942-6954.

SOSSIN, W. S., J. M. FISHER and R. H. SCHELLER, 1989 Cellular and molecular biology of neuropeptide processing and packaging. Neuron **2:** 1407-1417.

STANGIER, J., C. HILBICH, K. BEYREUTHER and R. KELLER, 1987 Unusual cardioactive peptide (CCAP) from pericardial organs of the shore crab Carcinus maenas. Proc Natl Acad Sci U S A **84:** 575-579.

STANLEY, B. G., and S. F. LEIBOWITZ, 1985 Neuropeptide Y injected in the paraventricular hypothalamus: a powerful stimulant of feeding behavior. Proc Natl Acad Sci U S A **82:** 3940-3943.

TAGHERT, P. H., 1999 FMRFamide neuropeptides and neuropeptide-associated enzymes in Drosophila. Microsc Res Tech **45:** 80-95.

TRUMAN, J. W., 2006 Steroid hormone secretion in insects comes of age. Proc Natl Acad Sci U S A **103:** 8909-8910.

TU, M. P., C. M. YIN and M. TATAR, 2005 Mutations in insulin signaling pathway alter juvenile hormone synthesis in Drosophila melanogaster. Gen Comp Endocrinol **142:** 347-356.

VEENSTRA, J. A., H. J. AGRICOLA and A. SELLAMI, 2008 Regulatory peptides in fruit fly midgut. Cell Tissue Res **334:** 499-516.

VENKATESH, K., and G. HASAN, 1997 Disruption of the IP3 receptor gene of Drosophila affects larval metamorphosis and ecdysone release. Curr Biol **7:** 500-509.

WADDELL, S., J. D. ARMSTRONG, T. KITAMOTO, K. KAISER and W. G. QUINN, 2000 The amnesiac gene product is expressed in two neurons in the Drosophila brain that are critical for memory. Cell **103:** 805-813.

WARD, R. E., P. REID, A. BASHIRULLAH, P. P. D'AVINO and C. S. THUMMEL, 2003 GFP in living animals reveals dynamic developmental responses to ecdysone during Drosophila metamorphosis. Dev Biol **256:** 389-402.

WRIGHT, W. E., D. A. SASSOON and V. K. LIN, 1989 Myogenin, a factor regulating myogenesis, has a domain homologous to MyoD. Cell **56:** 607-617.

ZHAI, R. G., P. R. HIESINGER, T. W. KOH, P. VERSTREKEN, K. L. SCHULZE *et al.*, 2003 Mapping Drosophila mutations with molecularly defined P element insertions. Proc Natl Acad Sci U S A **100:** 10860-10865.

ZHANG, H., J. LIU, C. R. LI, B. MOMEN, R. A. KOHANSKI *et al.*, 2009 Deletion of Drosophila insulin-like peptides causes growth defects and metabolic abnormalities. Proc Natl Acad Sci U S A **106:** 19617-19622.

ZHAO, T., T. GU, H. C. RICE, K. L. MCADAMS, K. M. ROARK *et al.*, 2008 A Drosophila gain-of-function screen for candidate genes involved in steroid-dependent neuroendocrine cell remodeling. Genetics **178:** 883-901.

ZITNAN, D., L. S. ROSS, I. ZITNANOVA, J. L. HERMESMAN, S. S. GILL *et al.*, 1999 Steroid induction of a peptide hormone gene leads to orchestration of a defined behavioral sequence. Neuron **23:** 523-535.